

Utah State University

DigitalCommons@USU

---

All Graduate Theses and Dissertations, Fall  
2023 to Present

Graduate Studies

---

12-2023

## Understanding the Impact of Physicochemical Modifications on the Cold Gelling Behavior of Micellar Casein Concentrate Dispersions

Nathan Pougher

Utah State University, [nathan.pougher@usu.edu](mailto:nathan.pougher@usu.edu)

Follow this and additional works at: <https://digitalcommons.usu.edu/etd2023>



Part of the [Food Science Commons](#), and the [Nutrition Commons](#)

---

### Recommended Citation

Pougher, Nathan, "Understanding the Impact of Physicochemical Modifications on the Cold Gelling Behavior of Micellar Casein Concentrate Dispersions" (2023). *All Graduate Theses and Dissertations, Fall 2023 to Present*. 23.

<https://digitalcommons.usu.edu/etd2023/23>

This Thesis is brought to you for free and open access by the Graduate Studies at DigitalCommons@USU. It has been accepted for inclusion in All Graduate Theses and Dissertations, Fall 2023 to Present by an authorized administrator of DigitalCommons@USU. For more information, please contact [digitalcommons@usu.edu](mailto:digitalcommons@usu.edu).



UNDERSTANDING THE IMPACT OF PHYSICOCHEMICAL MODIFICATIONS ON  
THE COLD GELLING BEHAVIOR OF MICELLAR CASEIN CONCENTRATE  
DISPERSIONS

by

Nathan Pougher

A thesis submitted in partial fulfillment  
of the requirements for the degree

of

MASTER OF SCIENCE

in

Nutrition and Food Sciences

Approved

---

Prateek Sharma, Ph.D.  
Major Professor

---

Marie K. Walsh, Ph.D.  
Committee Member

---

Almut Vollmer, Ph.D.  
Committee Member

---

D. Richard Cutler, Ph.D.  
Vice Provost for Graduate  
Studies

UTAH STATE UNIVERSITY  
Logan, Utah

2023

Copyright © Nathan Pougher 2023

All Rights Reserved

Any materials in this thesis can be used by the Western Dairy Center, the BUILD Dairy program, and Prateek Sharma.

## ABSTRACT

### Understanding the Impact of Physicochemical Modifications on the Cold Gelling Properties of Micellar Casein Concentrate Dispersions

by

Nathan Pougher, Master of Science

Utah State University, 2023

Major Professor: Dr. Prateek Sharma

Department: Nutrition, Dietetics, and Food Sciences

Highly Concentrated-Micellar Casein Concentrate (HC-MCC) is a dairy ingredient comprised of 17-23% protein. Obtained via microfiltration and vacuum evaporation, it can form a gel in cold conditions without any physicochemical modifications. With consumer preferences moving away from polysaccharide-based stabilizers in dairy products, there is potential for the gelling properties of HC-MCC to be applied in industry. This study investigates the gelling properties of HC-MCC various states to better understand the mechanism behind cold gelation.

The first study examined combinations of physicochemical modifications (dilution, calcium chelation, pH adjustment) to optimize gel strength. The second study examined certain treatments in further detail, i.e., examining additional physical properties. Lastly, the third study examined the cold gelling ability of diluted MCC and kappa carrageenan gels. A three-stage multiwave rheological protocol was applied to HC-MCC samples to observe gel strength and the temperature of cold gelation alongside texture analysis, particle size, and zeta potential measurements to observe additional

characteristics in response to treatments. Ultrastructure analysis was conducted on selected treatments using transmission electron microscopy (TEM) to observe morphological changes in casein micellar structure.

We observed that pH adjustment resulted in an exponential increase in gel strength as pH increased from 6.2 to 6.8 ( $R^2=0.99$ ), along with significantly higher gelation temperatures. The addition of a calcium chelating salt (trisodium citrate, or TSC) significantly increased gel strength in most combinations of treatments ( $P<0.05$ ), with 25mM concentrations consistently yielding the strongest gels. Ultrastructure analysis of samples showed that alkalization to pH 6.8 and 7.0 increasingly disintegrated the micellar structure of casein and released individual fragments into the aqueous phase, which was observed alongside a significantly increased gel strength and gelation temperature. The use of TSC at 25mM partially disintegrated micelles, whereas 50mM resulted in the formation of large aggregates with a concomitant decrease in gel strength. Kappa carrageenan addition resulted in gelation temperatures similar to modified higher protein samples, but gel strength was lower. TEM micrographs depicted minimal interaction between kappa carrageenan and casein, creating a biphasic solution. Overall, the gelling properties of HC-MCC can be significantly improved in response to physicochemical modification with significant changes in protein structure taking place.

## PUBLIC ABSTRACT

### Understanding the Impact of Physicochemical Modifications on the Cold Gelling Properties of Micellar Casein Concentrate Dispersions

Nathan Pougher

When skim milk is filtered via microfiltration, the amount of casein (one of the major milk proteins) in solution can be concentrated. When casein content is high enough (>15%), the solution forms a gel at cold temperatures. With growing trends in the food industry towards simplistic ingredient labels, commonly used gums and stabilizers in the dairy industry are becoming less preferred. In the future, there is potential for the gelling properties of micellar casein to be applied to dairy products as a thickener or stabilizer, but the mechanism behind gel formation isn't understood well. In this study, the gel strength, gelation temperature, and structural changes of casein in response to modifications were studied to understand how they may affect gelation. These modifications included reductions in protein content (from 18.5 to 10%), pH adjustment (from 6.2 to 6.8), addition of a calcium chelating salt (sequesters calcium, a structural component of casein), and addition of a common dairy stabilizer: kappa carrageenan. Protein content was the main determinant of gel strength; reductions from the original protein content of 18.5% to less than 15% resulted in weaker gels that required lower temperatures to form a gel. We found that as the pH increased from 6.2 to 6.8, stronger

gels can be formed at a higher temperature. The addition of calcium chelating salts improved these qualities as well but increasing concentrations from moderate (25mM) to high (50mM) resulted in a reduction in gel strength. Microstructure analysis of gels via transmission electron microscopy revealed that with increasing pH, the micellar structure of casein was disintegrating, forming a dispersion of free casein fragments. Calcium chelation at moderate concentrations partially disintegrated the protein structure, but high concentrations led to the formation of large casein aggregates causing a reduction in gel strength. When kappa carrageenan was added, it allowed samples diluted to 10% protein to form a gel which was not previously possible. Kappa carrageenan had minimal interaction with casein, but it was responsible for a stronger gel. Overall, modifications of casein can increase the gel strength and temperature of gelation due to the structural changes in casein.

## ACKNOWLEDGMENTS

My family has been an incredible help for me getting through this project, not just my immediate family but extended as well. Having a support net in that regard proved to be invaluable, especially from my parents and my old grand-dad. My fellow lab mates in the dungeon were a massive help, especially Ashutos, who helped me not just with experiment advice, but also for just being a friendly face. Everyone in the lab has my thanks. Additional thanks to my professor Dr. Prateek Sharma, especially in the closing days of my program where we spent long hours toiling over data. Furthermore, I'd also like to thank Dr. Almut Vollmer for her assistance in not just conducting the TEM experiments but helping me interpret them as well.

Besides lab work, I'd like to thank the crew that I won multiple product development competitions with. Because of Chandler, Melissa, and Mackenzie, I had the opportunity to grow and have a deeper social life than what I thought graduate school could offer. Additional thanks to Dr. Marie Walsh, not just for being on my committee, but also for putting up with our extensive technical reports for competitions.

Lastly, my thanks go out to the BUILD Dairy program, Dairy West, and the Utah Agricultural Experiment Station. Without the funding and assistance from them, I would not be writing this.

P.S. Thanks for the food, Tara and Lamis



## CONTENTS

	Page
ABSTRACT.....	iii
PUBLIC ABSTRACT.....	v
LIST OF FIGURES .....	xiv
LIST OF TABLES .....	xii
LIST OF ABBREVIATIONS.....	xvii
Chapter 1: Introduction .....	1
Research Hypothesis .....	3
Objectives.....	3
Chapter 2: Literature Review.....	4
2.1: HC-MCC Manufacture .....	4
2.2: Casein Structure and Gel Formation .....	5
2.3: Effect of pH on Casein .....	7
2.4: Calcium Chelating Salts on the Casein Micelle .....	9
2.5: Carrageenan-Casein Interactions.....	10
2.6: Rheology of MCC dispersions .....	11
References .....	14
Chapter 3: Effect of Protein Concentration, Calcium Chelation, and pH Adjustment on the Cold Gelling Properties of Highly Concentrated-Micellar Casein Concentrate (HC- MCC) .....	19
Abstract .....	19
3.1: Introduction .....	20
3.2: Materials and Methods .....	23
3.2.1: HC-MCC Manufacture and Storage .....	23
3.2.1.1: HC-MCC Modifications .....	23

3.2.2: Simulated Milk Ultrafiltrate (SMUF) Preparation .....	24
3.2.3: Experimental Design .....	25
3.2.4: Rheological testing .....	25
3.2.5: Particle Size analysis and Zeta Potential measurements .....	27
3.2.6: Transmission Electron Microscopy (TEM) .....	28
3.2.7: Statistical Analysis .....	29
3.3: Results .....	29
3.3.1: Particle Size .....	29
3.3.2: Zeta Potential .....	34
3.3.3: Transmission Electron Microscopy .....	37
3.3.4: Rheology .....	39
3.4: Discussions .....	51
3.5: Conclusions .....	55
References .....	56
Chapter 4: Rheological and Ultrastructural Analysis of Modified Micellar Casein Cold Gels .....	60
Abstract .....	60
4.1: Introduction .....	61
4.2: Materials and Methods .....	64
4.2.1: Sample Preparation .....	64
4.2.1.1: HC-MCC Production .....	64
4.2.1.3: Sample modification .....	65
4.2.2: Rheological Testing .....	66
4.2.2.1: Sample loading .....	66
4.2.2.2: Rheological Protocol .....	66
4.2.2.3: Multiwave Measurements .....	67
4.2.4: Transmission Electron Microscopy .....	68
4.2.5: Gel Electrophoresis .....	69
4.2.6: Texture Analysis .....	69
4.2.7: Statistical Analysis .....	70

4.3: Results .....	70
4.3.1: pH Measurements Pre- and Post-Rheological testing .....	70
4.3.2: Rheological Testing .....	71
4.3.2.1: Effect of pH and Calcium Chelation on Cold Gel Formation .....	71
4.3.2.2: Gelation Measurements .....	76
4.3.2.3: Frequency Dependence .....	77
4.3.2.4: Effect of Holding on Gel Strength .....	81
4.3.3: Gel Electrophoresis .....	81
4.3.4: Texture Analysis .....	83
4.3.5: Transmission Electron Microscopy .....	85
4.4: Discussions .....	89
4.5: Conclusions .....	92
References .....	93
 Chapter 5: Effect of Kappa-Carrageenan Addition on Cold Gelling Behavior of Micellar Casein Dispersions .....	 98
Abstract .....	98
5.1: Introduction .....	99
5.2: Materials and Methods .....	101
5.2.1: Materials .....	101
5.2.1.1: HC-MCC Modifications .....	102
5.2.2: SMUF Preparation .....	103
5.2.3: Rheological testing .....	103
5.2.4: Texture Analysis .....	104
5.2.5: Transmission Electron Microscopy .....	105
5.2.6: Particle Size .....	106
5.2.7: Zeta Potential .....	106
5.2.8: Statistical Analysis .....	107
5.3: Results .....	107
5.3.1: Particle Size .....	107
5.3.2: Zeta Potential .....	110
5.3.3: Texture Analysis .....	110

5.3.4: Rheology.....	112
5.3.4.1: Effect of KC addition.....	112
5.3.4.2: Effect of Calcium Chelation and Alkalization.....	115
5.3.5: TEM Micrographs .....	117
5.4: Discussions.....	120
5.5: Conclusions .....	125
References .....	126
Chapter 6: Conclusion.....	129
APPENDIX.....	131

## LIST OF TABLES

	Page
Table 3-1: SMUF Reagent Concentrations .....	25
Table 3-2: Cold gelation temperature (CGT) values of HC-MCC with different protein and TSC content .....	48
Table 3-3: Storage Modulus Values of 18.5% protein HC-MCC with different pH and TSC content.....	49
Table 3-4: Storage Modulus Values of 15% protein HC-MCC with different pH and TSC content.....	50
Table 4-1: Gel Strength Measurements and CGT Values for HC-MCC treatments.....	73
Table 4-2: Tables for Frequency Dependence of HC-MCC Treatments at Different Temperatures.....	80
Table 4-3: Texture Analysis Results.....	84
Table 5-1: Comparison of Particle Size ( $d_{4,3}$ ) Against KC Content and Treatment.....	109
Table 5-2: Texture Analysis Results.....	112
Table 5-3: Comparison of storage modulus values between treatments and Temperatures for kappa carrageenan added MCC samples.....	114

Table 5-4: Gelation Temperatures of Modified MCC Dispersions.....	115
Table A-1: Confidence Intervals of 18.5% Protein Sample Gelation Temperatures.....	131
Table A-2: Confidence Intervals of 15% Protein Sample Gelation Temperatures.....	131

## LIST OF FIGURES

	Page
Figure 2-1: A proposed model of interaction from casein micelles with calcium ions forming a bridge between individual protein strands (adopted from Lu et al., 2015).....	7
Figure 3-1: Scheme of rheological testing protocol.....	26
Figure 3-2: Effect of temperature on casein micelle size.....	30
Figure 3-3: Particle size data of TSC and temperature levels during pH testing.....	32
Figure 3-4: Effect of pH and TSC on particle size.....	33
Figure 3-5: Zeta potential of unmodified HC-MCC while reducing from 60°C to 5°C...	34
Figure 3-6: Zeta potential in response to temperature and pH.....	36
Figure 3-7: TEM Micrographs of HC-MCC at different temperatures under 5,000 and 20,000x magnification.....	37
Figure 3-8: TEM Micrograph Showing Presence of Fragmented Casein Structures. The sample was harvested at 25°C, and the micrograph was taken at 20,000x magnification.....	39
Figure 3-9: Dynamic moduli of select pH levels during temperature sweep testing.....	41
Figure 3-10: Changes in dynamic moduli with respect to pH after holding MCC sample at 5°C for 10hrs.....	43

Figure 3-11: Changes in dynamic moduli with respect to TSC concentration.....	44
Figure 3-12: Effect of TSC addition on the storage modulus of 18.5% protein gels adjusted to different pH levels.....	45
Figure 3-13: The effect of TSC on storage modulus values of pH 6.8 samples at different protein concentrations.....	47
Figure 3-14: Storage modulus values of select treatments in response to temperature change fitted to an Arrhenius equation.....	53
Figure 4-1: A comparison of dynamic moduli ( $G'$ and $G''$ ) between the different treatments of HC-MCC and their effect on pH.....	72
Figure 4-2: Temperature sweep data for select treatments.....	75
Figure 4-3: Gelation curves of select treatments.....	77
Figure 4-4: Frequency dependency of selected treatments.....	79
Figure 4-5: Urea PAGE of modified HC-MCC supernatants.....	82
Figure 4-6: Compressional testing of pH adjusted gels.....	84
Figure 4-7: TEM micrographs of treatments at 20,000x and 2,000x magnification.....	88
Figure 4-8: Emulsification effect observed in 50mM TSC micrographs.....	89
Figure 5-1: Comparison of particle size distributions across KC concentrations.....	109
Figure 5-2: Compressional testing of KC-MCC gels.....	111



Figure 5-3: Temperature sweep data for 25mM TSC treatments.....	116
Figure 5-4: TEM micrographs of cold gels made from treated MCC samples (10% protein) at 2000x magnification.....	118
Figure 5-5: TEM micrographs of cold gels made from treated MCC samples (10% protein) at 20000x magnification .....	119
Figure 5-6: A comparison in gelation behavior between 18.5% protein HC-MCC and 10% protein samples with 0.3% KC.....	122
Figure 5-7: A comparison of frequency measurements at 20°C, 5°C, and 5°C after 10 hours between unmodified HC-MCC and a diluted sample with 0.3% kappa carrageenan added.....	123
Figure A-1: 95% Confidence Intervals of G' Values – 18.5% Protein and 0mM TSC....	132
Figure A-2: 95% Confidence Intervals of G' Values - 18.5% Protein and 10mM TSC....	133
Figure A-3: 95% Confidence Intervals of G' Values – 18.5% Protein and 25mM TSC...	134
Figure A-4: 95% Confidence Intervals of G' Values – 18.5% Protein and 50mM TSC...	135

## LIST OF ABBREVIATIONS

HC-MCC – Highly Concentrated-Micellar Casein Concentrate

MCC – Micellar Casein Concentrate

CCP – Colloidal Calcium Phosphate

MF – Microfiltration

GDL – Glucono-Delta Lactone

TSC – Trisodium Citrate

SMUF – Simulated Milk Ultrafiltrate

KC – Kappa Carrageenan

CGT – Cold Gelling Temperature

$G'$  – Storage Modulus

$G''$  – Loss Modulus

LT – Loss Tangent

TEM – Transmission Electron Microscopy

## CHAPTER 1

### INTRODUCTION

In addition to manufacturing consumer products such as fluid milk, ice cream and cheese, the dairy industry is known for producing large amounts of commodity products. Many of these commodity products are utilized as ingredients in other food products. For example, non-fat dry milk powder is a frequent addition to ice-cream to increase the dairy solids content, similarly, mozzarella cheese made by a dairy industry for another company to use in a pre-made frozen pizza. One such commodity product is micellar casein concentrate (MCC), which is casein-rich product (9-10% protein), concentrated by using a membrane processing technique known as microfiltration (MF) and produced in either a liquid or powder form. MCC has the potential to be used in the production of cheese to adjust the casein to fat ratio to increase the cheese yield and to produce a consistent quality product throughout the year (Lu et al., 2017). A downside of using liquid forms of MCC in cheese making is that it forms a gel at cold temperatures, which slows down cheese production, because in order to make cold MCC usable, it requires a heating step to bring it back to a liquid state prior to addition to the cheese milk (Lu et al., 2017). This effect is amplified due to a higher concentration of casein micelles during evaporation of regular MCC, resulting in Highly Concentrated-Micellar Casein Concentrate (HC-MCC). While cold gelling behavior of HC-MCC is considered

disadvantageous in the production of cheese and beverages, it could be seen as a positive attribute if used as a stabilizer/thickener in ice-cream and yogurt manufacture.

Many consumer dairy products, such as yogurt and ice cream, utilize polysaccharide-based gums derived from plants as a stabilizer. These gums prevent whey syneresis in the products, as well as increase consumer preference in categories such as texture, viscosity, and mouthfeel (Rafiq et al., 2020). With increasing awareness of clean label practices within the dairy industry, these gums and stabilizers are negatively perceived by conscious consumers (Maruyama et al., 2021). With growing reservations against these gums, potential utilization of HC-MCC to stabilize dairy products could yield a viable clean label alternative in high protein dairy products.

This research investigated the impact of physicochemical modifications of HC-MCC on the cold gelling properties of HC-MCC and focuses on finding optimum conditions to enhance these characteristics. Advanced rheological testing was conducted in order to observe the effects of these modifications on gelling behavior and overall physical properties. Additional testing such particle size, zeta potential and transmission electron microscopy (TEM) was conducted to determine the effects of these modifications at a microscopic scale. Results from this study will serve as a basis for additional research into HC-MCC and potential applications within the dairy industry.

## **Research Hypothesis**

Overall hypothesis: Physicochemical modifications of HC-MCC will affect gel strength and gelation temperature during cooling because of changes to protein-protein and protein-water interactions.

## **Objectives**

Study the effects of changes in protein content, pH, and the addition of calcium chelating salts on the cold gelling properties in HC-MCC.

Understand the impact of kappa carrageenan addition on the cold gelling behavior of micellar casein concentrate solutions.

Study the changes in protein structure in response to physicochemical modifications and how they relate to gelling properties.

## CHAPTER 2

### LITERATURE REVIEW

#### **2.1: HC-MCC Manufacture**

Highly Concentrated-Micellar Casein Concentrate (HC-MCC) is an emerging bovine dairy ingredient notable for its high casein content, ranging from 17-23% in solution. Casein is one of the major proteins found in milk which provides unique structure in various dairy products, such as cheese and yogurt. HC-MCC is produced through microfiltration (MF) of milk. The casein in its native micellar state is retained by the MF membrane (pore size 0.145  $\mu\text{m}$ ), resulting permeation of the whey proteins, lactose, minerals, and much of the moisture. MCC can also undergo a diafiltration step as well; these repeat filtration cycles result in a purified form of MCC retentate. The resulting MF retentate (or MCC) is then subjected to vacuum evaporation which reduces additional moisture content. The evaporation process can continue until the desired level of casein is reached. Traditional MCC powders are produced using drying methods such as spray drying, but liquid forms of HC-MCC require less energy input to meet final specifications. There are tradeoffs however, as the casein is in solution, there is additional weight to the product, and refrigeration is still required.

Liquid HC-MCC is unique compared to other sources of casein since it is retained in the native micellar state (Saboyainsta & Maubois, 2000). This offers a unique advantage in terms of functionality compared to many other dry sources of casein where solubility is

drastically reduced due to heat or acid induced irreversible changes in the protein structure. In addition, the use of MF in HC-MCC manufacturing results in relatively lower levels of whey (serum) proteins, which are sensitive to heat. The reduction in these proteins can lead to higher stability at elevated temperatures (Lu et al., 2015). Due to high levels of casein within the solution, a thermo-reversible gel is observed at lower temperatures. The gelling capability of this solution is dependent on the composition and physical properties of the HC-MCC produced.

## **2.2: Casein Structure and Gel Formation**

The four main casein proteins ( $\alpha$ S1,  $\alpha$ S2,  $\beta$ ,  $\kappa$ ) can form a micellar structure with diameters ranging from 100-200 nm that is colloidally dispersed within milk solution (McMahon & Brown, 1984). The most important protein that protects the structure of the micelle is kappa casein, which is found on the exterior of the micelle. Kappa casein forms many of the protruding hairlike structures (strands) on the micelle surface and acts as the hydrophilic exterior of the micelle as it interacts with the aqueous phase while also binding to the hydrophobic casein proteins on the inside of the micelle (Dalglish, 1998). Another notable component that holds the casein micellar structure intact is colloidal calcium phosphate (CCP). CCP is a calcium salt that tends to form nanoclusters within the micelle and helps binding two sub-micelles together (Broyard & Gaucheron, 2015). These clusters are the major source of stability for the inter-protein complex due to the crosslinking observed between calcium ions and phosphoserine residues in casein proteins. The structure of the micelle itself has an outer shell with a strong net negative charge. Casein micelles are unique compared to other known micelles such as detergents. The interior of

the casein micellar structure contains the hydrophobic portions of the micellar proteins. In addition, the structure contains considerable amounts (more than twice the weight of the protein molecule) of bound water (Huppertz et al., 2017). The hydrophobic interactions between proteins are the secondary source of stability within the micelle. However, protein cross-linking through CCP remains the strongest force that contributes towards stabilization of the micellar structure.

Casein micelles are best known for their ability to form a gel under specific conditions, particularly when acid or rennet is introduced to milk. In the case of HC-MCC however, cold gel formation is observed with casein in an unmodified state (Lu et al., 2015). When caseins are reduced in temperature, the energy within the system is reduced which leads to various conformational changes. As the temperature is lowered, CCP solubilizes into the aqueous phase; in return, water within the system begins to enter the micelles, causing swelling and an increase in particle size. As described by Dunn et al. (2021), gelation can be attributed to the increase in the voluminosity of casein micelles as the increase in particle size at native pH levels results in a vast reduction in space between the micelles. This is combined with reduced energy within the system from lowered temperatures (Dunn et al., 2021). When the micelles are in very close proximity to one another, the friction between particles is heightened, leading to the occurrence of gelation via the excessive packing of particles. Lu et al. (2015) described another situation in which this gelation behavior is amplified, that is via casein strands interlinking and forming a matrix (Lu et al., 2015). The role of calcium in this interaction is important as it can cause the linking of the casein strands with one another (Figure2-1). When added to HC-MCC,



this can enhance the cross-linking ability of casein micelles, resulting in stronger gels and higher gelling temperatures.

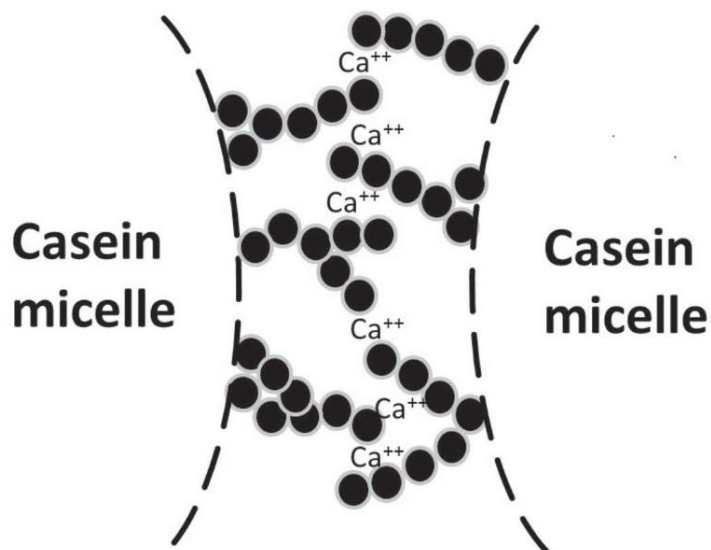


**Figure 2-2:** A proposed model of interaction from casein micelles with calcium ions forming a bridge between individual protein strands (adopted from Lu et al., 2015)

### 2.3: Effect of pH on Casein

Casein micelles have a net negative charge while in a milk solution. This charge remains on the micelle until the pH is reduced to the isoelectric point of 4.6. As the pH of the solution declines from the initial milk pH of 6.6, the negatively charged sites on the molecule begin to neutralize. When reaching the isoelectric point, casein proteins aggregate

and undergo a process known as acid coagulation. The reduction in pH to near the isoelectric point can result in increases in particle sizes, as well as in forming a matrix within the solution (Eshpari et al., 2016). Minor reductions in pH also have similar but less drastic effects on the micellar structure. As the pH declines within the solution, the negative charge on the kappa casein protein is reduced, the kappa casein layer partially collapses due to weakened submicelle interactions, which results in a reduction in steric hindrance between micelles (Li & Zhao, 2019). Prior to reaching the isoelectric point, this minor reduction in pH can result in the reduction of the casein micelle size (Sinaga et al., 2017). When considering this reduction in particle size with the packing effect described in Dunn et al. (2021), gel strength could potentially be reduced by lowering the pH from 6.6 to 6.0. As the casein micelle size is reduced, there is more space between micelles allowing for a weaker gel formation (Dunn et al., 2021).

As the pH declines, CCP solubilizes and exits the micelle into the serum phase; the inorganic phosphate ions are solubilized near a pH of 5.2 while the remaining calcium ions are fully solubilized at the isoelectric point of casein, which is at pH 4.6 (Li & Zhao, 2019). Collapse of kappa casein with concomitant solubilization of CCP results in the aggregation of micelles most typically found in many dairy foods, either through direct acidification or the use of lactic acid generating bacteria. Compared to cow's milk, HC-MCC has a much higher casein content; this would mean that the effect of acidification would have a stronger effect on physical properties compared to milk.

While the reduction in pH can result in coagulation and CCP solubilization, the increase in pH results in changes in physical properties as well. Adjusting the pH of casein within a solution higher than 6.6 yields an increase in particle size (Y. Liu & Guo, 2008).

The reason for this effect is the opposite of acidification: as the pH increases, the net charge on the casein micelle continues to grow more negative, increasing the repulsion effect within the micelle, promoting protein-water molecule interactions. This effect results in the micelle swelling until it fully dissociates, at a pH of around 8.5 (Sinaga et al., 2017). In addition, since CCP solubility in the aqueous phase decreases with increases in pH, there is an increase of CCP bound to the micellar structure. While this can increase the calcium content within the micelle, it can also reduce the hydrophobic interactions between proteins, which can contribute to micellar dissociation at elevated pH levels (Madadlou et al., 2009).

#### **2.4: Calcium Chelating Salts on the Casein Micelle**

The use of calcium chelating salts is a common practice in the dairy industry, particularly in products such as processed cheese. These salts encourage the sequestration of calcium from the casein micelles, resulting in the release of non-sedimentable casein fragments (Broyard & Gaucheron, 2015). When specific emulsifying salts, such as trisodium citrate (TSC) and disodium hydrogen phosphate ( $\text{Na}_2\text{HPO}_4$ ), are added to the casein solution, they function by chelating calcium molecules found in CCP. This sequestration of calcium from the micelle destabilizes the quaternary structure of the micelle and causes the dissociation of casein micelles (Culler et al., 2017). The excessive buildup of free caseins in the solution creates a situation where these proteins bind the remaining portions of micelles together, creating a stronger gel matrix.

When TSC is added to dairy products such as yogurt, there is a notable increase in gel strength (Ozcan-Yilsay et al., 2007). There appears to be an optimum concentration of

TSC to add to a sample though, with higher quantities reducing gel strength. One potential explanation is that while a lower concentration of TSC may cause the dissociation of caseins into the solution, a high enough concentration has the potential to chelate all CCP within the solution which could completely disrupt the micellar structure and yield a weaker yogurt gel (Ozcan-Yilsay et al., 2007). Since HC-MCC has a concentrated amount of casein micelles dispersed within the solution, it has a much higher calcium and overall ash content compared to regular milk (Lu et al., 2016). Because of this, HC-MCC solutions would likely require a higher amount of a given calcium chelating salt to result in higher gel strengths. The effect of high concentrations of TSC, or “over-salting” the product, is assumed to be similar. Introducing calcium chelating salts to milk solutions can also result in increases in pH levels, meaning that some of the effects of elevated pH may be observed when some of these salts are introduced to the solution. There is a lack of research observing the effect of calcium chelation compared to the effect of alkalization to a similar pH level.

## **2.5: Carrageenan-Casein Interactions**

Carrageenan is one of the most commonly used stabilizers in dairy products; especially since the three main forms ( $\kappa$ ,  $\iota$ , and  $\lambda$ ) offer different results for specific uses (Campbell & Hotchkiss, 2017).  $\kappa$  and  $\iota$  forms of carrageenan are best known for their ability to create a cold gel in the presence of proteins while the lambda form serves only as a thickener (Langendorff et al., 2000). The Kappa form of carrageenan facilitates cold gel formation with the sulfate group on each disaccharide portion of the chain: this sulfate group then bonds with the positively charged section of the  $\kappa$ -casein molecule, effectively

increasing the size of the casein micelle, and reducing the space between micelles. This effect can be observed with the employment of particle size analysis (Spagnuolo et al., 2005). In addition, temperature changes result in the conformational change of the polysaccharide chain as well: above temperatures of 50°C the chain exists in a coiled shape, but this conformation changes to a helix structure as the temperature is reduced (Bourriot et al., 1999). This newly formed helix shape also helps facilitate the gelation of solutions as well (Drohan et al., 1997). Spagnuolo et al. (2005) conducted an analysis of the carrageenan bound to micelles at 25°C, noting that the carrageenan was in a helix form.

As Pang et al. (2015) find, the addition of a 50:50 mixture of  $\kappa$  and  $\iota$  carrageenan in small quantities (0.02%) to an acid milk gel yields a gelation point at a higher temperature but a weaker overall gel. In higher concentrations (0.2%), the carrageenan inhibits the gelation of the milk. This is because of the aggregation of carrageenan on the casein molecules: this casein-carrageenan aggregate is inhibiting the normally present casein-casein aggregation that happens under acidic conditions, resulting in a decrease in storage modulus with increasing carrageenan content (Pang et al., 2015). While there has been sufficient rheological research on casein with respect to carrageenan and acidity, there has been minimal research conducted on the combination of calcium chelating salts and carrageenan to the casein dispersions.

## **2.6: Rheology of MCC dispersions**

HC-MCC is considered a viscoelastic material at low temperature, meaning that it exhibits both viscous (liquid) and elastic (solid) properties (Zad Bagher Seighalani et al., 2021). Rheological measurements on viscoelastic materials consist of measurements for

these two properties. The storage modulus, or  $G'$ , is the measurement of elastic properties (gel strength) in a sample. The loss modulus, or  $G''$ , is the measurement of viscous properties within a sample, meaning that it is an indicator of liquid-like properties within a measured sample. Calculating the ratio of  $G''$  to  $G'$  results in a measurement known as the loss tangent which indicates the relative proportion of viscous and elastic behavior of a material and the time dependence.

There have been multiple extensive rheological studies conducted on dairy products (Bouchoux et al., 2009; Keogh & O'kenney, 1998; Muliawan & Hatzikiriakos, 2007; Ozcan-Yilsay et al., 2007), but there are only few publications on the products like HC-MCC. In these studies, only preliminary measurements have been conducted. Lu et al. (2015) measured the temperature at which the crossover from viscoelastic liquid to viscoelastic solid takes place during cooling of HC-MCC. Using the crossover point, where the storage modulus becomes greater than the loss modulus, to determine the gelation temperature has a drawback as the sample often exhibits properties of a viscoelastic liquid after the point in question. Utilizing this method is a pseudo estimate of the gelling point because the crossover point is greatly dependent on the frequency applied during rheological testing as well as other factors such as the rate of sample cooling (Zad Bagher Seighalani et al., 2021). A method utilizing measurements at multiple frequencies (simultaneously) shows an improvement in determining a more accurate gelation temperature. Rather than measuring the crossover point, this method measures the loss tangent at multiple frequencies; the point where these loss tangents converge is considered the gelation point (Zad Bagher Seighalani et al., 2021). The former system fails to take into

consideration the measurement at different frequencies, while the ladder relies on these different frequencies to determine the gelation temperature.

## References

- Bouchoux, A., Debbou, B., Gésan-Guiziou, G., Famelart, M.-H., Doublier, J.-L., & Cabane, B. (2009). Rheology and phase behavior of dense casein micelle dispersions. *The Journal of Chemical Physics*, *131*(16), 165106.  
<https://doi.org/10.1063/1.3245956>
- Bourriot, S., Garnier, C., & Doublier, J.-L. (1999). Micellar-casein- $\kappa$ -carrageenan mixtures. I. Phase separation and ultrastructure. *Carbohydrate Polymers*, *40*(2), 145–157. [https://doi.org/10.1016/S0144-8617\(99\)00044-2](https://doi.org/10.1016/S0144-8617(99)00044-2)
- Broyard, C., & Gaucheron, F. (2015). Modifications of structures and functions of caseins: A scientific and technological challenge. *Dairy Science & Technology*, *95*(6), 831–862. <https://doi.org/10.1007/s13594-015-0220-y>
- Campbell, R., & Hotchkiss, S. (2017). Carrageenan Industry Market Overview. In A. Q. Hurtado, A. T. Critchley, & I. C. Neish (Eds.), *Tropical Seaweed Farming Trends, Problems and Opportunities: Focus on Kappaphycus and Eucheuma of Commerce* (pp. 193–205). Springer International Publishing.  
[https://doi.org/10.1007/978-3-319-63498-2\\_13](https://doi.org/10.1007/978-3-319-63498-2_13)
- Culler, M. D., Saricay, Y., & Harte, F. M. (2017). The effect of emulsifying salts on the turbidity of a diluted milk system with varying pH and protein concentration. *Journal of Dairy Science*, *100*(6), 4241–4252. <https://doi.org/10.3168/jds.2017-12549>
- Dagleish, D. G. (1998). Casein Micelles as Colloids: Surface Structures and Stabilities. *Journal of Dairy Science*, *81*(11), 3013–3018. [https://doi.org/10.3168/jds.S0022-0302\(98\)75865-5](https://doi.org/10.3168/jds.S0022-0302(98)75865-5)



- Drohan, D. D., Tziboula, A., McNulty, D., & Horne, D. S. (1997). Milk protein-carrageenan interactions. *Food Hydrocolloids*, *11*(1), 101–107.  
[https://doi.org/10.1016/S0268-005X\(97\)80016-1](https://doi.org/10.1016/S0268-005X(97)80016-1)
- Dunn, M., Barbano, D. M., & Drake, M. (2021). Viscosity changes and gel formation during storage of liquid micellar casein concentrates. *Journal of Dairy Science*, *104*(12), 12263–12273. <https://doi.org/10.3168/jds.2021-20658>
- Eshpari, H., Tong, P. S., & Corredig, M. (2016). Changes in particle size, calcium and phosphate solubilization, and microstructure of rehydrated milk protein concentrates, prepared from partially acidified milk. *Dairy Science & Technology*, *96*(3), 329–343. <https://doi.org/10.1007/s13594-015-0270-1>
- Huppertz, T., Gazi, I., Luyten, H., Nieuwenhuijse, H., Alting, A., & Schokker, E. (2017). Hydration of casein micelles and caseinates: Implications for casein micelle structure. *International Dairy Journal*, *74*, 1–11.  
<https://doi.org/10.1016/j.idairyj.2017.03.006>
- Keogh, M. k., & O’kennedy, B. t. (1998). Rheology of Stirred Yogurt as Affected by Added Milk Fat, Protein and Hydrocolloids. *Journal of Food Science*, *63*(1), 108–112. <https://doi.org/10.1111/j.1365-2621.1998.tb15687.x>
- Lamichhane, P., Sharma, P., Kennedy, D., Kelly, A. L., & Sheehan, J. J. (2019). Microstructure and fracture properties of semi-hard cheese: Differentiating the effects of primary proteolysis and calcium solubilization. *Food Research International*, *125*, 108525. <https://doi.org/10.1016/j.foodres.2019.108525>
- Langendorff, V., Cuvelier, G., Michon, C., Launay, B., Parker, A., & De kruif, C. G. (2000). Effects of carrageenan type on the behaviour of carrageenan/milk

- mixtures. *Food Hydrocolloids*, 14(4), 273–280. [https://doi.org/10.1016/S0268-005X\(99\)00064-8](https://doi.org/10.1016/S0268-005X(99)00064-8)
- Li, Q., & Zhao, Z. (2019). Acid and rennet-induced coagulation behavior of casein micelles with modified structure. *Food Chemistry*, 291, 231–238. <https://doi.org/10.1016/j.foodchem.2019.04.028>
- Liu, Y., & Guo, R. (2008). PH-dependent structures and properties of casein micelles. *Biophysical Chemistry*, 136(2), 67–73. <https://doi.org/10.1016/j.bpc.2008.03.012>
- Lu, Y., McMahon, D. J., Metzger, L. E., Kommineni, A., & Vollmer, A. H. (2015). Solubilization of rehydrated frozen highly concentrated micellar casein for use in liquid food applications. *Journal of Dairy Science*, 98(9), 5917–5930. <https://doi.org/10.3168/jds.2015-9482>
- Lu, Y., McMahon, D. J., & Vollmer, A. H. (2016). Investigating cold gelation properties of recombined highly concentrated micellar casein concentrate and cream for use in cheese making. *Journal of Dairy Science*, 99(7), 5132–5143. <https://doi.org/10.3168/jds.2015-10791>
- Lu, Y., McMahon, D. J., & Vollmer, A. H. (2017). Investigating rennet coagulation properties of recombined highly concentrated micellar casein concentrate and cream for use in cheese making. *Journal of Dairy Science*, 100(2), 892–900. <https://doi.org/10.3168/jds.2016-11648>
- Madadlou, A., Mousavi, M. E., Emam-Djomeh, Z., Sheehan, D., & Ehsani, M. (2009). Alkaline pH does not disrupt re-assembled casein micelles. *Food Chemistry*, 116(4), 929–932. <https://doi.org/10.1016/j.foodchem.2009.03.048>

Maruyama, S., Streletskaia, N. A., & Lim, J. (2021). Clean label: Why this ingredient but not that one? *Food Quality and Preference*, 87, 104062.

<https://doi.org/10.1016/j.foodqual.2020.104062>

McMahon, D. J., & Brown, R. J. (1984). Composition, Structure, and Integrity of Casein Micelles: A Review. *Journal of Dairy Science*, 67(3), 499–512.

[https://doi.org/10.3168/jds.S0022-0302\(84\)81332-6](https://doi.org/10.3168/jds.S0022-0302(84)81332-6)

Muliawan, E. B., & Hatzikiriakos, S. G. (2007). Rheology of mozzarella cheese.

*International Dairy Journal*, 17(9), 1063–1072.

<https://doi.org/10.1016/j.idairyj.2007.01.003>

Ozcan-Yilsay, T., Lee, W.-J., Horne, D., & Lucey, J. A. (2007). Effect of Trisodium Citrate on Rheological and Physical Properties and Microstructure of Yogurt.

*Journal of Dairy Science*, 90(4), 1644–1652. <https://doi.org/10.3168/jds.2006-538>

Pang, Z., Deeth, H., & Bansal, N. (2015). Effect of polysaccharides with different ionic charge on the rheological, microstructural and textural properties of acid milk gels. *Food Research International*, 72, 62–73.

<https://doi.org/10.1016/j.foodres.2015.02.009>

Rafiq, L., Zahoor, T., Sagheer, A., Khalid, N., Rahman, U. ur, & Liaqat, A. (2020).

Augmenting yogurt quality attributes through hydrocolloidal gums. *Asian-Australasian Journal of Animal Sciences*, 33(2), 323–331.

<https://doi.org/10.5713/ajas.18.0218>

Rosmaninho, R., Santos, O., Nylander, T., Paulsson, M., Beuf, M., Benezech, T.,

Yiantsios, S., Andritsos, N., Karabelas, A., Rizzo, G., Müller-Steinhagen, H., & Melo, L. F. (2007). Modified stainless steel surfaces targeted to reduce fouling –

- Evaluation of fouling by milk components. *Journal of Food Engineering*, 80(4), 1176–1187. <https://doi.org/10.1016/j.jfoodeng.2006.09.008>
- Saboyainsta, L. V., & Maubois, J.-L. (2000). Current developments of microfiltration technology in the dairy industry. *Le Lait*, 80(6), 541–553. <https://doi.org/10.1051/lait:2000144>
- Sinaga, H., Bansal, N., & Bhandari, B. (2017). Effects of milk pH alteration on casein micelle size and gelation properties of milk. *International Journal of Food Properties*, 20(1), 179–197. <https://doi.org/10.1080/10942912.2016.1152480>
- Spagnuolo, P. A., Dalgleish, D. G., Goff, H. D., & Morris, E. R. (2005). Kappa-carrageenan interactions in systems containing casein micelles and polysaccharide stabilizers. *Food Hydrocolloids*, 19(3), 371–377. <https://doi.org/10.1016/j.foodhyd.2004.10.003>
- Zad Bagher Seighalani, F., McMahon, D. J., & Sharma, P. (2021). Determination of critical gel-sol transition point of Highly Concentrated Micellar Casein Concentrate using multiple waveform rheological technique. *Food Hydrocolloids*, 120, 106886. <https://doi.org/10.1016/j.foodhyd.2021.106886>

## CHAPTER 3

### EFFECT OF PROTEIN CONCENTRATION, CALCIUM CHELATION, AND PH ADJUSTMENT ON THE COLD GELLING PROPERTIES OF HIGHLY CONCENTRATED-MICELLAR CASEIN CONCENTRATE (HC-MCC)

#### ABSTRACT

Highly Concentrated-Micellar Casein Concentrate (HC-MCC) is a dairy ingredient with a high casein content, ranging from 17-23%. Under cold temperatures ( $<10^{\circ}\text{C}$ ), it transforms from a liquid state to a viscoelastic solid state. However, the mechanism behind gelation is currently unknown. This chapter presents a body of work which helps to understand how the gelation of HC-MCC can be affected using physicochemical modifications such as changes in protein concentration, pH adjustment, and the addition of a calcium chelating salt. Viscoelastic properties such as storage modulus ( $G'$ ) and cold gelation temperature (CGT) were measured using a three-stage rheological protocol utilizing a multiwave technique. Additional metrics, such as particle size and zeta potential, were also analyzed in response to physicochemical modifications. In addition, transmission electron microscopy (TEM) was conducted on unmodified samples to understand the effect of temperature on cold gelation. Rheological results showed that the gel strength of cold gels was highly dependent upon protein concentration, with reduced protein samples being weaker than undiluted ones. Gel strength and CGT both increased in response to trisodium citrate (TSC) addition, but

there appeared to be a limit of TSC addition before a reduction in these qualities was observed. Reduction in pH from the native state of 6.6 resulted in a decrease in gel strength, gelation temperature, particle size and net charge. Alkalization of the sample however, increased strength, but the effect of calcium chelation in conjunction with higher pH improved gel qualities less than at native and acidic pH levels. Overall, this data can serve as a foundation for future research on HC-MCC to better understand what factors may lead to optimum gelling qualities for the product, leading to potential novel applications in the future.

### **3.1: Introduction**

Casein is one of two major proteins found in milk alongside whey proteins. Made of four subunits ( $\alpha$ S1,  $\alpha$ S2,  $\beta$ ,  $\kappa$ ), casein is known to form a micellar structure that is colloiddally dispersed within the aqueous phase of milk. As an important component of the micelle, colloidal calcium phosphate (CCP) functions as a structural base holding subunits together in the form of nanoclusters (Broyard & Gaucheron, 2015). Individual subunits of casein bind to the nanoclusters and enhance stability within the structure.

HC-MCC is produced via the microfiltration of skim milk. The size of the pores within the filter ( $0.145\mu\text{m}$ ) is large enough for whey proteins, minerals, lactose, and additional moisture to pass through, effectively concentrating casein into a retentate phase in the form of MCC. Further concentration via vacuum evaporation yields HC-MCC, with a protein content ranging from 17% to 23%. Compared to other common

dairy ingredients, such as milk protein concentrate or powdered MCC, HC-MCC is unique as it is still in a liquid state, meaning no changes to the micellar structure of casein took place during the drying process (Saboyainsta & Maubois, 2000).

Under physicochemical modifications such as acidification or rennet addition, casein micelles undergo significant structural changes that cause the irreversible gelation of milk. Unlike other dairy products such as cheese and yogurt, gel formation in HC-MCC is possible due to cooling while the casein is still in a native micellar conformation. Holding HC-MCC at low temperatures ( $<10^{\circ}\text{C}$ ) results in the formation of a thermoreversible cold gel (Lu et al., 2015). Multiple studies have examined the potential causes behind gelation. Authors from one of these studies propose a packing transition as the reason where the space between micelles is so small that steric hindrance was a likely driving force for the transition into a gel (Lu et al., 2015). Another potential cause for this effect could be the increase in micellar size in response to CCP migration from colloidal phase to the soluble phase, resulting in swelling of the casein micelle structure and further reduction in space between micelles (Dunn et al., 2021).

When casein micelles are in solution, they have a net negative charge. Changes in the pH of the solution can affect the stability of the micelle by changing the net charge of the structure, and this in turn may affect the strength of a cold gel. During acidification, the net negative charge on the micelle is neutralized due to the excess of  $\text{H}^{+}$  ions in solution until the isoelectric point (IP) is reached (Francis et al., 2019). At the IP, there are not enough negative charges remaining on the caseins to maintain their micellar stability, therefore an acid gelation, or precipitation occurs (Eshpari et al., 2016). In addition to this, CCP solubility increases with increasing acidity, further destabilizing the

micelle. A reverse effect is expected if pH is adjusted towards an alkaline solution. The negative charge on casein increases in response to increases in pH, which promotes protein-water interactions rather than hydrophobic interactions (Y. Liu & Guo, 2008). As the solubility of CCP decreases with increases in pH, there is also more available calcium for casein subunits to bind to each other (Madadlou et al., 2009)

In order to improve the heat stability of casein micelles, it is common practice in the dairy industry to use a calcium chelating salt such as tri-sodium citrate (TSC) which is able to sequester CCP within the micellar structure. TSC and other calcium chelating salts are often referred to as emulsifying salts in the processed cheese industry due to its ability to open the micellar structure of casein due to the removal of structural CCP, releasing individual casein fractions at higher concentrations. These free caseins can act as an emulsifier by interacting with fat globules within the system, effectively stabilizing fat in molten protein matrix (Culler et al., 2017; Deshwal et al., 2023). Some studies suggest that the addition of calcium chelating salts can result in an increase in the gel strength of yogurt, but higher concentrations can reduce strength (Ozcan-Yilsay et al., 2007). This outcome shows that while there is an improvement on casein strength using calcium chelating salts, there is a limit to the amount of increase possible while utilizing them.

While previous studies have proposed models of gelation, the formation of a cold gel is still not known. The aim of this study is to better understand the mechanism behind the cold gelation of HC-MCC and the factors impacting this phenomenon. In addition, gathering knowledge on the gelation properties of physicochemically modified samples will help us understand how HC-MCC will behave in response to different treatments.



This will help optimize the cold gelling properties of HC-MCC and potentially create a gel requiring lower protein content, reducing the quantity of material required to encourage a desired effect within a product.

## **3.2: Materials and Methods**

### **3.2.1: HC-MCC Manufacture and Storage**

HC-MCC used in the study was produced at South Dakota State University as described in Lu et al., (2015). The MF system consisted of a four-vessel continuous design utilizing polyvinylidene fluoride membranes with a combined surface area of 57.4m<sup>2</sup>. The subsequent vacuum evaporation of the MCC was conducted at 63°C at a pressure of -680mbar. The samples were held in large pails at -20°C. Frozen samples were thawed and melted into a liquid state in a water bath at 50°C. The liquid HC-MCC was thoroughly mixed and poured into screw-cap plastic containers in ~120g quantities. Spoilage of the samples due to potential microbial growth was prevented by the addition of a chemical preservative (0.05% wt/wt sodium azide). Samples were kept frozen at -20°C until ready for use. Sample cups were thawed in a water bath and stored at 4°C between tests. All tests were performed in triplicate.

#### **3.2.1.1: HC-MCC Modifications**

In this study, HC-MCC samples were treated in three ways: protein concentration was varied (18.5% and 15%), pH adjusted (6.2, 6.4, 6.6, 6.8), and TSC added (0, 10, 25,

50 mM). The HC-MCC used in the study had an original protein content of 18.5% and a pH of 6.6 at 60°C. Adjustment of protein content was performed with deionized water. Adjustment of pH was accomplished utilizing glucono-delta-lactone as an acid and sodium hydroxide (NaOH) as a base. For pH adjustment, samples were first homogenized using an overhead mixer for two minutes, followed by the addition of GDL/NaOH and further mixing for three minutes. The samples were then held at room temperature for two hours to allow for the additions to dissolve. The calcium chelating salt used in this study was food grade trisodium citrate dihydrate (TSC), sourced from Cargill (Eddyville, IA). TSC at 10mM, 25mM, and 50mM levels was added to the samples at 60°C with constant stirring using a glass rod immediately prior to loading into the rheometer. For some samples, additional heating for five seconds in a microwave was required to fully incorporate the salt.

### **3.2.2: Simulated Milk Ultrafiltrate (SMUF) Preparation**

SMUF was prepared using ingredients listed in Table 1 for diluting HC-MCC sample for particle size and zeta potential analysis. Reagent salts were measured and mixed in proportion to create SMUF in one-liter quantities. The salt solution was filtered using a vacuum flask and a Millipore 1.2µm filter (Bedford, MA). To prevent precipitation of phosphates in the completed buffer, the SMUF was stored in a refrigerator at 5°C in between uses.

**Table 3-1:** SMUF reagent concentrations

Reagent	Concentration (mM)
$\text{KH}_2\text{PO}_4$	11.61
$\text{K}_3 \text{ citrate}^* \cdot \text{H}_2\text{O}$	3.70
$\text{Na}_3 \text{ citrate}^* \cdot 2\text{H}_2\text{O}$	6.09
$\text{K}_2\text{SO}_4$	1.03
$\text{K}_2\text{CO}_3$	2.17
KCl	8.05
$\text{CaCl}_2 \cdot 2\text{H}_2\text{O}$	8.98
$\text{MgCl}_2 \cdot 6\text{H}_2\text{O}$	3.21
*Citrate= $\text{C}_6\text{H}_8\text{O}_3^-$	Table adopted from (Rosmaninho et al., 2007)

### 3.2.3: Experimental Design

Factorial design was used for this study, with two protein concentration levels, four pH levels, and four TSC concentration levels for each pH level. In addition, unmodified MCC (18.5% protein, pH 6.6, and 0mM TSC) acted as a control sample. Each sample was tested in triplicate.

### 3.2.4: Rheological testing

Rheological measurements were performed using an Anton Paar MCR 302 rheometer (Anton Paar GMBH, Graz, Austria) using a concentric cylinder geometry setup (model no. CC27). For sample loading, 20ml of sample was heated to 60°C and poured into the bottom of the sample cylinder. An oil layer was added on the top via a pipette to prevent dehydration during the rheological protocol. Rheological testing was conducted in three stages (Figure 3-1). In the first stage a time sweep was conducted by

holding the sample at 60°C for one hour taking measurements every 30 seconds for a total of 120 data points. The second stage was a temperature sweep where the temperature was decreased from 60°C to 5°C over the course of 56 minutes, taking a measurement every 41.25 seconds for a total of 81 data points. Lastly, the third stage held the sample at 5°C for at least ten hours, making measurements every minute. Rheological testing was conducted by applying simultaneously multiple angular frequencies (3, 6, 12, 24, and 48 rad/s), and the gelation point was determined by using the criteria described in Zad Bagher Seighalani et al., (2021). Here, the gelation point was defined as the point where the loss tangent of the sample is independent of frequencies applied (Winter & Chambon, 1986). Storage modulus ( $G'$ ) values obtained during the temperature sweep at 20°C, 8°C, and 5°C at the end of the temperature sweep, and holding 5°C for ten hours during the time sweep was used to compare the gel strength between different treatments.

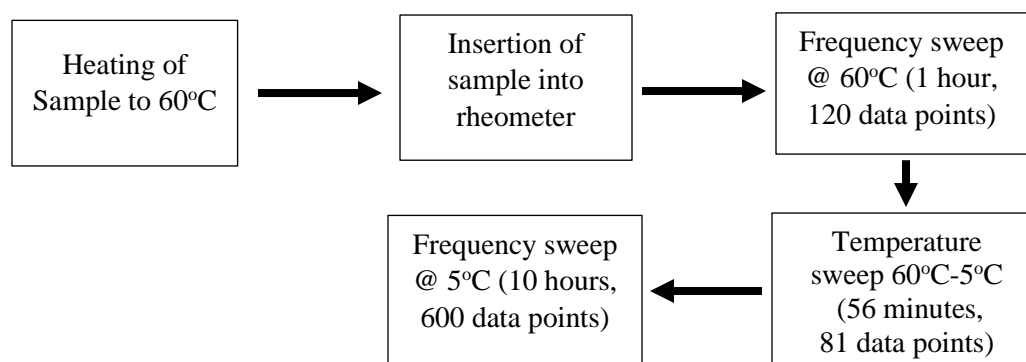


**Figure 3-1:** Scheme of rheological testing protocol

### 3.2.5: Particle Size Analysis and Zeta Potential Measurements

Tests examining casein particle size and zeta potential was measured in Sarstedt disposable cuvettes (Nümbrecht, Germany) using an Anton Paar Litesizer 500 (Anton Paar GMBH, Graz, Austria). Changes in the particle size of unmodified HC-MCC during cooling were measured using a temperature series set up; with readings taken starting from 60°C every 5 degrees until 5°C is reached. HC-MCC was diluted by 1000x in simulated milk ultrafiltrate (SMUF) buffer. Zeta potential measurements on unmodified HC-MCC were conducted in the same manner utilizing a model no. 225288 zeta potential cuvette (Anton Paar GMBH, Graz, Austria). All zeta potential readings were recorded at 18V with a maximum of 300 measurements for each reading. Zeta potential data was analyzed using Smoluchowski approximation in the Kalliope software version 2.26.3 (Anton Paar, Graz, Austria).

Testing with respect to pH adjustment were conducted using a Metrohm AG model 867 pH module as a dosing system with model 800 Dosinos (Herisau, Switzerland) in conjunction with the particle size analyzer utilizing the same Anton Paar model no. 225288 zeta potential cuvette (Graz, Austria). For testing, 25ml of HC-MCC in SMUF solution was poured into the dosing system mixing cup, which is connected to the zeta potential cuvette. The mixing cup was also connected to solutions of 0.1M HCL and NaOH solutions controlled by testing software. Acid or base solutions were added to the solution within the mixing cup via the Dosinos to adjust the pH to a desired level, followed by a fraction of the sample solution being transferred to the cuvette for testing. The dosing system was used to adjust the pH of the sample in a range from 6.6 to 5.8, taking a reading of both particle size and zeta potential every  $0.1 \pm 0.02$  pH change. These

measurements were conducted at three temperatures: 5°C, 20°C, and 45°C. Samples with 10, 25, and 50mM TSC were prepared prior to testing and diluted into SMUF 1000x where it will undergo the same pH range testing.

### **3.2.6: Transmission Electron Microscopy (TEM)**

Ultrastructure analysis of HC-MCC mixtures was performed using the TEM method described by (Lu et al., 2015). Samples underwent rheological testing using the sample loading and testing method described above. Testing occurred within the rheometer but stopped at certain points (25°C, 11°C, 5°C at the end of the temperature sweep) to observe the effect of temperature on the micellar structure. After testing was complete, the CC27 geometry was removed from the rheometer. The bottom of the geometry was removed to reveal the sample which was used for TEM analysis. Samples were fixed using 2% glutaraldehyde and formaldehyde for at least two hours. Samples were then rinsed in a sodium cacodylate buffer and postfixes in 2% osmium tetroxide solution for 1 hour, followed by rinsing with distilled water in two 10-minute stints. After dehydration of the samples via a progressive ethanol series (20 min each in 50%, 70%, twice in 95%, and three times in 100% EtOH) samples were transitioned into plastic resin and infiltrated with a resin-acetone mix. Infiltration with pure resin followed, and polymerization of sample blocks occurred overnight at 65°C. Sections (70-100nm) were cut on a Leica EM UC6 ultramicrotome (Leica Microsystems Inc., Buffalo Grove, IL) using a diamond knife (Diatome, Hatfield, PA). Sections were double stained for 20 minutes with saturated aqueous uranyl acetate followed by 10 minutes with Reynold's lead citrate. Sections were then analyzed using a transmission electron microscope (TEM,

JEM 1400 Plus, Jeol USA Inc., Peabody, MA) operated at 120kV, and digital images were captured using a Gatan camera (Gatan Inc., Pleasanton, CA).

### **3.2.7: Statistical Analysis**

Data points from rheological tests were compared using a GLM model in SAS to compare the effects of modifications. Differences were evaluated using ANOVA and Tukey's HSD adjustment with  $P \leq 0.05$  considered statistically significant. Statistical comparisons against pH levels were accomplished via 95% confidence intervals.

## **3.3: Results and Discussion**

### **3.3.1: Particle Size**

HC-MCC at an unmodified pH of 6.6 (at 60°C) diluted 1000x into a SMUF buffer exhibited a nonsignificant ( $P > 0.05$ ) but general increase in particle size from 165nm to 209nm in response to lowering temperatures from 60°C to 5°C (Figure 3-2). This phenomenon can be attributed to the fact that micellar structures gain additional hydration in cold temperatures due to the release of CCP into solution (Broyard & Gaucheron, 2015).

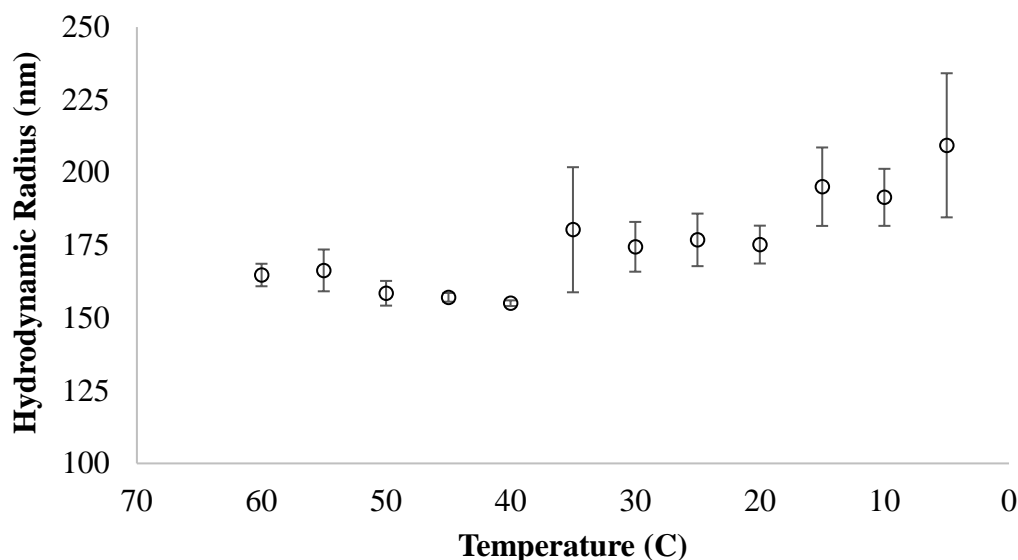


**Figure 3-2:** Effect of temperature on casein micelle size. Sample used was unmodified HC-MCC at natural pH, diluted with SMUF. Each data point represents mean of triplicate measurements and error bars indicates standard error of mean.

Decreasing pH from 6.6 to 5.8 led to a consistent, linear decrease in the particle size of MCC at all three TSC treatment levels (10, 25, and 50mM) (Figure 3-3). Higher pH is usually associated with larger size of the casein micelle due to increased negative charge and therefore, increased hydration. Conversely, acidification (decline in pH), leads to a decline in net negative charge on the casein micelles, causing increased protein and protein interaction which results in a tighter micellar structure, reduction in particle size (Figure 3-4) and expulsion of the aqueous phase (Sinaga et al., 2017). The reducing effect of pH on particle size was more pronounced for samples added with 25mM TSC. Samples added with 25mM TSC exhibited higher values of hydrodynamic diameter



(315nm to 254nm) followed samples added with 50mM (234nm to 208nm) and 10 mM (199nm to 168nm). The effect of TSC on particle size indicated that calcium chelation may cause changes in the micellar structure, such as swelling (de Kort et al., 2011).

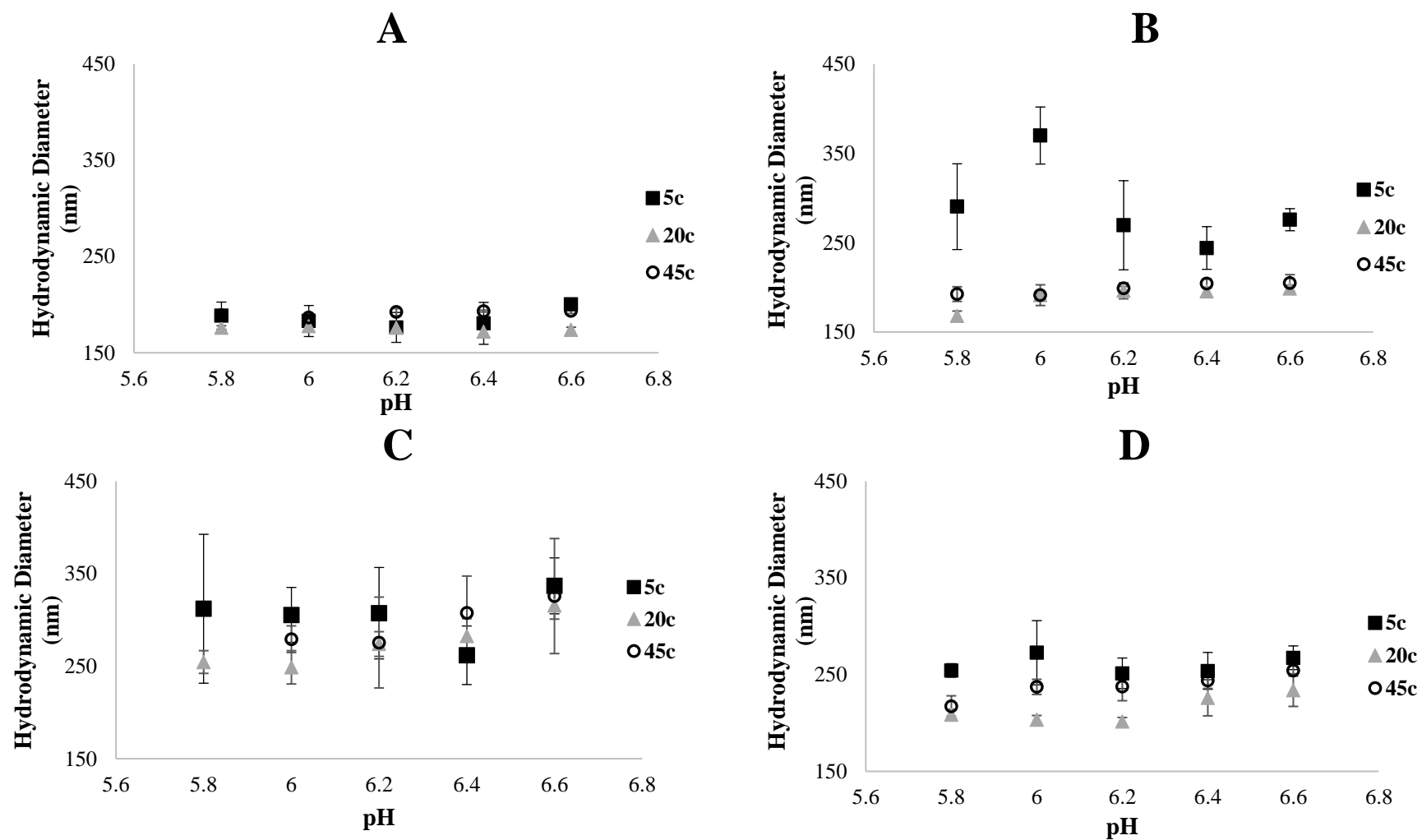


**Figure 3-3:** Particle size data of TSC and temperature levels during pH testing. A: Unmodified, B: 10mM TSC, C: 25mM TSC, D: 50mM TSC

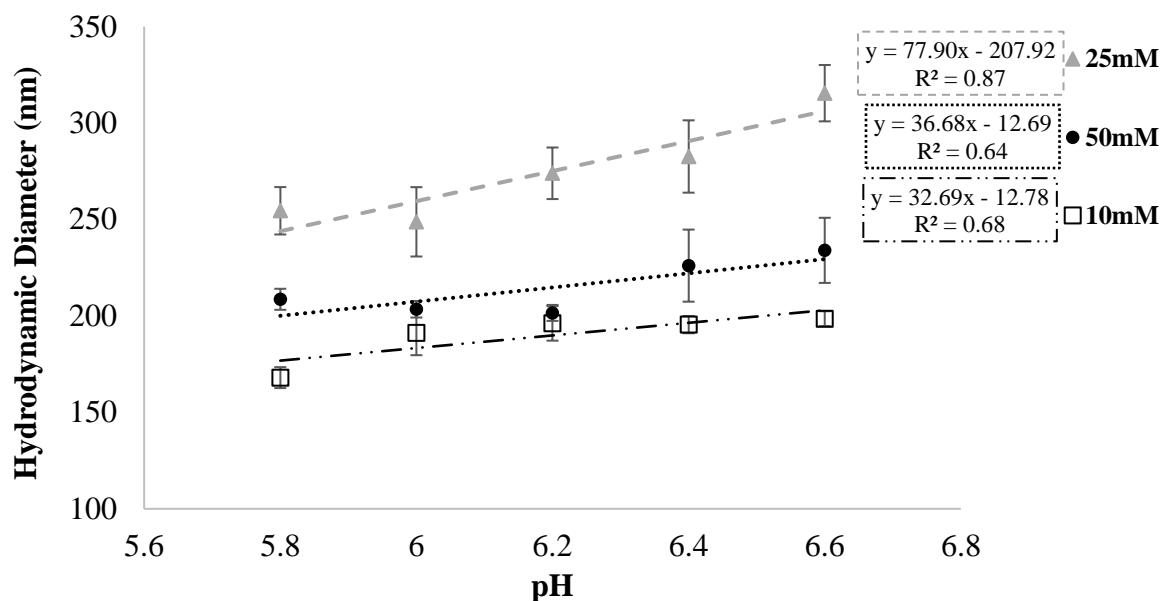


**Figure 3-4:** Effect of pH and TSC on particle size. Average Particle sizes during pH sweep testing at 3 different concentrations of TSC. All samples were tested at 20°C.

At higher temperatures (20 and 45°C), the effect of pH on particle size of HC-MCC was not as pronounced compared to samples at 5°C (Figure 3-3). Samples kept at 5°C exhibited a slight trend but not very consistently. At pH 6.0 and 5°C, HC-MCC samples (10mM and 50mM TSC content) exhibited the smallest particle size; these variations could be attributed to combined effect of calcium chelation and pH decline. We are unsure of the exact mechanism causing this phenomenon, but the water binding capacity of calcium phosphate within the micelle could be a potential reason.

### 3.3.2: Zeta Potential

Cooling unmodified HC-MCC (pH 6.6) from 60°C to 5°C changed the zeta potential from -16.8mV to -19.7mV (Figure 3-5), indicating that even at low temperature there was still sufficient repulsion between micelles. Decreasing pH 6.6 to 5.8 reduced the net negative charge on the casein micelles, linearly, from -13.2mV to -7.2mV for samples treated with 10mM TSC (Figure 3-6). Figure 3-6 displays the linear relationship of the zeta potential change that occurs irrespective of temperature or TSC concentration of the sample. This effect has been described in previous studies; as casein approaches its isoelectric point of 4.6, the charge on the proteins molecules become neutralized due to increased H<sup>+</sup> ions (Anema & Klostermeyer, 1996). The gradual movement towards 0mV as the pH moves in the direction of the IP in this test is further evidence of this phenomenon.

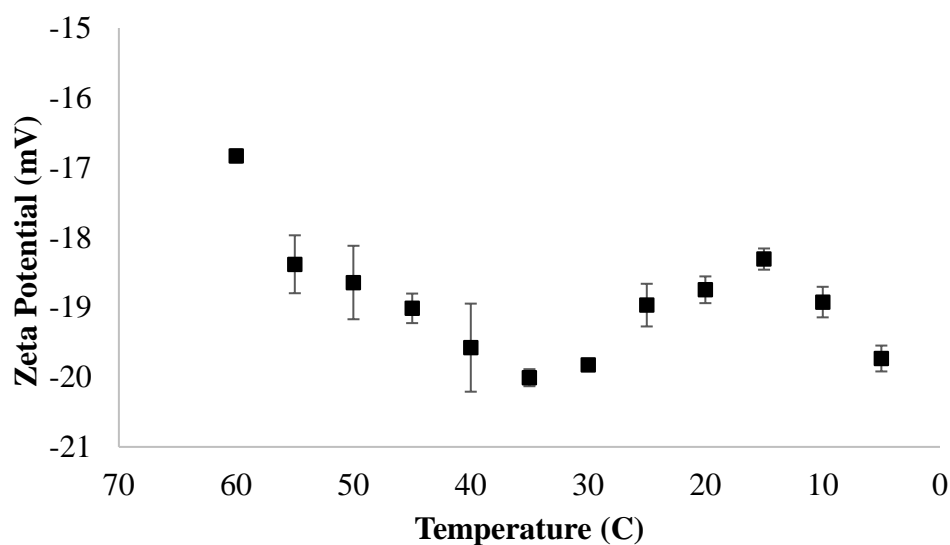


**Figure 3-5:** Zeta potential of unmodified HC-MCC while reducing from 60°C to 5°C.

29           A similar but less intense trend was observed at 50mM TSC level (Figure 3-6).  
30   These results also indicate that more calcium chelation led to more retention of net  
31   negative charge on the casein micelle, suggesting that structural integrity is inversely  
32   linked to robustness against pH change. Addition of TSC to a milk system may lead to an  
33   increase in pH because of its buffering effect and/or calcium chelation. The impact of  
34   these two processes on zeta potential may be contradictory, which may lead to  
35   inconsistent trends across different pH and TSC levels. However, it was evident that the  
36   effect of pH decline on reduction of net negative charge was less pronounced with  
37   increasing amounts of TSC regardless of temperature. Interestingly, unmodified MCC  
38   demonstrated a higher buffering tendency and a greater charge than TSC added samples  
39   at the selected temperatures, which could be attributed to the fact that in native state,  
40   more CCP was attached with proteins. Greater amounts of CCP bound to protein help  
41   exhibit a stronger buffering effect and retention of charge. However, addition of TSC  
42   would cause chelation of calcium i.e., mobilizing calcium from the colloidal phase to  
43   soluble phase. With calcium mobility, some of the phosphate groups may be released into  
44   the aqueous phase, causing a decrease of the net charge on the micelles (Horne, 2017).  
45   With increasing TSC concentration, this phenomenon may be reversing, therefore,  
46   increasing net negative charge at a given pH (Figure 3-6).

47

48

49

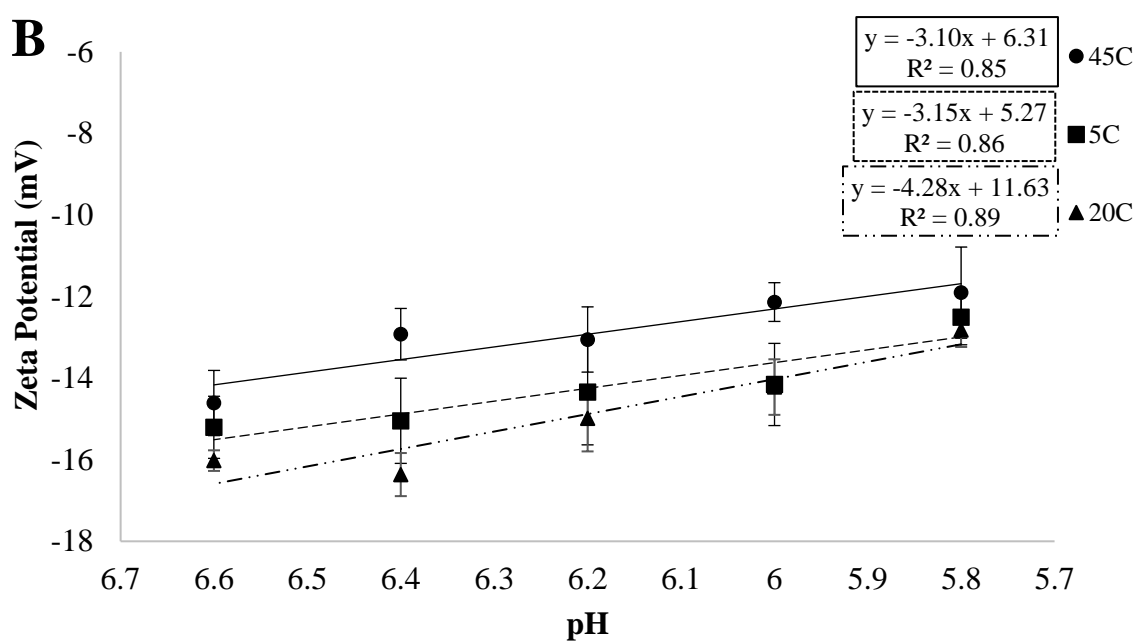
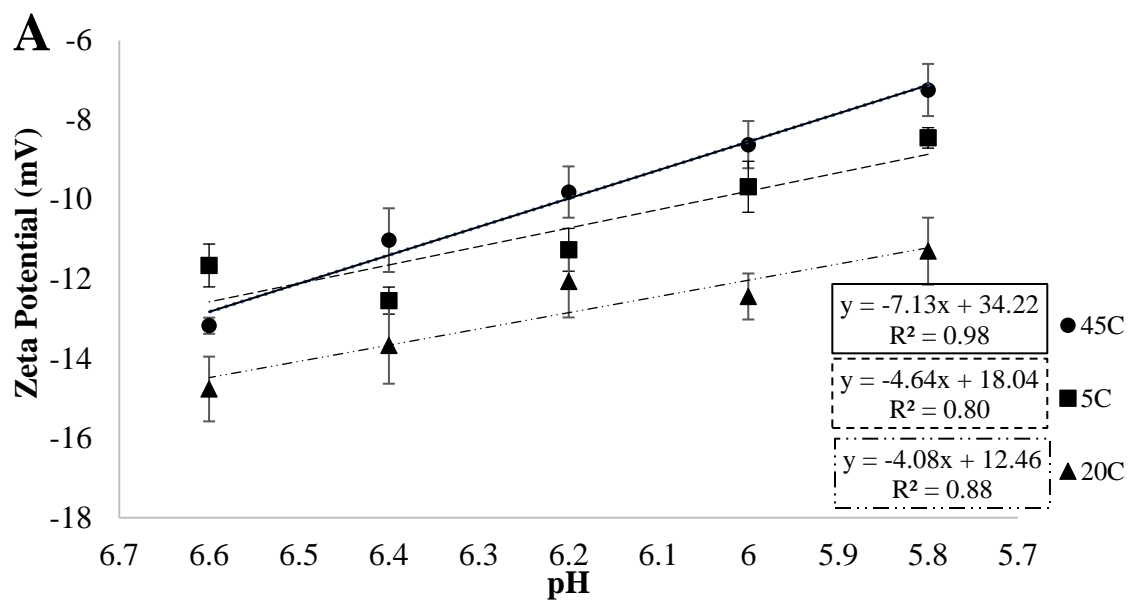


**Figure 3-6:** Zeta potential in response to temperature and pH. A: 10mM TSC added,  
B: 50mM TSC added.

### 56 3.3.3: Transmission Electron Microscopy

57 TEM micrographs of unmodified HC-MCC samples harvested at the three  
58 temperatures i.e., above (25°C), at (11°C) and below the gelling point (5°C) exhibit clear  
59 differences in micellar structure, particularly at higher magnification level (20,000x)  
60 (Figure 3-7). Based upon visual observations, it was apparent that the concentration of  
61 dense particles (casein micelles) and their distribution was similar at all three  
62 temperatures. At temperatures above gelation (25°C), the overall shape of casein micelles  
63 appears to be more irregular and distorted, indicating a structural change in response to  
64 higher temperatures (Figure 3-7). Additionally, at elevated temperatures, there is  
65 evidence of free casein fragments forming less dense pockets within solution rather than  
66 maintaining a micellar structure (Figure 3-8). This could be related to several factors,  
67 such as the shear forces acting during microfiltration of skim milk to produce HC-MCC  
68 (Gebhardt et al., 2012) or phase separation arising from higher hydrophobic interaction at  
69 elevated temperatures (Lucey & Horne, 2018) or simply the fluid-like nature of the  
70 material at 25°C (Zad Bagher Seighalani et al., 2021). The casein micelles from samples  
71 harvested at the gel-sol transition point at 11°C had a spherical, round shape and defined  
72 boundary structures. In addition, they appeared to be swollen and more densely packed  
73 and possibly interactive with water compared to the higher temperature samples. Below  
74 the gelation temperature (5°C), this phenomenon was more prevalent, giving the  
75 impression of the typical cold gel structure observed by others (Lu et al., 2015).

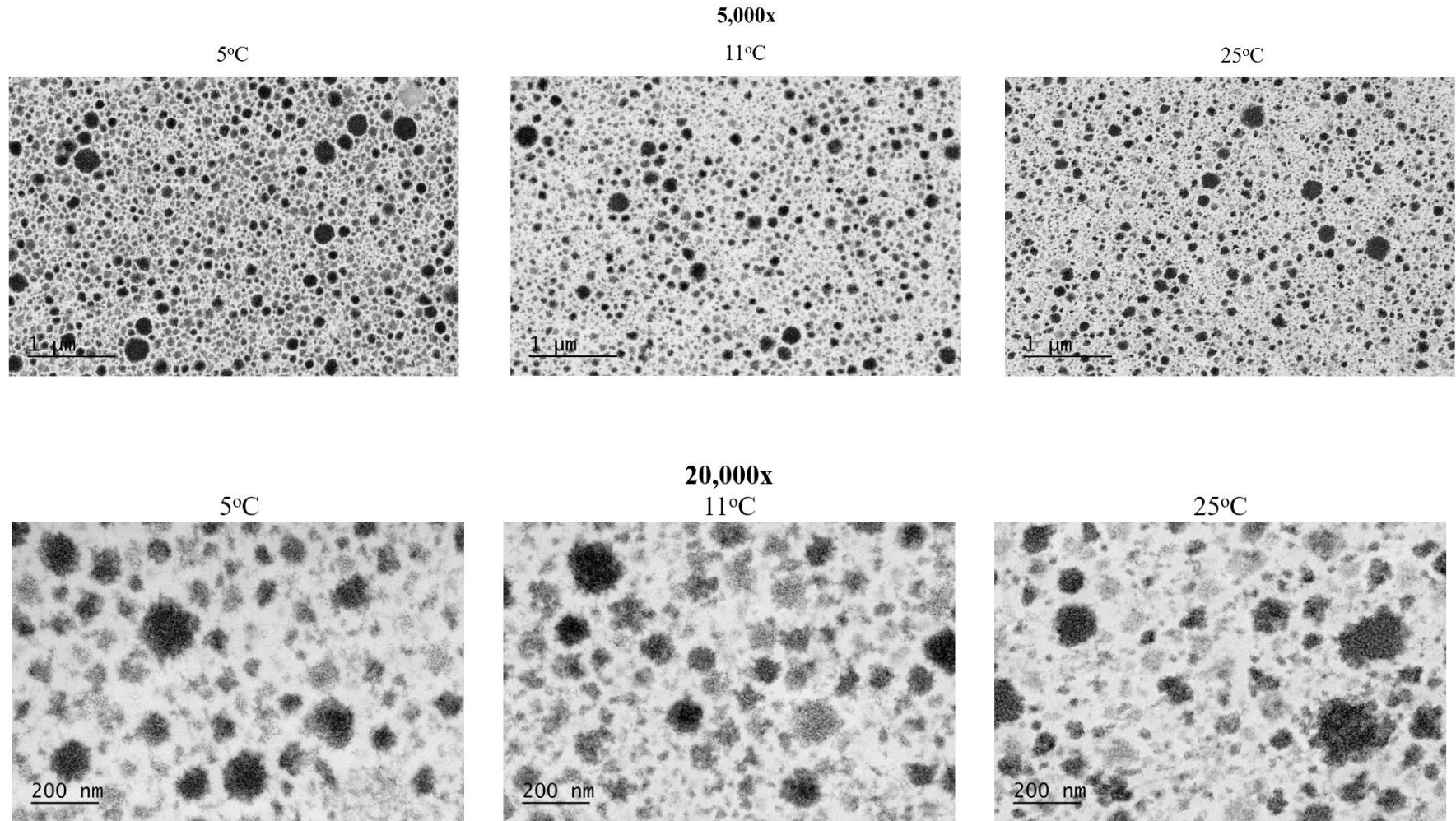
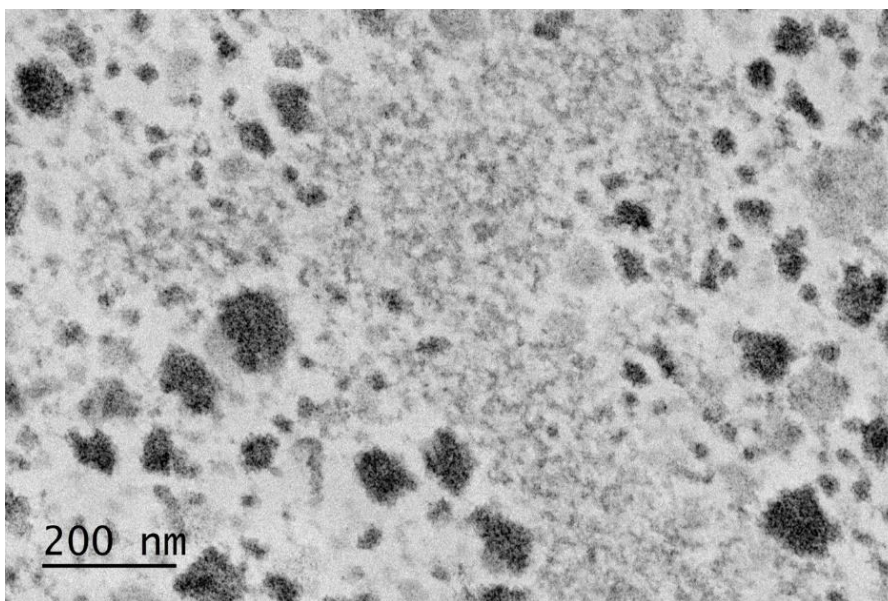


**Figure 3-7:** TEM micrographs of HC-MCC at different temperatures at 5,000x and 20,000x instrumental magnification. Casein micelles can be seen as electron-dense (dark), more or less spherical structures.





81

82 **Figure 3-8:** TEM Micrograph Showing Presence of Fragmented Casein Structures. The  
 83 sample was harvested at 25°C, and the micrograph was taken at 20,000x magnification.

84

85

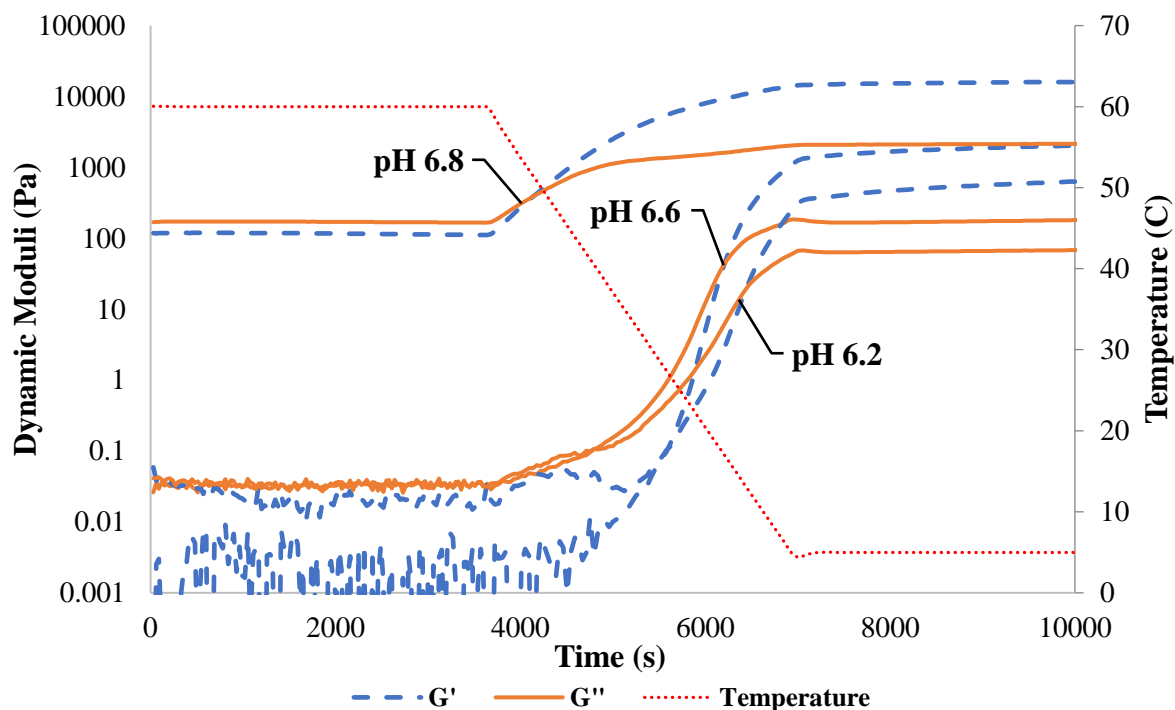
### 86 **3.3.4: Rheology**

87 Figure 3-9 represents the dynamic moduli ( $G'$  and  $G''$ ) of HC-MCC at different  
 88 pH levels (6.2, 6.6, 6.8) while holding at 60°C, cooling to 5°C to form a cold and curing  
 89 of the gel at 5°C. At 60°C, all the samples behaved as a viscoelastic liquid ( $G' < G''$ ). At a  
 90 higher pH, both  $G'$  and  $G''$  had higher values, indicating that the pH had a large effect on  
 91 the viscoelastic characteristics of the material. This could be attributed to the fact that at  
 92 higher pH, casein micelles have a greater net negative charge and particle size (Figure 3-  
 93 6, Figure 3-4). During cooling, the material went through a phase transition from liquid  
 94 like ( $G' < G''$ ) to a solid like ( $G' > G''$ ) material state, exhibiting a cross over point for  $G'$   
 95 and  $G''$ . The strengthening of HC-MCC network during cooling was attributed to the

96 morphological changes in the micellar casein concentrate electrostatic charge and  
97 swelling (Table 3-3). With an increase in pH, the cross over point between dynamic  
98 moduli ( $G'$  and  $G''$ ) was occurring at a higher temperature during the temperature sweep  
99 stage of testing (Figure 3-9). This could also be related to an increase in micellar  
100 hydration and swelling of the structure at a higher pH. True cold gelling temperature  
101 (CGT) as determined using the protocol described by Zad Bagher Seighalani et al.,  
102 (2021) also indicated a similar pattern (at pH 6.2, CGT 7.80°C; pH 6.8, CGT 26.99°C)  
103 (Table 3-2). Protein concentration had an impact on the CGT (Table 3-2). Samples  
104 diluted to 15% casein content formed cold gels at a lower temperature compared to  
105 samples with 18.5% protein. A similar effect was observed with  $G'$  values, with 15%  
106 protein samples forming weaker gels. (Table 3-3, Table 3-4). The effect of protein  
107 content was significant ( $P < 0.05$ ) on the  $G'$  values of the MCC during cooling from 60°C  
108 to 5°C and holding at 5°C (Table 3-3, Table 3-4). At natural pH (6.6), diluting protein  
109 content from 18.5% to 15% decreased  $G'$  at 20°C by ~4 fold (from 6.95Pa to 1.69Pa).

110

111



112

113 **Figure 3-9:** Dynamic moduli of select pH levels during temperature sweep testing. Black  
 114 arrows designate pH level and crossover point of  $G'$  and  $G''$ . The testing was conducted  
 115 using 1% amplitude strain and 1rad/s frequency.

116

117

118 At the end of the temperature sweep, the strength of the cold gels increased by  
 119 approximately an order of magnitude from pH 6.2 ( $G'=261$  Pa) to 6.6 ( $G'=901$  Pa) to 6.8  
 120 ( $G'=12100$  Pa) (Table 3-3). The reinforcement of the gel structure due to pH  
 121 modifications could be attributed to the increase in net charge and changes in the  
 122 dynamics of CCP mobility from colloidal phase to soluble phase (Gonzalez-Jordan et al.,  
 123 2015). Holding cold gels at 5°C for 10h further increased the gel strength. The majority  
 124 of increases in dynamic moduli appeared to take place within the first 2 hours of holding,

125 with minimal increases after. The highest ( $P < 0.05$ ) relative increase was for pH 6.2 (from  
126 261Pa to 1490Pa), and smallest ( $P > 0.05$ ) relative increase was for pH 6.8 (from 12100Pa  
127 to 15800Pa) (Table 3-3). Samples at pH 6.8 appear to maintain a high gel strength even at  
128 elevated temperatures such as 20°C (Table 3-3). We attribute these differences to the fact  
129 that soluble calcium levels vary based on pH values and there is a limit of volume  
130 fraction casein micelles can take up in the given circumstances due to the high  
131 concentration of protein in solution (Lu et al., 2015). The relationship between pH and  
132 the dynamic moduli ( $G'$  and  $G''$ ) of the cold gels held at 5°C for 10 hours followed an  
133 exponential equation, indicating a slow increase in the moduli at low pH values, followed  
134 steeper increase at higher pH levels (Figure 3-10).

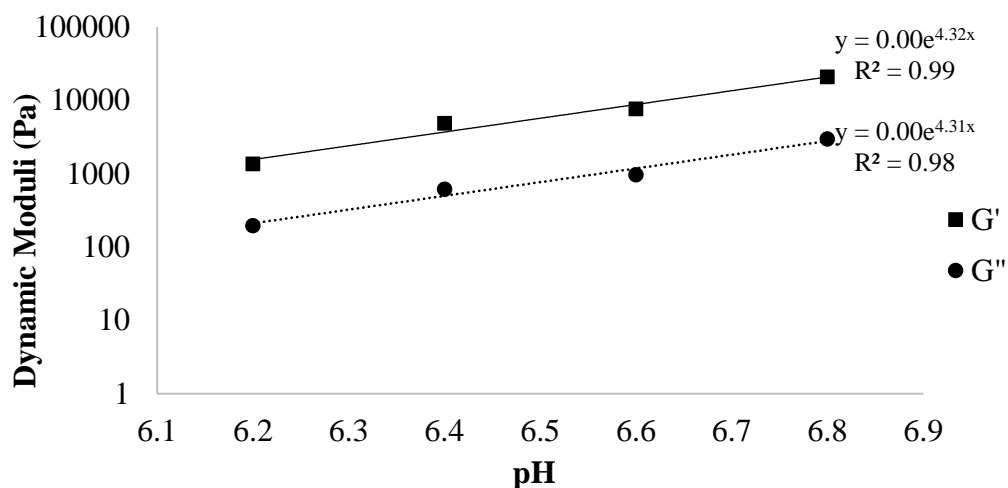
135

136

137

138

139



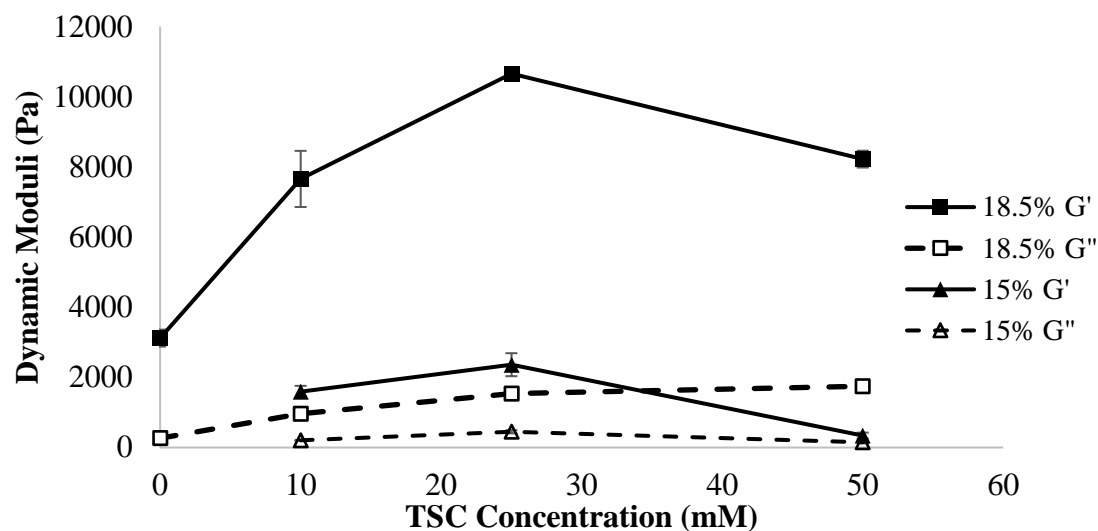
140

141 **Figure 3-10:** Changes in dynamic moduli with respect to pH after holding MCC sample  
 142 at 5°C for 10 hrs. Average modulus values of HC-MCC with respect to pH adjustment.  
 143 The samples used in the following tests were 18.5% protein and had 10mM of TSC  
 144 added.

145

146

147 The impact of TSC addition on the viscoelastic properties of final cold gels (after  
 148 holding at 5°C for 10hrs) prepared at both protein content levels can be seen in Figure 3-  
 149 11. It was clearly evident that diluting the protein content from 18.5% to 15% decreased  
 150 G' values by 4-fold at all TSC levels. Addition of TSC caused an increase in gel strength  
 151 at all levels (Figure 3-11) and at all pH treatments (Table 3-3). However, the maximum  
 152 increase in gel strength was observed at 25mM for both protein levels (Figure 3-11). This  
 153 was due to calcium chelation activity of TSC, possibly causing changes in the micellar  
 154 structure (Kaliappan & Lucey, 2011). On the other hand, excessive amounts of TSC (e.g.,  
 155 50mM), led to a decline in gel strength and CGT (Figure 3-11, Table 3-2, and Table 3-3).



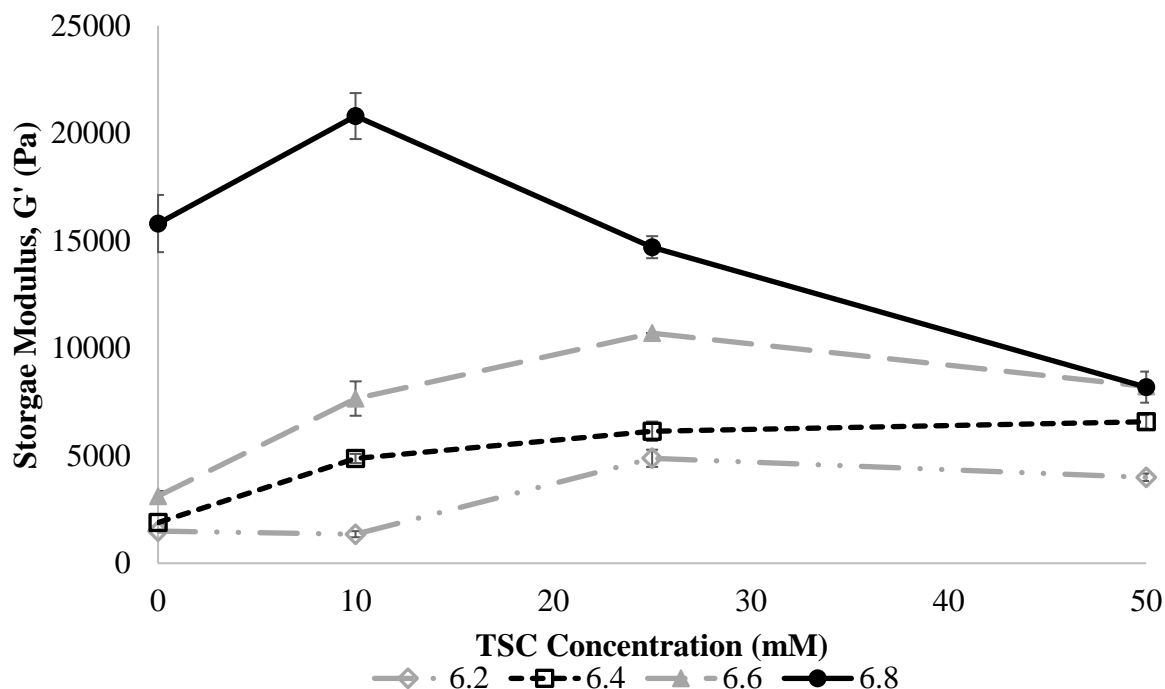
156

157 **Figure 3-11:** Changes in dynamic moduli with respect to TSC concentration. Average  
 158 modulus ( $G'$  and  $G''$ ) values of HC-MCC with respect to TSC concentration. The  
 159 samples used in these tests were at a native pH of 6.6 prior to the addition of TSC.

160

161 Samples with 15% protein content and no modifications formed a very weak  
 162 structure, not strong enough to hold its shape. With lower pH values, the required amount  
 163 of TSC to obtain the maximum  $G'$  value increased (Figure 3-12). This can be attributed  
 164 to the fact that at low pH, more soluble calcium is released from the micelle, requiring a  
 165 larger amount of the TSC to chelate excess calcium. It is likely that TSC interacts first  
 166 with the soluble calcium and then it starts interacting with casein bound calcium (CCP).  
 167 We hypothesize that changes in CCP due to TSC addition contributes to the increase in  
 168 the strength only after it is able chelate all the solubilized portion of CCP and remaining  
 169 portion disturbs the micellar integrity. More work is needed to test this hypothesis.

170



171

172 **Figure 3-12:** Effect of TSC addition on the storage modulus of 18.5% protein gels

173 adjusted to different pH levels.

174

175

176 At 25mM TSC levels, the impact of protein content on CGT was slightly

177 diminished, indicating that there is an optimum concentration of TSC (25mM) needed to

178 increase CGT. Interestingly, at lower pH levels (<6.8) and 10mM TSC concentrations,

179 gel formation was not observed during cooling MCC from 60°C to 5°C (Table 3-2). This

180 can be attributed to the fact that excessive calcium dissociation from the micelle and its

181 sequestration by TSC made less calcium available for participating in forming protein-

182 protein bridges. On the other hand, complete removal of CCP (without a drastic pH

183 change) may lead to formation of irreversible aggregates, losing ability to form a  
184 thermoreversible gels. However, to prove this hypothesis more work is needed.

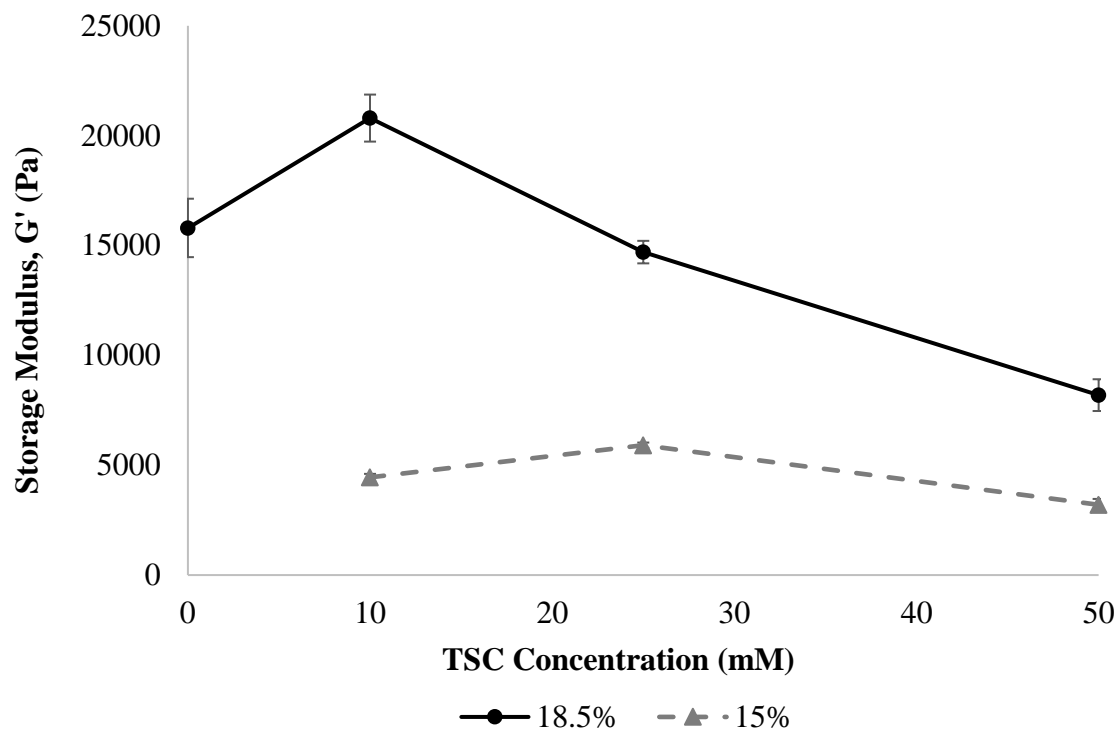
185         In response to alkalized samples, the amount of TSC needed to form a stronger  
186 cold gel at pH 6.8 decreased with higher concentration of protein (10mM at 18.5% and  
187 25mM at 15%) (Figure 3-13). We hypothesize that there is a dependency between the  
188 spacing of casein micelles and amount of soluble calcium needed to form cross-links  
189 between structures. At higher protein concentrations, spacing between casein micelles  
190 reduces; this necessitates less quantity of TSC needed to solubilize calcium from the  
191 colloidal phase and make bridges between protein structures. There are some indications  
192 in literature on the role of calcium in forming bridges during cold gelling (Lu et al., 2015;  
193 Zad Bagher Seighalani, 2021). However, there is more work needed to test our  
194 hypothesis.

195

196

197





198

199 **Figure 3-13:** The effect of TSC on storage modulus values of pH 6.8 samples at different  
 200 protein concentrations.

201

**Table 3-2:** Cold gelation temperature (CGT) values of HC-MCC with different protein and TSC content.

pH	TSC Concentration (mM)	Protein concentration, w/w	
		15%	18.5%
6.8	0	X	26.99±0.23 <sup>AB</sup>
	10	19.90±0.40 <sup>ABb</sup>	27.68±0.23 <sup>Aa</sup>
	25	21.50±0.61 <sup>Ab</sup>	25.39±0.40 <sup>Ba</sup>
	50	17.84±0.40 <sup>Bb</sup>	20.81±0.61 <sup>Ca</sup>
6.6	0	X	8.01±0.23 <sup>C</sup>
	10	No Gel*	20.58±0.69 <sup>B</sup>
	25	20.94±1.62 <sup>Ab</sup>	25.84±0.46 <sup>Aa</sup>
	50	13.72±0.68 <sup>Bb</sup>	21.27±0.40 <sup>Ba</sup>
6.4	0	X	7.79±0.23 <sup>C</sup>
	10	No Gel*	17.61±0.91 <sup>B</sup>
	25	17.38±0.83 <sup>Bb</sup>	21.72±0.61 <sup>Aa</sup>
	50	24.92±0.83 <sup>Aa</sup>	19.21±0.69 <sup>ABb</sup>
6.2	0	X	7.80±0.23 <sup>C</sup>
	10	No Gel*	7.78±0.23 <sup>BC</sup>
	25	No Gel*	21.49±0.82 <sup>A</sup>
	50	12.81±1.65 <sup>b</sup>	14.63±0.23 <sup>Ba</sup>

A comparison of gelation temperatures in response to different protein concentrations and TSC content. \* Designates no gel formation during the temperature sweep. Values are mean ± standard error. Capital letters denote significance within the same protein concentration, while lower case denotes significance within the same TSC concentration. Statistics were not conducted across different pH levels. Significance is at P<0.05.

**Table 3-3:** Storage Modulus Values of 18.5% protein HC-MCC with different pH and TSC content.

18.5% Protein		Storage Modulus (G') Value (kPa)			
pH	TSC Concentration (mM)	20°C	8°C	5°C	5°C + 10 Hours
6.8	0	6.95±0.633 <sup>Bc</sup>	11.0±0.897 <sup>Bbc</sup>	12.1±0.969 <sup>Bab</sup>	15.8±1.33 <sup>Ba</sup>
	10	10.7±0.657 <sup>Ac</sup>	16.0±0.937 <sup>Ab</sup>	17.4±1.01 <sup>Aab</sup>	20.8±1.07 <sup>Aa</sup>
	25	7.79±0.251 <sup>Bc</sup>	11.9±0.342 <sup>Bb</sup>	13.0±0.362 <sup>Bb</sup>	14.7±0.512 <sup>Ba</sup>
	50	3.77±0.366 <sup>Cb</sup>	6.87±0.581 <sup>Ca</sup>	7.76±0.640 <sup>Ca</sup>	8.19±0.723 <sup>Ca</sup>
6.6	0	0.00419± 0.00180 <sup>Dc</sup>	0.519± 0.0912 <sup>Ccb</sup>	0.901±0.127 <sup>Cb</sup>	3.12±0.242 <sup>Ca</sup>
	10	1.12±0.236 <sup>Cc</sup>	3.18±0.477 <sup>Bcb</sup>	3.94±0.548 <sup>Bb</sup>	7.66±0.800 <sup>Ba</sup>
	25	3.59±0.0635 <sup>Ad</sup>	6.62±0.0665 <sup>Ac</sup>	7.57±0.00652 <sup>Ab</sup>	10.7±0.00751 <sup>Aa</sup>
	50	2.83±0.0668 <sup>Bd</sup>	5.80±0.141 <sup>Ac</sup>	6.76±0.164 <sup>Ab</sup>	8.22±0.240 <sup>Ba</sup>
6.4	0	0.000864± 0.0000388 <sup>Cd</sup>	0.161± 0.00874 <sup>Cc</sup>	0.352±0.0170 <sup>Cb</sup>	1.89±0.0586 <sup>Ca</sup>
	10	0.395±46.1 <sup>Bc</sup>	1.71±0.109 <sup>Bb</sup>	2.29±0.134 <sup>Bb</sup>	4.87±0.212 <sup>Ba</sup>
	25	1.34±107 <sup>Ac</sup>	3.28±0.207 <sup>Ab</sup>	3.98±0.241 <sup>Ab</sup>	6.14±0.450 <sup>ABa</sup>
	50	1.29±101 <sup>Ac</sup>	3.51±0.176 <sup>Ab</sup>	4.32±0.195 <sup>Ab</sup>	6.58±0.311 <sup>Aa</sup>
6.2	0	0.000610± 0.000142 <sup>Bd</sup>	0.109± 0.00289 <sup>Bc</sup>	0.261± 0.00801 <sup>Bb</sup>	1.49±0.045.8 <sup>Ba</sup>
	10	0.0018± 0.000944 <sup>Bb</sup>	0.118± 0.0347 <sup>Bb</sup>	0.248± 0.0547 <sup>Bb</sup>	1.35±0.142 <sup>Ba</sup>
	25	0.494±0.113 <sup>Ac</sup>	1.76±0.289 <sup>Ac</sup>	2.43±0.343 <sup>Ab</sup>	4.88±0.400 <sup>Aa</sup>
	50	0.545±0.0377 <sup>Ad</sup>	2.00±0.0980 <sup>Ac</sup>	2.64±0.115 <sup>Ab</sup>	4.00±0.174 <sup>Aa</sup>

A comparison of storage modulus values for 18.5% protein samples in response to different TSC concentrations. Values are mean ± standard error. Capital letters denote significance within the same protein concentration, while lower case denotes significance within the same TSC concentration. Statistics were not conducted across different pH levels. Significance is at P<0.05.

**Table 3-4:** Storage Modulus Values of 15% protein HC-MCC with different pH and TSC content.

15% Protein		Storage Modulus (G') Value (kPa)			
pH	TSC Concentration (mM)	20°C	8°C	5°C	5°C + 10 Hours
6.8	10	1.69±0.0786 <sup>Bc</sup>	3.15±0.116 <sup>Bb</sup>	3.34±0.129 <sup>Bb</sup>	4.45±0.156 <sup>Ba</sup>
	25	2.64±0.0507 <sup>Ad</sup>	4.40±0.0688 <sup>Ac</sup>	4.86±0.0740 <sup>Ab</sup>	5.91±0.121 <sup>Aa</sup>
	50	0.899±0.0579 <sup>Cc</sup>	2.26±0.154 <sup>Cb</sup>	2.72±0.189 <sup>Cab</sup>	3.20±0.265 <sup>Ca</sup>
6.6	10	0.00235± 0.00141 <sup>Bb</sup>	0.135±0.0354 <sup>Bb</sup>	0.273±0.0588 <sup>Bb</sup>	1.60±0.163 <sup>Aa</sup>
	25	0.358± 0.0818 <sup>Ac</sup>	1.12±0.191 <sup>Abc</sup>	1.40±0.226 <sup>Aab</sup>	2.36±0.328 <sup>Aa</sup>
	50	0.0164± 0.00683 <sup>Bb</sup>	0.0860±0.0247 <sup>Bb</sup>	0.129±0.0344 <sup>Bab</sup>	0.340±0.0851 <sup>Ba</sup>
6.4	10	0.00000154± 0.000000123 <sup>Bb</sup>	0.00179±0.293 <sup>Bb</sup>	0.0104±0.00144 <sup>Bb</sup>	0.566±0.0191 <sup>Ca</sup>
	25	0.0456± 0.00217 <sup>Ad</sup>	0.332±0.0119 <sup>Ac</sup>	0.480±0.0169 <sup>Ab</sup>	1.41±0.0467 <sup>Aa</sup>
	50	0.0479± 0.00216 <sup>Ad</sup>	0.307±0.0133 <sup>Ac</sup>	0.466±0.0198 <sup>Ab</sup>	1.10±0.0465 <sup>Ba</sup>
6.2	10	0.000000291± 0.000000162 <sup>Bb</sup>	0.00000677± 0.00000139 <sup>Bb</sup>	0.000317± 0.000103 <sup>Bb</sup>	0.143±0.0312 <sup>Ca</sup>
	25	0.000252± 0.0000735 <sup>Bb</sup>	0.0412±0.0121 <sup>Ab</sup>	0.105±0.0247 <sup>Ab</sup>	0.957±0.104 <sup>Aa</sup>
	50	0.00679± 0.0000970 <sup>Ac</sup>	0.0742±0.00785 <sup>Abc</sup>	0.129±0.0118 <sup>Ab</sup>	0.479±0.0400 <sup>Ba</sup>

A comparison of storage modulus values for 15% protein samples in response to different TSC concentrations. Values are mean ± standard error. Capital letters denote significance within the same protein concentration, while lower case denotes significance within the same TSC concentration. Statistics were not conducted across different pH levels. Significance is at P<0.05.

### 3.4: Discussions

226

227

228

229

230

231

In this work we found that there are several factors which can influence the formation of cold gels. For example, cooling MCC from 60°C to 5°C causes an increase in particle size and net negative charge on the casein micelle, as well as solubilizes CCP so that it can act as bridging element during formation of cold gels.

232

233

234

235

236

237

238

239

240

241

242

The rheology of a system depends upon the volume fraction of the dispersed phase (in our case casein micelles), rigidity of dispersed particles, interaction between particles, viscosity of the solvent, and temperature of the system. Swelling of the casein micelles at low temperatures increases the volume fraction, therefore viscosity and gel strength of the system (D.Z. Liu et al., 2013). Increasing concentration of dispersed phase or volume fraction increases the interaction between particles. When the volume fraction reaches a maximum packing effect, jamming of particles takes place where particles exert steric hindrance to the extent where they cannot move. On the other hand, at low temperatures, the kinetic energy of the system decreases to the extent where molecules cannot move past each other and get arrested (Lu et al., 2015). Both concepts offer a potential explanation behind cold gelation.

243

244

245

246

247

248

The Arrhenius equation is widely used for explaining temperature dependence of a system based upon the kinetic theory of the molecular movement. In our case, we are taking  $G'$  as a factor dependent upon mobility of particles influenced by temperature. Figure 3-14 shows the storage modulus of 4 selected treatments during the temperature sweep fitted to an Arrhenius equation (Eq 1). Using the following equation, we can obtain the activation energy ( $E_a$ ) of deformation for each sample and temperature

249 dependence of storage moduli ( $G'$ ) (Tunick, 2010). Lower activation indicates ease of gel  
250 formation and stability of the gel.

251

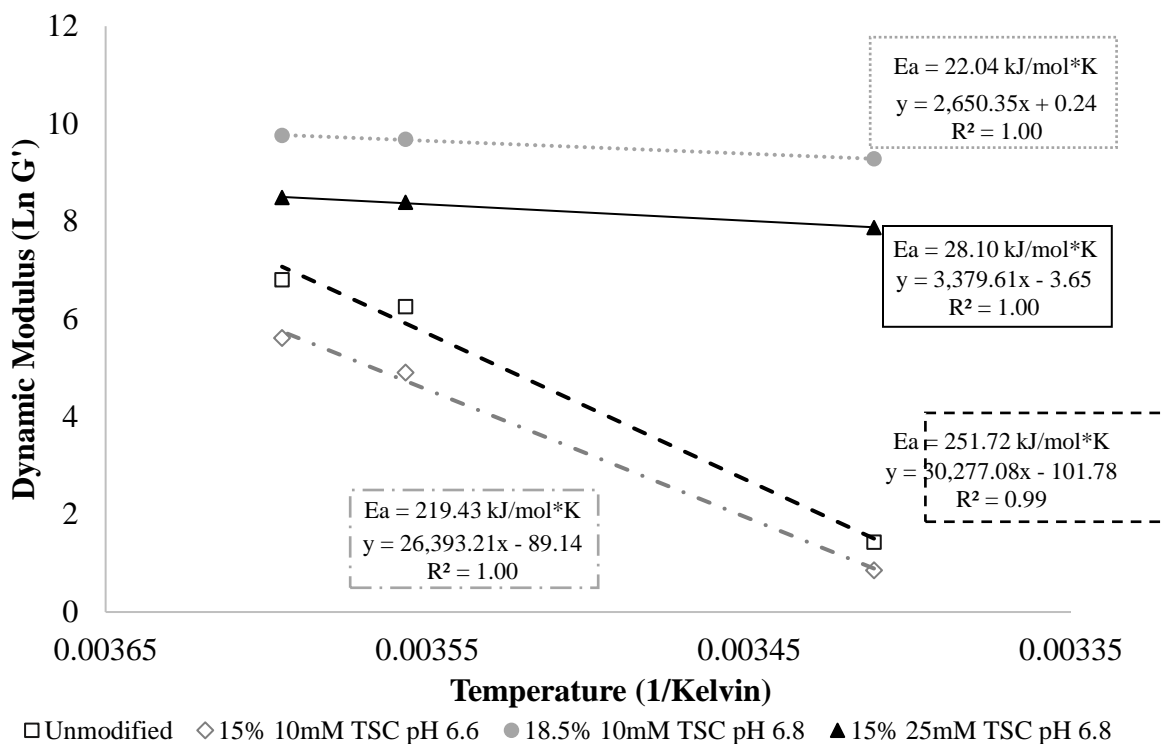
$$252 \quad k = Ae^{\frac{-Ea}{RT}} \quad (1)$$

253

254 As expected, since both of the strongest samples (18.5% protein with 10mM TSC  
255 at pH 6.8, and 15% protein with 25mM TSC at pH 6.8) for their respective protein  
256 concentrations had formed a gel by 20°C (0.00341 in 1/Kelvin), their activation energy is  
257 a lower value. The control sample and weaker 15% protein sample, however, did not  
258 form a gel by 20°C, and as such they have a higher activation energy (>200 kJ/mol.K)  
259 and more temperature dependence in the given temperature range.

260

261



262

263 **Figure 3-14:** Storage modulus values of select treatments in response to temperature

264 change fitted to an Arrhenius equation. Control samples are 18.5% protein at pH 6.6 with

265 0mM TSC added.

266

267

268 The initial increase and subsequent decrease in particle size in response to

269 increasing the TSC content (Figure 3-4) follows the same pattern observed for gel

270 strength with the same quantities of TSC, indicating that there could be a potential link

271 between size of particles in solution and gel strength, conforming the hypothesis related

272 to the volume fraction. A similar effect can be observed in the TEM results, where

273 micrographs of samples taken well above gelation (25°C) exhibited free hydrated casein

274 pockets released from casein micelle where particle size is minimal (Figure 3-8). This  
275 observation was concomitant with the irregular structures exhibited, indicating a less  
276 homogeneous and less interactive dispersed phase, possibly due to residual hydrophobic  
277 interactions of casein micelle. The presence of these fragmented casein pockets at slightly  
278 higher temperature was contradictory to the behavior of  $\beta$ -casein, which is known to  
279 migrate from the micelle to the aqueous phase in response to low temperature ( $<15^{\circ}\text{C}$ )  
280 (O'Connell et al., 2003). Such pockets were not observed at CGT ( $11^{\circ}\text{C}$ ) and below;  
281 instead, there was evidence of protein structures smaller than those seen for the typical  
282 micelle size. The formation of these smaller structures indicates that there are entropic  
283 forces in response to changes in temperature causing the formation of regular, well  
284 hydrated and interactive structures observed in the sample (Holt et al., 2013).

285         The effect of TSC on samples falls in line with previous rheological research  
286 conducted on dairy samples (de Kort et al., 2011; Ozcan-Yilsay et al., 2007). As TSC can  
287 remove the CCP from the interior of the casein micelle, the resulting destabilization can  
288 open the structure, releasing individual casein fractions at higher concentrations  
289 (Deshwal, 2017). In addition to this release of casein fractions, the remaining structure  
290 gains additional size due to increased hydration (de Kort et al., 2011). Increases in casein  
291 hydration are the likely cause of increases in gel strength and CGT, but there is additional  
292 research required to better understand how the release of casein fractions may impact  
293 rheological properties.

294         The decrease in zeta potential values in response to alkalization is a possible  
295 explanation for increased CGT and  $G'$  values in these samples. With a greater negative  
296 charge on caseins within solution, there is a potentially higher degree of protein-water



297 interaction than what is observed at native or acidified pH levels (Vaia et al., 2006).  
298 Higher protein-water interactions could prove beneficial for gel strength by preventing  
299 syneresis and long-term stability in a sample. Another potential explanation can come  
300 from particle size data: with higher pH, there is a greater average hydrodynamic diameter  
301 (Figure 3-4). If the pH is high enough to encourage swelling of the micellar structure, it  
302 could encourage the packing transition proposed in prior literature (Dunn et al., 2021; Y.  
303 Liu & Guo, 2008; Lu et al., 2015). More analysis is required to better understand the  
304 effect of alkalization on both the structure of casein, and how it impacts gelling behavior.

305

### 306 **3.5: Conclusions**

307

308 The effects of the protein concentration, pH adjustment and calcium chelation had  
309 a significant impact on the cold gelling behavior of HC-MCC. We propose that cold gel  
310 formation in MCC takes place due to increased hydration, net negative charge and  
311 solubilization of calcium. Acidification of the sample resulted in the reduction of gel  
312 qualities and particle size, whereas alkalization improved gel strength and increased  
313 CGT, owing to increased particle size and zeta potential. Addition of TSC at both protein  
314 levels (18.5% and 15%) led to formation stronger gels, indicating significant role of  
315 calcium in cold gel formation. The quantity of TSC needed to form stronger gels is  
316 dependent on the pH, and protein content of the MCC samples. Additional research is  
317 needed to get further insights into understanding the mechanism of cold gel formation.

318

## References

- Anema, S. G., & Klostermeyer, H. (1996).  $\zeta$ -Potentials of casein micelles from reconstituted skim milk heated at 120 °C. *International Dairy Journal*, 6(7), 673–687. [https://doi.org/10.1016/0958-6946\(95\)00070-4](https://doi.org/10.1016/0958-6946(95)00070-4)
- Broyard, C., & Gaucheron, F. (2015). Modifications of structures and functions of caseins: A scientific and technological challenge. *Dairy Science & Technology*, 95(6), 831–862. <https://doi.org/10.1007/s13594-015-0220-y>
- Culler, M. D., Saricay, Y., & Harte, F. M. (2017). The effect of emulsifying salts on the turbidity of a diluted milk system with varying pH and protein concentration. *Journal of Dairy Science*, 100(6), 4241–4252. <https://doi.org/10.3168/jds.2017-12549>
- de Kort, E., Minor, M., Snoeren, T., van Hooijdonk, T., & van der Linden, E. (2011). Effect of calcium chelators on physical changes in casein micelles in concentrated micellar casein solutions. *International Dairy Journal*, 21(12), 907–913. <https://doi.org/10.1016/j.idairyj.2011.06.007>
- Deshwal, G. K., Gómez-Mascaraque, L. G., Fenelon, M., & Huppertz, T. (2023). A Review on the Effect of Calcium Sequestering Salts on Casein Micelles: From Model Milk Protein Systems to Processed Cheese. *Molecules*, 28(5), Article 5. <https://doi.org/10.3390/molecules28052085>
- Dunn, M., Barbano, D. M., & Drake, M. (2021). Viscosity changes and gel formation during storage of liquid micellar casein concentrates. *Journal of Dairy Science*, 104(12), 12263–12273. <https://doi.org/10.3168/jds.2021-20658>

- 341 Eshpari, H., Tong, P. S., & Corredig, M. (2016). Changes in particle size, calcium and  
 342 phosphate solubilization, and microstructure of rehydrated milk protein  
 343 concentrates, prepared from partially acidified milk. *Dairy Science & Technology*,  
 344 96(3), 329–343. <https://doi.org/10.1007/s13594-015-0270-1>
- 345 Francis, M. J., Glover, Z. J., Yu, Q., Povey, M. J., & Holmes, M. J. (2019). Acoustic  
 346 characterisation of pH dependant reversible micellar casein aggregation. *Colloids  
 347 and Surfaces A: Physicochemical and Engineering Aspects*, 568, 259–265.  
 348 <https://doi.org/10.1016/j.colsurfa.2019.02.026>
- 349 Gebhardt, R., Steinhauer, T., Meyer, P., Sterr, J., Perlich, J., & Kulozik, U. (2012).  
 350 Structural changes of deposited casein micelles induced by membrane filtration.  
 351 *Faraday Discussions*, 158(0), 77–88. <https://doi.org/10.1039/C2FD20022H>
- 352 Gonzalez-Jordan, A., Thomar, P., Nicolai, T., & Dittmer, J. (2015). The effect of pH on  
 353 the structure and phosphate mobility of casein micelles in aqueous solution. *Food  
 354 Hydrocolloids*, 51, 88–94. <https://doi.org/10.1016/j.foodhyd.2015.04.024>
- 355 Holt, C., Carver, J. A., Ecroyd, H., & Thorn, D. C. (2013). Invited review: Caseins and  
 356 the casein micelle: Their biological functions, structures, and behavior in foods1.  
 357 *Journal of Dairy Science*, 96(10), 6127–6146. <https://doi.org/10.3168/jds.2013-6831>  
 358 6831
- 359 Horne, D. S. (2017). A balanced view of casein interactions. *Current Opinion in Colloid  
 360 & Interface Science*, 28, 74–86. <https://doi.org/10.1016/j.cocis.2017.03.009>
- 361 Kaliappan, S., & Lucey, J. A. (2011). Influence of mixtures of calcium-chelating salts on  
 362 the physicochemical properties of casein micelles. *Journal of Dairy Science*,  
 363 94(9), 4255–4263. <https://doi.org/10.3168/jds.2010-3343>

- 364 Liu, D. Z., Weeks, M. G., Dunstan, D. E., & Martin, G. J. O. (2013). Temperature-  
365 dependent dynamics of bovine casein micelles in the range 10–40°C. *Food*  
366 *Chemistry*, 141(4), 4081–4086. <https://doi.org/10.1016/j.foodchem.2013.06.130>
- 367 Liu, Y., & Guo, R. (2008). PH-dependent structures and properties of casein micelles.  
368 *Biophysical Chemistry*, 136(2), 67–73. <https://doi.org/10.1016/j.bpc.2008.03.012>
- 369 Lu, Y., McMahon, D. J., Metzger, L. E., Kommineni, A., & Vollmer, A. H. (2015).  
370 Solubilization of rehydrated frozen highly concentrated micellar casein for use in  
371 liquid food applications. *Journal of Dairy Science*, 98(9), 5917–5930.  
372 <https://doi.org/10.3168/jds.2015-9482>
- 373 Lucey, J. A., & Horne, D. S. (2018). Perspectives on casein interactions. *International*  
374 *Dairy Journal*, 85, 56–65. <https://doi.org/10.1016/j.idairyj.2018.04.010>
- 375 Madadlou, A., Mousavi, M. E., Emam-Djomeh, Z., Sheehan, D., & Ehsani, M. (2009).  
376 Alkaline pH does not disrupt re-assembled casein micelles. *Food Chemistry*,  
377 116(4), 929–932. <https://doi.org/10.1016/j.foodchem.2009.03.048>
- 378 O’Connell, J. E., Grinberg, V. Ya., & de Kruif, C. G. (2003). Association behavior of  $\beta$ -  
379 casein. *Journal of Colloid and Interface Science*, 258(1), 33–39.  
380 [https://doi.org/10.1016/S0021-9797\(02\)00066-8](https://doi.org/10.1016/S0021-9797(02)00066-8)
- 381 Ozcan-Yilsay, T., Lee, W.-J., Horne, D., & Lucey, J. A. (2007). Effect of Trisodium  
382 Citrate on Rheological and Physical Properties and Microstructure of Yogurt.  
383 *Journal of Dairy Science*, 90(4), 1644–1652. <https://doi.org/10.3168/jds.2006-538>
- 384 Rosmaninho, R., Santos, O., Nylander, T., Paulsson, M., Beuf, M., Benezech, T.,  
385 Yiantsios, S., Andritsos, N., Karabelas, A., Rizzo, G., Müller-Steinhagen, H., &  
386 Melo, L. F. (2007). Modified stainless steel surfaces targeted to reduce fouling –

- 387 Evaluation of fouling by milk components. *Journal of Food Engineering*, 80(4),  
388 1176–1187. <https://doi.org/10.1016/j.jfoodeng.2006.09.008>
- 389 Saboyainsta, L. V., & Maubois, J.-L. (2000). Current developments of microfiltration  
390 technology in the dairy industry. *Le Lait*, 80(6), 541–553.  
391 <https://doi.org/10.1051/lait:2000144>
- 392 Sinaga, H., Bansal, N., & Bhandari, B. (2017). Effects of milk pH alteration on casein  
393 micelle size and gelation properties of milk. *International Journal of Food*  
394 *Properties*, 20(1), 179–197. <https://doi.org/10.1080/10942912.2016.1152480>
- 395 Tunick, M. H. (2010). Activation energy measurements in rheological analysis of cheese.  
396 *International Dairy Journal*, 20(10), 680–685.  
397 <https://doi.org/10.1016/j.idairyj.2010.03.010>
- 398 Vaia, B., Smiddy, M. A., Kelly, A. L., & Huppertz, T. (2006). Solvent-Mediated  
399 Disruption of Bovine Casein Micelles at Alkaline pH. *Journal of Agricultural and*  
400 *Food Chemistry*, 54(21), 8288–8293. <https://doi.org/10.1021/jf061417c>
- 401 Winter, H. H., & Chambon, F. (1986). Analysis of Linear Viscoelasticity of a  
402 Crosslinking Polymer at the Gel Point. *Journal of Rheology*, 30(2), 367–382.  
403 <https://doi.org/10.1122/1.549853>
- 404 Zad Bagher Seighalani, F., McMahon, D. J., & Sharma, P. (2021). Determination of  
405 critical gel-sol transition point of Highly Concentrated Micellar Casein  
406 Concentrate using multiple waveform rheological technique. *Food Hydrocolloids*,  
407 120, 106886. <https://doi.org/10.1016/j.foodhyd.2021.106886>
- 408
- 409

## CHAPTER 4

## RHEOLOGICAL AND ULTRASTRUCTURAL ANALYSIS

## OF MODIFIED MICELLAR CASEIN COLD GELS

**ABSTRACT**

The purpose of this study was to examine the effect of calcium chelation and alkalization on the cold gelling properties of Highly Concentrated-Micellar Casein Concentrate (HC-MCC). Rheological measurements of dynamic moduli ( $G'$  and  $G''$ ) were measured on HC-MCC gels at multiple frequencies to determine gelation via Winter–Chambon criterion. In addition, Transmission Electron Microscopy (TEM) micrographs for each of the treatments were produced to understand the effect of modification on the micellar structure of casein. All modifications performed resulted in a significant increase ( $P < 0.05$ ) in gel strength and gelation temperature, with samples adjusted to pH 7.0 yielding the strongest gels. Both forms of treatments raise sample pH, but TEM micrographs show evidence of different mechanisms causing morphological changes to casein micelles in solution. The addition of 25mM of TSC resulted in the partial disintegration of the micellar structure whereas samples treated with 50mM (TSC) show formation of large aggregate structures. pH adjusted samples show an increasingly disintegrated micellar structure, with pH 7.0 samples displaying complete micellar dissolution and the formation of a casein matrix. These findings show that the effect of

433 calcium chelation and alkaline pH adjustment greatly affect both the structure of casein  
434 micelles and the rheological properties of HC-MCC. The mechanism behind both forms  
435 of modification appear to be different, additional research is required to better understand  
436 the effect of these modifications on micellar structure.

437

#### 438 **4.1: Introduction**

439

440 Highly Concentrated Micellar Casein Concentrate (HC-MCC) is a dairy product  
441 with the unique capability of creating a gel without modification (Lu et al., 2016). HC-  
442 MCC is produced in a similar manner to MCC via the microfiltration and diafiltration of  
443 milk; the difference between the two being that HC-MCC undergoes an additional stage  
444 of vacuum evaporation to increase the solids content. The final protein content ranges  
445 from 17% to 23% while maintaining the native conformation of the casein micelle  
446 (Saboyainsta & Maubois, 2000). The cold gelling nature of HC-MCC has been  
447 documented and is the subject of research in order to understand it better (Dunn et al.,  
448 2021; Lu et al., 2016; Zad Bagher Seighalani et al., 2021). Lu et al. (2015) proposed a  
449 mechanism of gelation behavior where the high amount of casein micelles within solution  
450 created a packing effect where there is little viscoelastic flow due to the minimal space  
451 between protein supramolecules. In conjunction with this, additional gel strength was  
452 attributed to bridging between micelles via bridging of Colloidal Calcium Phosphate  
453 (CCP).

454 The effect of calcium bridging between micellar structures can be modified by  
455 utilizing a calcium chelating salt such as trisodium citrate (TSC). CCP is also considered

456 an important molecule for the overall stability of a casein micelle (Younes, 2017).  
457 Calcium chelating salts have the ability to remove CCP from the micelle resulting in  
458 conformational changes in the tertiary structure, potentially resulting in crosslinking  
459 between strands of caseins. Previous rheological studies have shown that TSC in casein  
460 gels has an effect on gel strength, likely due to this effect (Ozcan-Yilsay et al., 2007).  
461 When TSC is added to casein solutions, there is a notable increase in gel strength. In the  
462 event of a high concentration of TSC added to casein, there is a notable decrease in gel  
463 strength compared to a lower concentration of salt. One potential explanation is that  
464 while a lower concentration of TSC may cause the dissociation of caseins into the  
465 solution, a high enough concentration has the potential to chelate all CCP within the  
466 solution which could completely disrupt the micellar structure and yield a weaker gel  
467 (Ozcan-Yilsay et al., 2007).

468         Adjustment in sample pH can also affect calcium equilibrium within casein.  
469 Increases in pH result in a decrease in CCP solubility, and by extension a reduction in  
470 hydrophobic interactions between caseins (McMahon & Oommen, 2008). In the event of  
471 alkalization, the charge on individual caseins changes in response to the increase in  $\text{OH}^-$   
472 within solution (Touhami et al., 2022). This reduction in the hydrophobic interactions can  
473 result in the dissolution of the micelle, leading to the release of free casein proteins within  
474 solution (Vaia et al., 2006). If calcium bridging between individual caseins were to occur  
475 in a highly dissociated casein solution, there is potential for strong gel formation. Mild  
476 increases in pH (as in not alkalized enough for micellar destabilization) have been found  
477 to result in particle size increases as well, potentially increasing gel strength due to a  
478 heightened version of the packing effect proposed in Lu et al. (2015).



479           As with many other food gels, HC-MCC exhibits viscoelastic behavior where it  
480 acts more like a viscoelastic fluid at elevated temperatures and transitions into a  
481 viscoelastic solid as temperature within the system decreases. Applying rheological  
482 techniques to measure the properties of an HC-MCC gel offers an excellent opportunity  
483 to better understand the gelling characteristics of casein, and the effect of modification on  
484 casein gels. To determine the temperature where a viscoelastic material transitions to a  
485 gel requires the use of a technique based on the data recorded during testing. A common  
486 method utilized is the crossover point method, where the storage modulus ( $G'$ ), or  
487 measurement of elastic properties yields a greater value than the loss modulus ( $G''$ ) or  
488 measurement of liquid properties. This is seen as a pseudo-gelation point as the  
489 determined gelation point is highly dependent on the frequency used during testing (Liu  
490 et al., 2016). Zad Bagher Seighalani et al., (2021) utilized a multiwave method originally  
491 devised by Winter & Chambon, (1986) where gelation was defined as the point where the  
492 loss tangent of the sample was independent of the frequency that oscillatory shear was  
493 applied to the sample. This method resulted in a significantly lower temperature of  
494 transition, but samples at gelation point behaved more accurately as a gel.

495           Transmission Electron Microscopy (TEM) is an imaging method that allows the  
496 direct observation of protein structures at high details and has been used to image the  
497 structure of dairy products in multiple forms (Lu et al., 2015; Marchin et al., 2007;  
498 Vollmer et al., 2021). Imaging of unmodified casein micelles in milk and concentrated  
499 dairy products has shown that the casein micelle structure is consistently spherical in  
500 shape and generally measures 100-200nm in diameter with fine protein strands of casein  
501 on the exterior (McMahon & Oommen, 2008). In conjunction with the strong imaging

potential it offers, TEM can also be used effectively in conjunction with rheological testing. A rheological testing protocol can be conducted on a sample and then can be used as a sample for TEM imaging, allowing two sources of data on a singular sample. Comparison of TEM micrographs to rheological data allows us to observe interactions on a micro scale while offering insight on how this can affect rheological data on the macro scale. In this study, we will observe the gelling properties of HC-MCC using oscillatory rheological protocols in conjunction with TEM imaging. Our goal is to find the strongest possible gel and the highest gelation temperature for HC-MCC using rheological testing, and to use TEM to understand the effect of modifications on the structure of casein micelles on a microscopic scale.

512

## 4.2: Materials and Methods

514

### 4.2.1: Sample Preparation

516

#### 4.2.1.1: HC-MCC Production

518

HC-MCC used in the study was produced at South Dakota State University in the same manner as described in Lu et al., (2015). The MF system was a 4-vessel continuous design utilizing polyvinylidene fluoride membranes with a combined surface area of 57.4m<sup>2</sup>. The subsequent vacuum evaporation of the MCC was conducted at 63°C at a pressure of -680mbar. The samples were held in large pails within a -20°C freezer. Frozen samples were taken out and molten to a liquid state in a water bath at 50°C. The liquid HC-MCC is thoroughly mixed and poured into screw cap plastic

524

525 containers in ~120g quantities. Spoilage of the samples via microbial growth was  
526 prevented by the addition of a chemical preservative in the form of 0.05% wt/wt sodium  
527 azide. Samples not in use will return to the -20°C freezer until ready for use. Sample cups  
528 will be thawed in a water bath and stored in refrigerators in between tests. All tests will  
529 be performed in triplicate.

530

#### 531 **4.2.1.3: Sample modification**

532 In this study, HC-MCC gels were given two forms of modifications in two  
533 different treatment levels: pH adjustment from a native pH of 6.6 to 6.8 and 7.0, and the  
534 addition of TSC in 25mM and 50mM quantities. For pH adjustment, samples were first  
535 homogeneously mixed using an overhead mixer for 2 minutes, followed by the addition  
536 of NaOH and were mixed further for 3 minutes. The samples were then held at room  
537 temperature for 2 hours to allow for the additions to dissolve. TSC at 25mM and 50mM  
538 levels was added to the samples at 60°C with constant stirring using a glass rod  
539 immediately prior to loading into the rheometer. For some samples, additional heating for  
540 5 seconds in a microwave was required to fully incorporate the salt. pH testing was  
541 performed using an ORIONSTAR A111 model pH meter (Thermoscientific, USA. CA)  
542 and sample pH was measured immediately prior to sample testing at 60°C.

543

544

545

## 546     **4.2.2: Rheological Testing**

547

### 548             **4.2.2.1: Sample loading**

549             Rheological measurements were performed using an Anton Paar model 302  
550     rheometer (Graz, Austria) using a CC27 concentric cylinder geometry setup. 20ml of  
551     sample was heated to 60°C using a heated water bath and mixed using a glass stirring rod  
552     to ensure a homogenous sample. Heated HC-MCC was then loaded into the test cylinder  
553     heated to the same temperature. A mineral oil layer was added to the top of the sample  
554     and solvent trap via a pipette to prevent dehydration during the rheological protocol.

555

### 556             **4.2.2.2: Rheological Protocol**

557             Testing took place in three stages and automatically advances to the next stage  
558     once the previous stage is complete (Figure 3-1). The first stage held the temperature of  
559     the geometry and sample at 60°C for one hour taking measurements every 30 seconds for  
560     a total of 120 data points. The second test was a temperature sweep where the  
561     temperature will decrease from 60°C to 5°C over the course of 56 minutes, taking a  
562     measurement every 41.25 seconds for a total of 81 data points. Lastly, the third stage held  
563     the sample at 5°C for 10 hours, making measurements every minute. Proper temperature  
564     of the sample was maintained using a Peltier temperature control system attached to a  
565     refrigerated water bath (CORIO CP-200F, Julabo GmbH, Seelbach, Germany).

566

### 4.2.2.3: Multiwave Measurements

The testing protocol conducted measurements at multiple angular frequencies simultaneously (3, 6, 12, 24, and 48 rad/s with a strain of 0.18, 0.16, 0.14, 0.11, 0.09, and 0.07% respectively) during all three testing phases. Lower strain values at higher frequencies were chosen to ensure the LVR limit of the sample was not exceeded according to the findings reported by Zad Bagher Seighalani et al., (2021). Signals from multiple frequencies were separated into individual signals using the Fourier transform package within RheoCompass software 1.31 (Anton Paar, Graz, Austria) connected to the rheometer. Gelation point was determined by using Winter and Chambon criteria described in Winter & Chambon, (1986) and Zad Bagher Seighalani et al., (2021), where gelation is defined as the point where the loss tangent of 3, 6, 12, 24, and 48 rad/s frequencies converge. This criterion can be defined in the following equations:

$$G' \propto \omega^n ; \quad G'' \propto \omega^n \quad (2)$$

and;

$$\tan \delta = G'' / G' = \tan(n\pi / 2) \quad (3)$$

where  $n$   $0 < n < 1$  is the slope of dynamic moduli within a frequency spectrum (Higham et al., 2014). Measurements of 6 rad/s storage and loss modulus ( $G'$ ) at 20°C, 8°C, 5°C at the end of the temperature sweep, and 5°C at the end of the frequency sweep was used to compare gel strength between the different treatments.

588

589 **4.2.4: Transmission Electron Microscopy**

590 Ultrastructure analysis of HC-MCC mixtures was performed using the TEM  
591 method described by (Lu et al., 2015). Samples underwent rheological testing using the  
592 sample loading and testing method described above. After testing was complete, the  
593 CC27 geometry was removed from the rheometer. The bottom of the geometry was  
594 removed to reveal the sample which were harvested for TEM. Samples were fixed using  
595 2% glutaraldehyde and formaldehyde for at least two hours. Samples were then rinsed in  
596 a sodium cacodylate buffer and postfixed in 2% osmium tetroxide solution for 1 hour,  
597 followed by rinsing with distilled water in two 10-minute stints. After dehydration of the  
598 samples via a progressive ethanol series (20 min each in 50%, 70%, twice in 95%, and  
599 three times in 100% EtOH) samples were transitioned into plastic resin and infiltrated  
600 with a resin-acetone mix. Infiltration with pure resin followed, and polymerization of  
601 sample blocks occurred overnight at 65°C. Sections (70-100nm) were cut on a Leica EM  
602 UC6 ultramicrotome (Leica Microsystems Inc., Buffalo Grove, IL) using a diamond knife  
603 (Diatome, Hatfield, PA). Sections were double stained for 20 minutes with saturated  
604 aqueous uranyl acetate followed by 10 minutes with Reynold's lead citrate. Sections were  
605 then analyzed using a transmission electron microscope (TEM, JEM 1400 Plus, Jeol USA  
606 Inc., Peabody, MA) operated at 120kV, and digital images were captured using a Gatan  
607 camera (Gatan Inc., Pleasanton, CA).

608

#### 609    **4.2.5: Gel Electrophoresis**

610           Molecular changes in the casein proteins was analyzed using a Urea-PAGE and  
 611    native PAGE technique using the protocol from Lamichhane et al. (2019). Control, 25  
 612    and 50mM TSC, pH 6.8 and pH 7.0 treated MCC samples were centrifuged at 50,000g  
 613    for 4 hours at 30°C using a Beckman model LE-80 Ultracentrifuge (Brea, CA) to  
 614    sediment intact casein structures. The supernatant of each treatment served as the protein  
 615    sample for electrophoresis. Supernatant containing 1mg of protein was mixed into sample  
 616    buffers and heated at 70°C for 30 minutes 5µl of sample (containing 5µg of protein) was  
 617    loaded into each well of a Biorad 15% Mini-PROTEAN TBE Urea gel (Hercules, CA)  
 618    where it was then run at 120V for 2.5 hours. Sample staining was accomplished using  
 619    Coomassie blue stain for 1 hour, followed by de-staining using distilled water. Imaging  
 620    of the finished gels was accomplished in red light with UV conditions and processed  
 621    within Bio-Rad Image Lab software (Hercules, CA).

622

#### 623    **4.2.6: Texture Analysis**

624           Texture analysis of treatments was conducted using a TA-XT Plus texture  
 625    analyzer (Stable Micro System Ltd., Surrey, UK) with a texture profile test using a two-  
 626    bite test with 25% compression. Samples of HC-MCC treatments were poured into 30mm  
 627    diameter cylindrical molds and were allowed to solidify overnight in a 5°C refrigerator  
 628    prior to testing. Fracture properties were tested in compression deformation modes using  
 629    a 1.5cm thick section of sample. Force and compressional data from testing was  
 630    converted into Hencky strain ( $\epsilon$ ) using equation 5 where  $L(t)$  is the height of the  
 631    compressed sample and  $L_0$  is the initial height. A metric to observe the strain hardening

potential of a sample is the strain hardening ratio (SHR), or the ratio of the slope at the beginning of testing compared to the end (Sharma et al., 2018)(Bast et al., 2015). As the sample continues to harden in response to strain, the slope will increase, and the ratio can describe the level of hardening possible.

636

$$\text{SHR} = \frac{\text{Maximum modulus}}{\text{Initial modulus}} \quad (4)$$

$$\varepsilon = \ln \frac{L(t)}{L_o} \quad (5)$$

639

#### 640 **4.2.7: Statistical Analysis**

Values for storage modulus measured at 6 rad/s, gelation temperature using the multiwave method, loss tangent values at the end of the temperature sweep and the slope of frequency dependent G' measurements were analyzed using SAS Studio (version 3.8) with analysis of variance (ANOVA) accompanied with Tukey's HSD to determine significant difference at (P < 0.05).

646

### 647 **4.3: Results and Discussion**

648

#### 649 **4.3.1: pH Measurements Pre- and Post-Rheological testing**

Utilization of TSC from 25mM to 50mM levels yielded an expected increase in pH, for pre-test pH of 6.78 and 6.93, and a post-test pH of 6.91 and 7.05 respectively

651



652 Samples adjusted via NaOH yielded pre-test pH values of 6.82 and 7.04, and post-test  
 653 values of 7.04 and 7.65 respectively. Since the post-test pH increased further, it indicates  
 654 the role of CCP solubilization on the final pH in response to temperature (Wang & Ma,  
 655 2020). The more pronounced increase in post-test pH values for NaOH samples as  
 656 compared to TSC samples could be due to the additional buffering effect of TSC; as there  
 657 is more calcium bound to TSC, there is less CCP to affect the pH in response to  
 658 temperature changes (On-Nom et al., 2010). Also, TSC itself acts as buffering agent,  
 659 manipulating final pH. In addition to this, caseins themselves also act as buffering agents.  
 660 The inherent buffering capacity of casein is at max around natural milk pH i.e., 6.6. If the  
 661 pH is near 7.00, the tendency to resist the pH decreases. This could be one of the  
 662 potential reason for a further rise in the pH while holding sample for 10hrs at 5°C (Salaün  
 663 et al., 2005).

664

### 665 **4.3.2: Rheological Testing**

666

#### 667 **4.3.2.1: Effect of pH and Calcium Chelation on Cold Gel Formation**

668 The effects of TSC addition and pH modifications (by adding NaOH) to HC-  
 669 MCC dynamic moduli are presented in Figure 4-1 and Table 4-1. Both methods of  
 670 modification resulted in higher values of G' throughout cooling of HC-MCC (Table 4-1),  
 671 indicating strengthening of the matrix with these modifications. Samples with TSC  
 672 treatments reached a peak in gel strength and gelation temperature at 25mM TSC,  
 673 whereas 50mM resulted in a reduction in these metrics (Figure 4-1). It is evident that the  
 674 effect of pH modifications (6.8, 7.0) dominated over the TSC addition (25mM and  
 675 50mM), with G' values being significantly higher ( $P < 0.05$ ) for the former treatment

(Table 4-1 and Figure 4-1). This effect is observed with increasing alkalization, with 7.0 samples being stronger than 6.80 samples (Figure 4-1). CGT values for pH 7.0 treatments were significantly higher ( $P>0.05$ ) than either concentration of TSC treatment. This indicates that the mechanism for gel formation in both treatments leads to a heightened degree of protein interaction. More work is needed to establish the nature of these interactions.

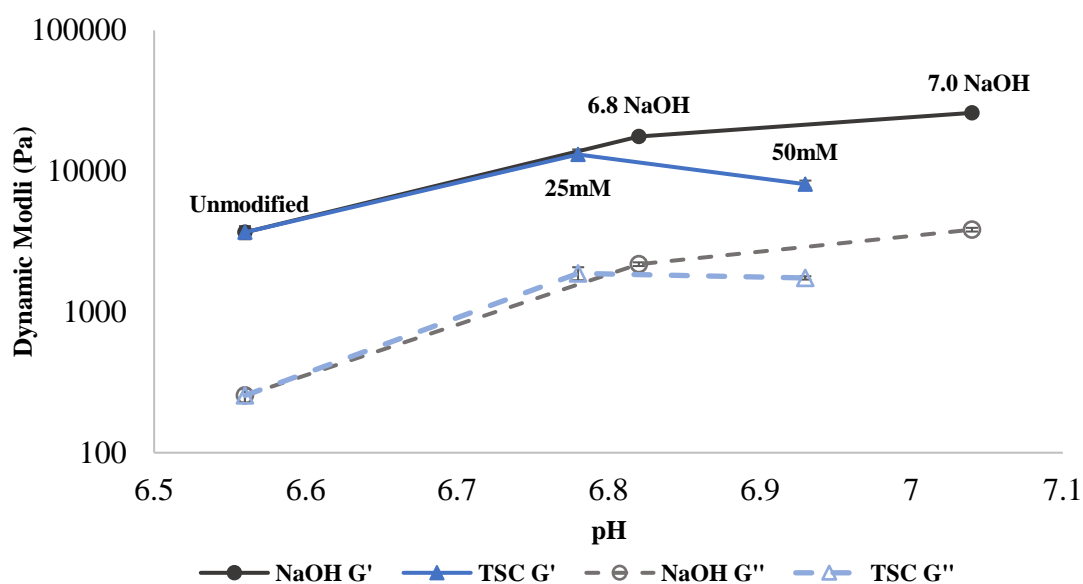


**Figure 4-1:** A comparison of dynamic moduli ( $G'$  and  $G''$ ) between the different treatments of HC-MCC and their effect on pH.

688 **Table 4-1:** Gel Strength Measurements and CGT Values for HC-MCC treatments.

Treatment	G' Value (kPa)				Loss Tangent	CGT
	20°C	8°C	5°C	10hr @ 5°C	5°C (48 rad/s)	(°C)
Control	0.0123±0.00620 <sup>Eb</sup>	0.671±0.147 <sup>Eb</sup>	1.13±0.197 <sup>Eb</sup>	3.68±0.388 <sup>Ea</sup>	0.123±0.011 <sup>B</sup>	8.93±0.69 <sup>D</sup>
TSC 25mM	4.56±0.532 <sup>Cb</sup>	8.16±0.794 <sup>Cb</sup>	9.29±0.863 <sup>Cab</sup>	13.1±1.14 <sup>Ca</sup>	0.141±0.0025 <sup>B</sup>	26.08±0.69 <sup>B</sup>
TSC 50mM	2.53±0.348 <sup>Db</sup>	5.50±0.480 <sup>Db</sup>	6.47±0.505 <sup>Db</sup>	8.10±0.470 <sup>Da</sup>	0.220±0.0035 <sup>A</sup>	21.61±0.34 <sup>C</sup>
NaOH 6.8	7.23±0.260 <sup>Bc</sup>	11.7±0.298 <sup>Bb</sup>	12.9±0.294 <sup>Bb</sup>	17.6±0.0730 <sup>Ba</sup>	0.127±0.005 <sup>B</sup>	27.79±0.34 <sup>AB</sup>
NaOH 7.0	15.1±0.0795 <sup>Ad</sup>	21.4±0.211 <sup>Ac</sup>	22.9±0.248 <sup>Ab</sup>	26.0±0.271 <sup>Aa</sup>	0.144±0.023 <sup>B</sup>	29.16±0.34 <sup>A</sup>

689 Letters denote significant difference at (P<0.05), capital letters denote significant difference across treatments in the same column, and  
 690 lowercase letters denote significant difference within the same row.

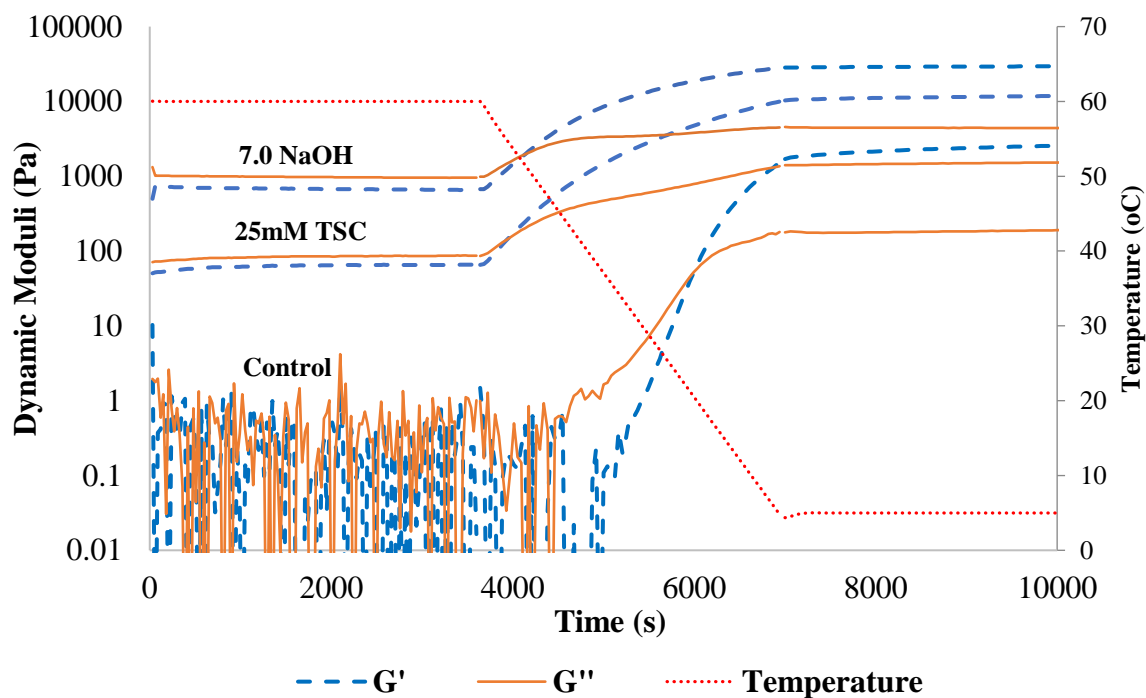
691 Rheological testing of the HC-MCC samples involved three steps: holding at  
 692 60°C for 1hr, followed formation of cold gels by cooling to 5°C in around 56 minutes and  
 693 holding the cold gels at 5°C for 10hrs for curing. While holding samples at 60°C, control  
 694 samples exhibited a higher variance in both  $G'$  and  $G''$  which is attributed to low  
 695 viscoelastic strength nearing the limit of reliable measurement by the rheometer (Sharma  
 696 et al., 2016). Having a low material strength that is near and below the inertia effect of  
 697 the geometry affects sensitivity of the instrument and can create large jumps in the data,  
 698 especially when on a logarithmic scale as seen in Figure 4-2. The material strength of the  
 699 samples added with 25mM TSC ( $G'=80$  Pa) and pH adjusted 7.0 ( $G'=950$ ) was much  
 700 higher than the control ( $\sim 0.5$  Pa) at 60°C. Higher  $G'$  values obtained for the treatment  
 701 samples significantly improved the reliability of the data. Impact of pH adjustment on  $G'$   
 702 values was significantly higher ( $P<0.05$ ) than 25mM TSC samples. Overall, minimal  
 703 changes were observed during holding these samples at 60°C for 1hrs, suggesting that the  
 704 samples were stable under these conditions.

705 As the temperature of the sample was reduced during temperature sweep, the  
 706 values of both dynamic moduli increased, resulting in less noisy data (Figure 4-2).  
 707 Cooling samples from 60°C to 5°C increased gel strength significantly for all four  
 708 treatments (Table 4-1). At the end of the temperature sweep,  $G'$  values obtained for the  
 709 samples were pH 7.0 (22.9kPa) > pH 6.8 (12.9kPa) > 25mM TSC (9.29kPa) < 50mM  
 710 TSC (6.47kPa) > control (1.13kPa) (Table 4-1). This indicates the pH 7.0 treatment was  
 711 most effective in manipulating gel strength of HC-MCC samples. Rate of increase in  $G'$   
 712 with cooling was more pronounced with control samples, possibly due to the fact in the

713 absence of other modifications (pH and TSC), more calcium is available to interact with  
 714 casein micelles which are relatively less hydrated than modified samples (Chapter 3.3.1).

715

716



717

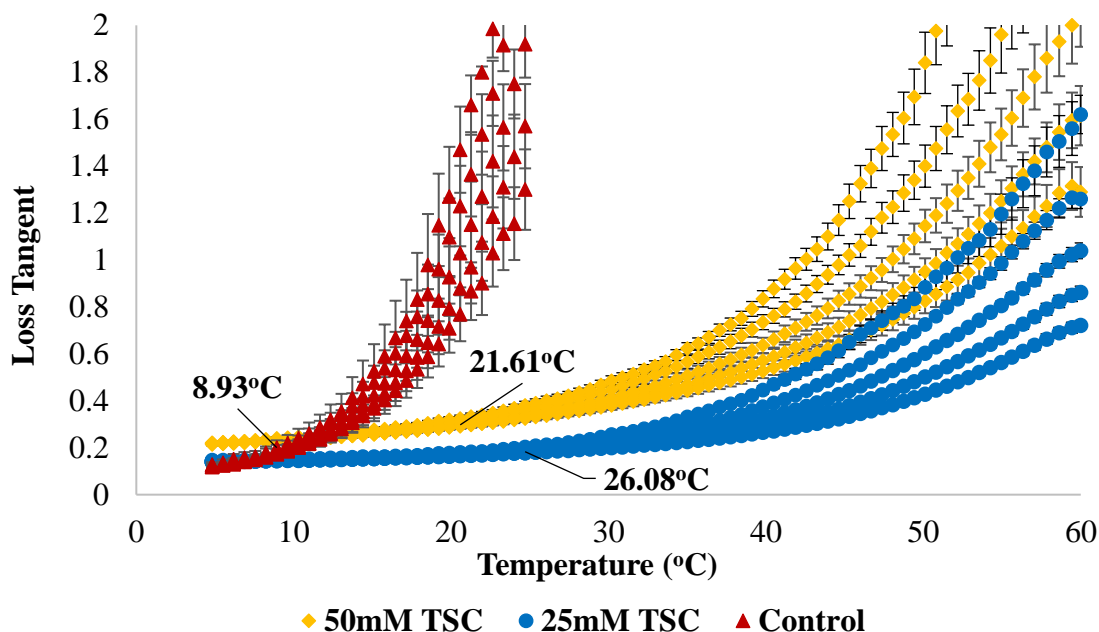
718 **Figure 4-2:** Temperature sweep data for select treatments. A comparison of dynamic  
 719 moduli in response to the temperature sweep in the rheological protocol using 1 rad/s  
 720 frequency

721

722

#### 4.3.2.2: Gelation Measurements

During cooling, we observed that the material was going through a phase transition from a viscoelastic liquid ( $G' < G''$ ) to a viscoelastic solid ( $G' > G''$ ) state with occurrence of a pseudo gelling point, or cross over temperature where  $G' = G''$  (Figure 4-2). This was later accompanied by a true gelling point, where the LT from multiple frequencies converged to one single point, where the values are independent of the frequency measured (Figure 4-3). The crossover temperature for highest gelling samples, i.e., pH 7.0 and 25mM TSC were almost similar (42.5°C and 46.7°C at 1 rad/s respectively), but both were higher than control sample, which crossed over at 15.8°C (Figure 4-2). Similarly, true gelling points were significantly higher for treatments (21.61°C and 29.16°C) than control (8.93°C) for both 25mM TSC and pH 7.0 treatments. After the occurrence of the true gelation point (CGT), the LT reduces further but at slower rate, denoting a further relative increase in elastic properties within the sample and changes in the gel structure. This phenomenon may be related to continuous migration of CCP at slow rate and reduction in kinetic energy and mobility of protein particles (Chapter 3.4).



743

744 **Figure 4-3:** Gelation curves of select treatments. A comparison of multiwave gelation  
 745 curves between three different treatments. Each sample has the loss tangent of 3, 6, 12,  
 746 24, and 48 rad/s measured to observe the convergence of each frequency. The gelation  
 747 point for each treatment was denoted with a temperature value.

748

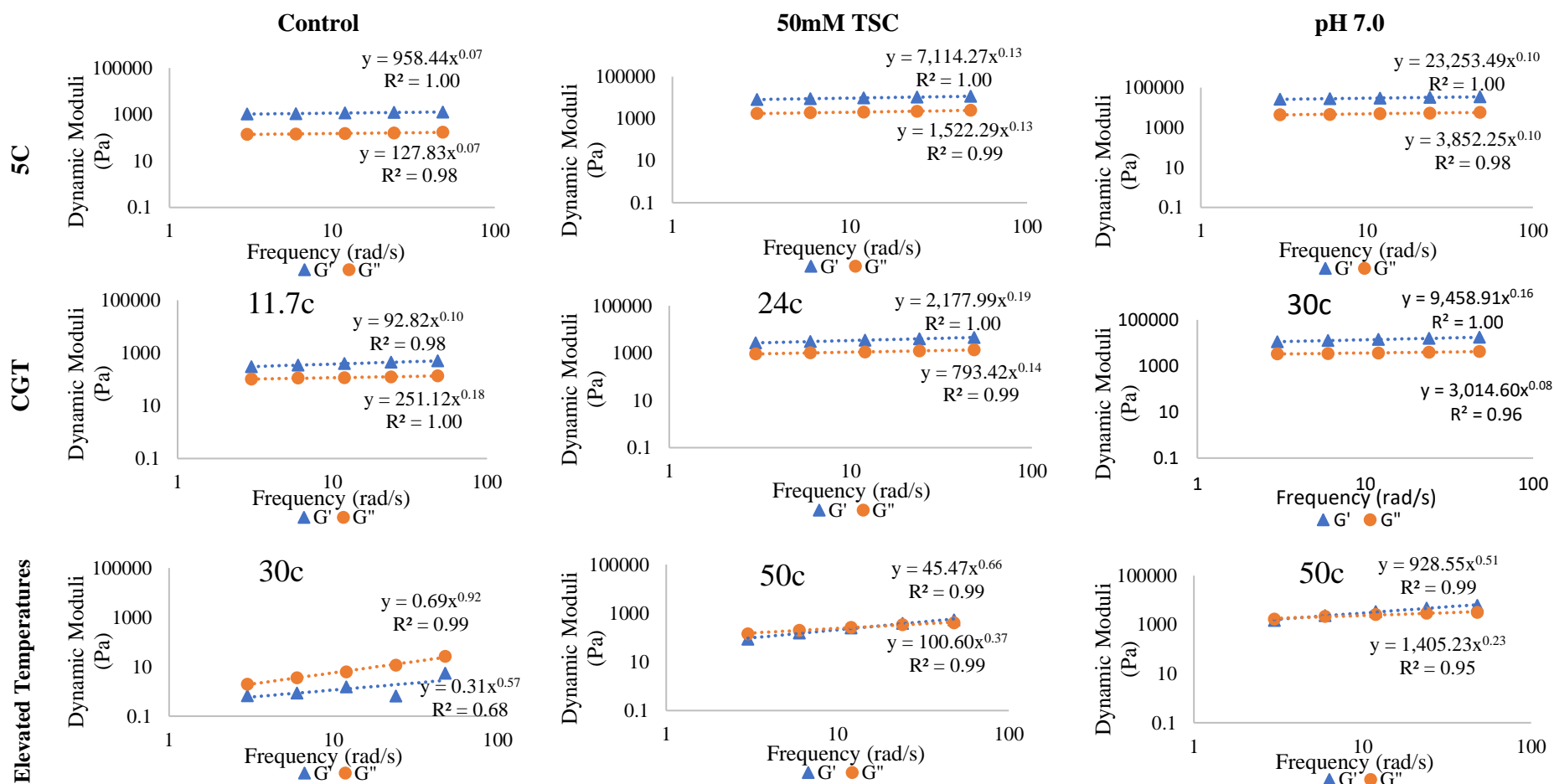
749

### 750 4.3.2.3: Frequency Dependence

751 Frequency sweeps are useful and alternate tools for tracking the phase transition  
 752 and exact state of material from the rheology data (Sharma et al., 2016). Frequency  
 753 dependence can indicate the type of bonding between various structural elements. Above  
 754 CGT,  $G'$  values for control samples had more frequency dependence ( $n > 0.9$ ) than TSC  
 755 and pH treated samples ( $n > 0.5$ ) (Figure 4-4). Higher frequency dependence of  $G'$  is  
 756 linked with weak interaction such as entanglement of polymer units, particularly at higher

757 frequencies (Gaspard et al., 2021; Nordby et al., 2003; Sharma et al., 2016; Tunick, 2011;  
758 Zad Bagher Seighalani et al., 2021). All samples behaved as a weak entangled polymer  
759 network above CGT, because colloidal casein micelles are relatively free to move around  
760 at these temperatures. However, at and below CGT, all samples behaved as crosslinked  
761 stronger gels as indicated by almost no frequency dependence ( $n < 0.2$ ) of  $G'$  (Table 4-2)  
762 (Zad Bagher Seighalani et al., 2021). At the sol-gel transition point, these samples  
763 exhibited almost equal frequency dependence both for  $G'$  and  $G''$ , conforming to the  
764 Winter and Chambon criteria of being LT independent of frequency (Zad Bagher  
765 Seighalani et al., 2021; Winter and Chambon, 1986).





766

767 **Figure 4-4:** Frequency dependency of selected treatments. A comparison of dependance is presented at below CGT (5°C), CGT, and

768 above CGT

769 **Table 4-2:** Tables for Frequency Dependence of HC-MCC Treatments at Different Temperatures.

TREATMENT	5°C				(CGT)				Temperatures above CGT			
	LG'	nG'	LG''	nG''	LG'	nG'	LG''	nG''	LG'	nG'	LG''	nG''
Control	1150±196 <sup>B</sup>	0.065±0.005 <sup>B</sup>	147±19.6 <sup>B</sup>	0.045±0.03 <sup>B</sup>	350±99 <sup>B</sup>	0.150±0.03 <sup>A</sup>	103±10.1 <sup>A</sup>	0.08 <sup>AB</sup>	0.195±0.12 <sup>B</sup>	0.955±0.39 <sup>A</sup>	0.88±0.19 <sup>A</sup>	0.90±0.02 <sup>A</sup>
25mM TSC	9370±935 <sup>AB</sup>	0.085±0.005 <sup>B</sup>	1390±160 <sup>AB</sup>	0.07 <sup>AB</sup>	2340±350 <sup>AB</sup>	0.135±0.005 <sup>A</sup>	635±81.5 <sup>A</sup>	0.045±0.005 <sup>B</sup>	186±45.5 <sup>AB</sup>	0.405±0.02 <sup>A</sup>	213±38 <sup>A</sup>	0.150 <sup>C</sup>
50mM TSC	6600±510 <sup>B</sup>	0.130 <sup>A</sup>	1450±70 <sup>AB</sup>	0.130 <sup>A</sup>	1880±300 <sup>AB</sup>	0.205±0.02 <sup>A</sup>	720±73 <sup>A</sup>	0.150±0.01 <sup>A</sup>	32.8±12.7 <sup>B</sup>	0.695±0.02 <sup>A</sup>	76.9±24.1 <sup>A</sup>	0.405±0.04 <sup>B</sup>
6.8 NaOH	13100±350 <sup>AB</sup>	0.080 <sup>B</sup>	1730±115 <sup>AB</sup>	0.065±0.005 <sup>AB</sup>	4290±220 <sup>AB</sup>	0.11 <sup>A</sup>	981±69.5 <sup>A</sup>	0.030±0.01 <sup>B</sup>	500±21.5 <sup>AB</sup>	0.335±0.02 <sup>A</sup>	470±22.5 <sup>A</sup>	0.080±0.02 <sup>C</sup>
7.0 NaOH	18800±4550 <sup>A</sup>	0.09±0.01 <sup>B</sup>	2860±970 <sup>A</sup>	0.080±0.02 <sup>AB</sup>	7020±2440 <sup>A</sup>	0.135±0.03 <sup>A</sup>	2065±945 <sup>A</sup>	0.055±0.03 <sup>B</sup>	711±219 <sup>A</sup>	0.430±0.08 <sup>A</sup>	960±451 <sup>A</sup>	0.170±0.06 <sup>C</sup>

770

771 Letters denote significant difference at ( $P < 0.05$ ) between values within the same column.

#### 4.3.2.4: Effect of Holding on Gel Strength

The last stage of rheological testing involved holding gelled samples at 5°C for 10hrs. The purpose of this step was to provide enough time for the sample to attain calcium equilibrium. G' increased by 300% for the control sample and 10-40 % for TSC and pH treated samples over the 10hrs of storage time (Table 4-1). The increase in G' for control sample was much steeper compared to the treated samples. This was attributed to the fact that control samples had more available calcium than treated samples, therefore was continuously participating in bridging links between hydrated casein micelles. Another reason for this steeper increase could be related to the fact that treated samples had a CGT, which meant that further cooling post gelling point kept decreasing temperature of the treatment gels and reducing the kinetic energy of the system. This can then result in less mobility of structural components including CCP (Chapter 3.3.3).

#### 4.3.3: Gel Electrophoresis

Urea PAGE conducted on supernatant of each of the 5 samples yielded differences in bands based on the treatment. There were clear indications of leaching out individual casein fractions in the aqueous phase of MCC. All MCC samples show a defined band found near the top of the wells which is absent from the sodium caseinate control. This is assumed to be a residual serum protein which remained in solution after microfiltration. A distinct  $\kappa$ -casein was evident in all lanes, meaning that regardless of treatment, there are free  $\kappa$ -casein strands within solution that were not sedimented during centrifugation (Figure 4-5). Like with  $\kappa$ -casein, there is a distinct and easily visible  $\alpha$ -casein band observable within all treatments and within the sodium caseinate control. The

ratio of  $\alpha$ -casein does not appear to change based off treatment, indicating that both methods of modification do not affect the release of  $\alpha$ -casein into solution. The main difference between treatments is evidenced within  $\beta$ -casein and its variants; control and sodium caseinate had a singular  $\beta$ -casein band (C), while pH adjusted and TSC added samples had the presence of an additional  $\beta$ -casein band (D) (figure 4-5). The concentration of this  $\beta$ -casein variant may be higher within the supernatant of treatment groups, resulting in a stronger band. Migration of beta-casein from casein micelles at low temperatures is a known phenomenon (O'Connell et al., 2003). However, the migration of individual casein fractions and their impact on cold gelling behavior is still unknown.

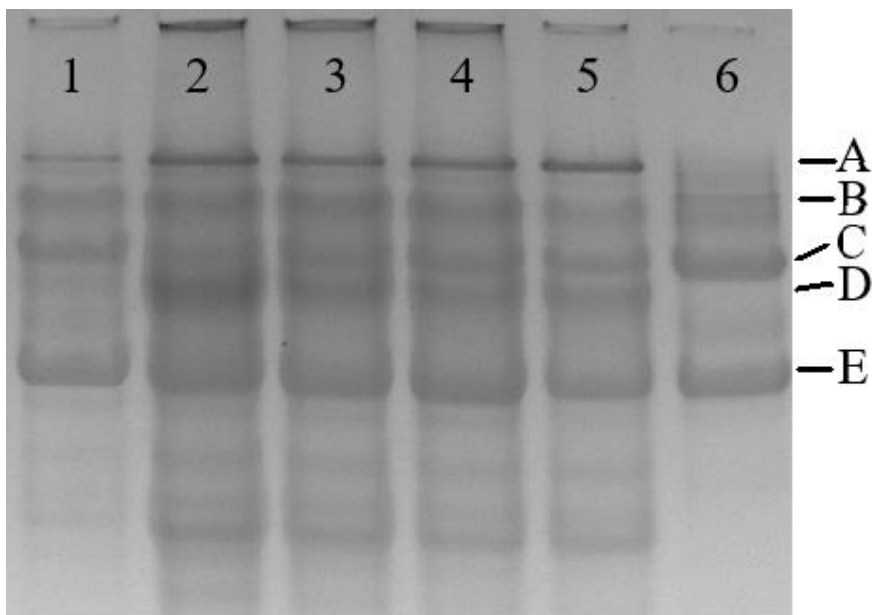


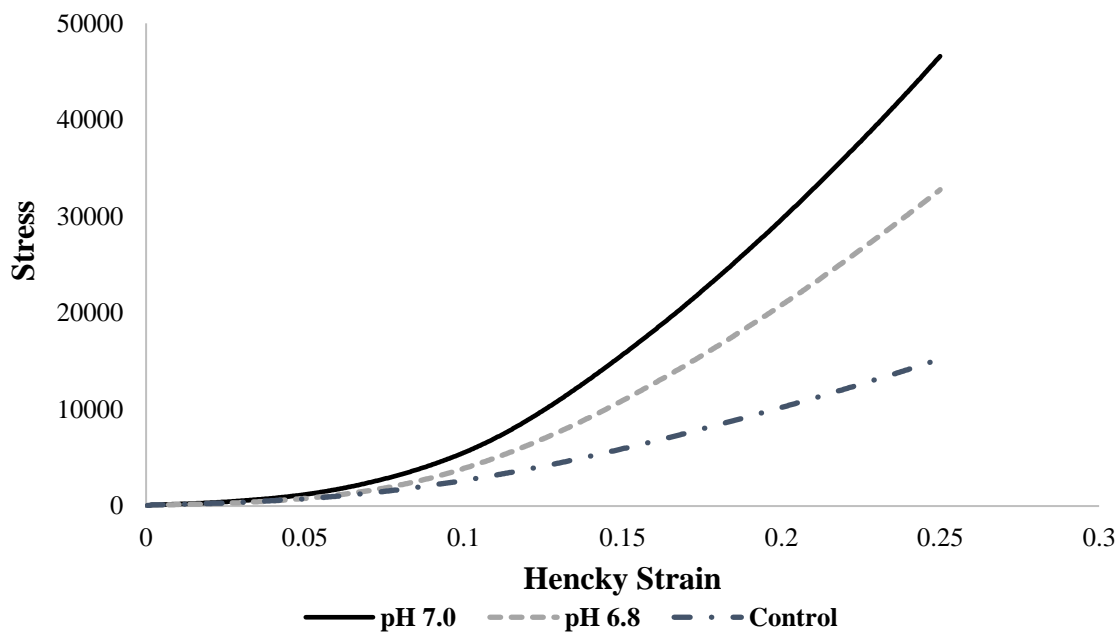
**Figure 4-5:** Urea PAGE of modified HC-MCC supernatants. 1: Unmodified HC-MCC 2: 25mM TSC 3: 50mM TSC 4: pH 6.8 5: pH 7.0 6: Sodium caseinate. A: Serum protein B:  $\kappa$ -casein C:  $\beta$ -casein D:  $\beta$ -casein E:  $\alpha_{s1}$ -casein

#### 810 4.3.4: Texture Analysis

811 Samples under texture profile analysis exhibited a strain hardening behavior,  
812 meaning that under deformation, the strength of the material increases with incremental  
813 increase in strain. pH adjusted samples had a higher degree of strain hardening compared  
814 to control and TSC samples, with pH 7.0 displaying the stronger tendency of strain  
815 hardening (SHR=7.0) (Figure 4-6). Strain hardening is a result of internal friction of  
816 structural elements and formation of new bonds during deformation (Sharma et al.,  
817 2018). Both maximum stress and hardness values were higher in treatment samples  
818 compared to the control. Highest hardness and maximum stress were observed with pH  
819 7.0 adjusted samples (Table 4-3). These results are in line with the linear viscoelastic  
820 parameters, such as  $G'$  as observed in rheological testing. TSC added groups had  
821 significantly lower values of mechanical properties compared to pH adjusted samples  
822 suggesting that the mechanism behind structural changes plays an important role in the  
823 textural properties of the gels.

824

825



826

827 **Figure 4-6:** Compressional testing of pH adjusted gels. Values are until 25% maximum  
 828 strain.

829

830

831 **Table 4-3:** Texture Analysis Results

Treatment	Control	25mM TSC	50mM TSC	pH 6.8	pH 7.0
Maximum Stress (Pa)	25500±1860 <sup>C</sup>	32100±1510 <sup>B</sup>	37300±2480 <sup>B</sup>	62500±1050 <sup>A</sup>	71200±3080 <sup>A</sup>
Strain Hardening Ratio (SHR)	2.35±0.110 <sup>D</sup>	2.91±0.125 <sup>CD</sup>	4.79±0.450 <sup>BC</sup>	6.32±0.660 <sup>AB</sup>	7.00±0.575 <sup>A</sup>
Hardness (g)	263±19.0 <sup>C</sup>	369±7.27 <sup>BC</sup>	452±33.8 <sup>B</sup>	715±12.3 <sup>A</sup>	799±30.7 <sup>A</sup>

832 Values are mean ± standard error. Letters designate significant difference between  
 833 treatments at a 0.05 significance level.

834

#### 835 4.3.5: Transmission Electron Microscopy

836 TEM images obtained from control samples indicated clear and distinctive  
837 micellar structures that had minimal space between structures exhibiting a potential  
838 jamming effect as observed by Lu et al., (2015). The effect of calcium chelation via TSC  
839 however, resulted in distinctive morphological changes in the micellar structure of casein  
840 and its fragments. At lower magnification (2000x), the structure from control samples,  
841 25mM TSC and pH 6.8 gels appeared to have only minor variations (Figure 4-7). At pH  
842 6.8, samples exhibited a slightly smaller particle size with more dispersion of casein in  
843 the aqueous phase. This phenomenon became more pronounced at pH 7.0 with even  
844 smaller size and more dispersion of casein fractions. This indicates the casein micelles  
845 may be undergoing a fragmentation of structure (dissociation) at higher pH levels, and  
846 the released fragments interact with the aqueous phase to a greater extent (more protein-  
847 water interactions). On the other hand, a very slight increase in the number of larger-size  
848 particles was observed for 25mM TSC samples compared to control samples, indicating  
849 relatively more protein-protein interactions compared to control and pH treatments.  
850 Samples with 50mM added TSC formed larger aggregates, often in sizes  $>1\ \mu\text{m}$ . We  
851 believe these aggregates are formed after casein micelles are disintegrated due to calcium  
852 chelation action of TSC.

853 It is clear from the high magnification images (20,000x) that control samples  
854 exhibited a distinctive border between micellar structures, which was also the case for  
855 residual intact micelles at pH 6.8, suggesting a better integrity of the casein micelles.  
856 However, TSC samples exhibited the disappearance of distinctive borders of intact  
857 micelles, and many of the smaller structures evident in the control sample were no longer

858 present. Rather than exhibiting a distinct border, the remaining structures were instead  
859 mixing with the adjacent aqueous phase, indicating release of CCP and by extension,  
860 casein fragments. The increased interactivity due to calcium chelation may occur first at  
861 the exterior surface of the micelle and then in the interior. The release of these individual  
862 casein fractions was confirmed through Urea-PAGE (Figure 4-5). We believe that the  
863 smaller micelles were disintegrating first due to the calcium chelating action of TSC. At  
864 50mM concentrations, the complete collapse of micellar structure was accompanied with  
865 the formation of new type of aggregated structure dispersed in a unique continuous  
866 protein network (hydrated matrix formed from fragmented casein fractions). The  
867 formation of the new aggregate structures indicates that the new structures were not  
868 interacting strongly with the aqueous phase, therefore causing a decline in the  $G'$  (Figure  
869 4-1; Table 4-1).

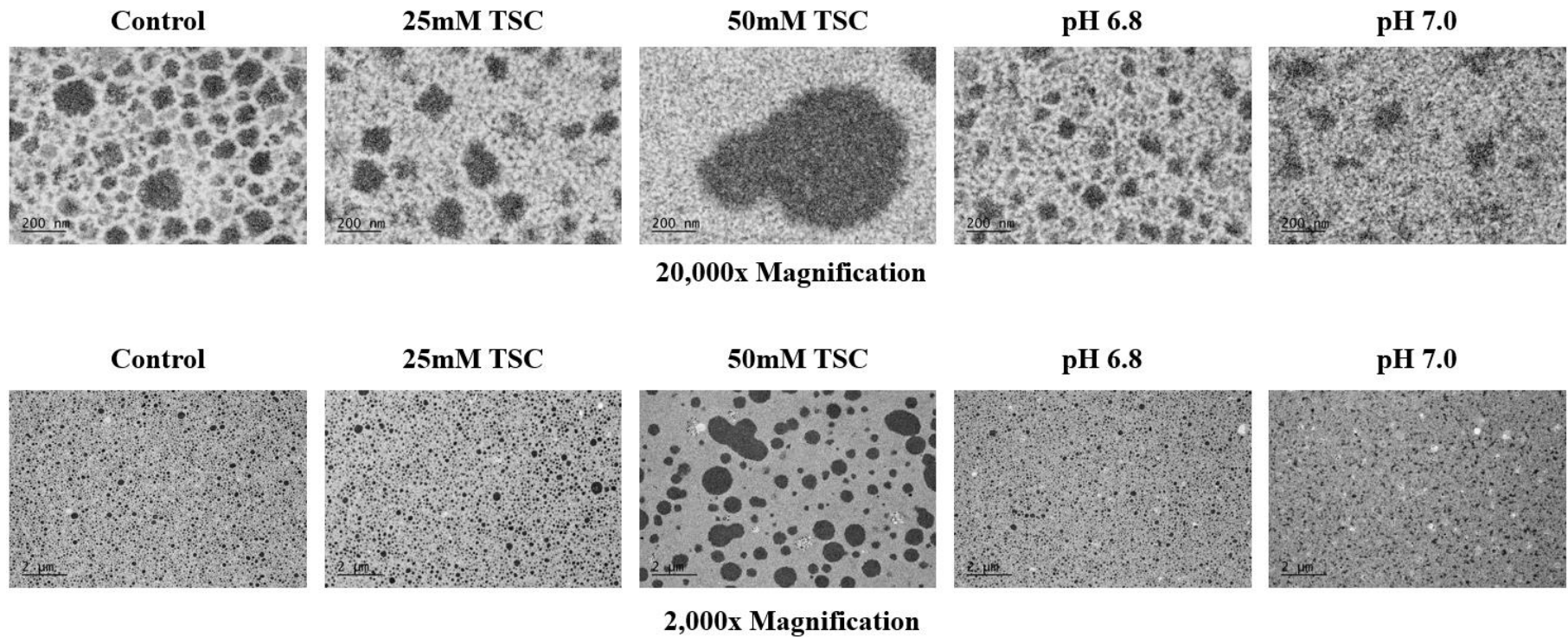
870         At pH 7.0 casein micelles and their fragmented structures interacted with the  
871 aqueous phase at a higher rate, therefore exhibited higher gel strength (Figure 4-1 and  
872 Table 4-1). Samples at pH 7.0 had an overall darker appearance in micrographs due to the  
873 dissociation of all micelles within solution. These individual caseins created a complete  
874 network which encompasses the sample. This dense network offers a good explanation as  
875 to why 7.0 pH samples formed the strongest gels within the study; the complete  
876 dissolution of micellar structures coupled with a high degree of crosslinking between  
877 caseins show much more interaction than control and TSC samples. While there is little  
878 research on alkalized casein micelle structure, the micrographs exhibiting this casein  
879 matrix are novel, allowing additional research to be conducted on casein matrix  
880 formation in alkaline conditions.



881           In the TEM micrographs, white spots were considered remnants of fat globules.  
882   We observed some indication of emulsified fat globule structures in the samples with  
883   50mM TSC via the presence of protein structures around fat globules (Figure 4-8). It is  
884   likely that these proteins are being released due to calcium chelation activity of TSC and  
885   acting as an emulsifier (Lazzaro et al., 2017).

886

887

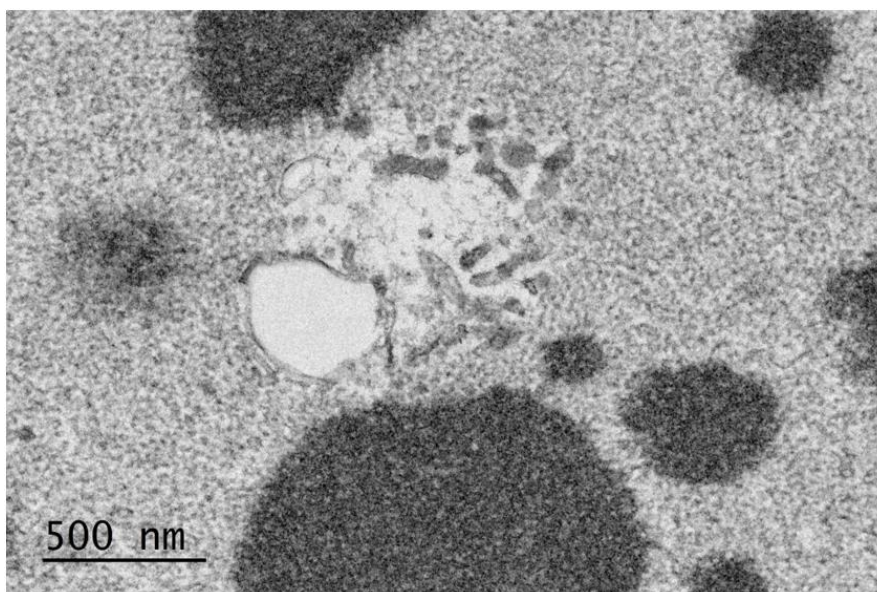


888

889 **Figure 4-7:** TEM micrographs of treatments at 20,000x and 2,000x magnification. Samples were harvested after holding at 5°C for 10  
890 hours.

891

892



893

894 **Figure 4-8:** Emulsification effect observed in 50mM TSC micrographs. Magnification  
895 level is 10,000x

896

897

898

#### 4.4: Discussions

899

900 Comparisons of gelling points obtained from the multiwave technique (Figure 4-  
901 3) and cross over temperature (Figure 4-2) indicated discrepancy which was dependent  
902 on the frequency measured. The discrepancy increases as dynamic moduli increases,  
903 suggesting that crossover point methodology is less accurate with stronger gels.

904

905 With a high strength gel, the  $G'$  must increase at the same proportional rate as a  
906 weaker gel in order to result in a lower LT value. However, for a strong gel with a high  
907 starting  $G'$  value, this means that an increase in the  $G'$  value must be far higher than a  
weak sample that is more sensitive to temperature. For reference, the  $G'$  values for pH

908 7.0 samples increased from 15100Pa to 26000Pa while cooling from 20°C to 5°C,  
909 whereas control samples raised from 12.3Pa to 3680Pa in the same timeframe. While  
910 control samples reached a higher G' value in proportion to its starting value, the samples  
911 at pH 7.0 gained more in plain numbers, which results in a larger difference between the  
912 gelling point observed from both methods. These results are in line with the observations  
913 made by Zad Bagher Seighalani et al. (2021)

914       Elevated temperatures (e.g. 40°C) in conjunction with elevated pH levels (pH 8)  
915 are known to encourage micellar destabilization (Vaia et al., 2006); the step where the  
916 sample was held at 60°C for 1hr might have encouraged the destruction of the micellar  
917 structure and was a major factor in catalyzing the formation of the matrix of individual  
918 caseins shown in 7.0 pH samples. TEM micrographs exhibiting the morphological  
919 changes in casein micelles with either type of treatment indicate the destabilization of  
920 casein. Both of these modifications indicated that the increase in gel strength was due to  
921 increasing interactions between casein fragments and the aqueous phase. It is still unclear  
922 how does these fragments interact among each other and water to form a stronger gel.  
923 Additional research into the development of these new structures is required to gather a  
924 better understanding of the destabilizing effect of calcium chelation and pH  
925 modifications.

926       TSC within solution appears to chelate the structural CCP from the micelle  
927 leading to partial structural dissociation resulting in a network seen in the micrographs  
928 (de Kort et al., 2011). Evidence of potential crosslinking between caseins supports  
929 rheological data (Figure 4-1), as 25mM TSC samples were significantly stronger and had  
930 a significantly higher gelation temperature ( $P < 0.05$ ).

931           When comparing findings from the TEM micrographs with rheological data, the  
932   formation of aggregates in 50mM TSC samples could offer insight as to why the gel  
933   strength is reduced at this concentration. As there is greater space (reduced volume  
934   fractions of new denser protein structures) between aggregates compared to the spaces  
935   between micelles in the control sample, there is potential for higher mobility within  
936   solution. As such, there is a greatly reduced packing and particle interaction effect  
937   between structures, which results in lower strength compared to other treatment samples.  
938   50mM samples also had significant rheological differences compared to other samples  
939   within the study; at 5°C the frequency dependence of  $G'$  of 50mM samples ( $n>0.1$ ) was  
940   found to be significantly higher than other samples ( $n<0.1$ ) within the study (Table 4-2).

941           The main determinant of gel strength in this study appears to be based on protein  
942   interactivity, with increased protein-water and protein-protein (outside of the micellar  
943   structure) resulting in increased strength. Control samples exhibited minimal interaction  
944   outside of the micellar structure, and as such, they had the lowest  $G'$  and CGT values.  
945   However, the disintegration of the micellar structure seen in pH 7.0 samples and the  
946   formation of one continuous phase resulted in the strongest samples measured. The same  
947   can be said between 25mM and 50mM TSC samples; while 50mM resulted in the  
948   disintegration of the original micellar structure, the new aggregates had less interaction  
949   with the aqueous phase due to the larger size of the structures compared to 25mM TSC.  
950   As such, the gel strength and CGT is significantly lower.

951

952

## 4.5: Conclusions

pH and TSC modifications at all levels of treatment resulted in an increase in gel strength and temperature of gelation. pH had larger impact on increase of gel strength than TSC treatments. TSC samples at 25mM concentrations formed stronger gels that transitioned earlier in rheological testing compared to 50mM TSC samples. 50mM TSC concentrations resulted in creation of unique aggregated structures which were less interactive with aqueous phase, slightly weakening gel matrix. The effect of calcium chelation and pH treatment resulted in the dissolution of micellar casein structure as observed through TEM and Urea-PAGE analysis. pH adjustment to 7.0 resulted in the strongest gels of all treatments. While both methods of treatment exhibited elevated material properties and changes in morphology, it is likely that the mechanisms for formation of cold gels may be different. Therefore, more research is needed to elucidate the exact mechanism of cold gel formation.

## References

- 968
- 969 Bast, R., Sharma, P., Easton, H. K. B., Dessev, T. T., Lad, M., & Munro, P. A. (2015).
- 970 Tensile testing to quantitate the anisotropy and strain hardening of mozzarella
- 971 cheese. *International Dairy Journal*, 44, 6–14.
- 972 <https://doi.org/10.1016/j.idairyj.2014.12.006>
- 973 de Kort, E., Minor, M., Snoeren, T., van Hooijdonk, T., & van der Linden, E. (2011).
- 974 Effect of calcium chelators on physical changes in casein micelles in concentrated
- 975 micellar casein solutions. *International Dairy Journal*, 21(12), 907–913.
- 976 <https://doi.org/10.1016/j.idairyj.2011.06.007>
- 977 Dunn, M., Barbano, D. M., & Drake, M. (2021). Viscosity changes and gel formation
- 978 during storage of liquid micellar casein concentrates. *Journal of Dairy Science*,
- 979 104(12), 12263–12273. <https://doi.org/10.3168/jds.2021-20658>
- 980 Gaspard, S. J., Sharma, P., Fitzgerald, C., Tobin, J. T., O'Mahony, J. A., Kelly, A. L., &
- 981 Brodkorb, A. (2021). Influence of chaperone-like activity of caseinomacropptide
- 982 on the gelation behaviour of whey proteins at pH 6.4 and 7.2. *Food*
- 983 *Hydrocolloids*, 112, 106249. <https://doi.org/10.1016/j.foodhyd.2020.106249>
- 984 Higham, A. K., Garber, L. A., Latshaw, D. C. I., Hall, C. K., Pojman, J. A., & Khan, S.
- 985 A. (2014). Gelation and Cross-Linking in Multifunctional Thiol and
- 986 Multifunctional Acrylate Systems Involving an in Situ Comonomer Catalyst.
- 987 *Macromolecules*, 47(2), 821–829. <https://doi.org/10.1021/ma402157f>
- 988 Lamichhane, P., Sharma, P., Kennedy, D., Kelly, A. L., & Sheehan, J. J. (2019).
- 989 Microstructure and fracture properties of semi-hard cheese: Differentiating the

- 990 effects of primary proteolysis and calcium solubilization. *Food Research*  
991 *International*, 125, 108525. <https://doi.org/10.1016/j.foodres.2019.108525>
- 992 Lazzaro, F., Saint-Jalmes, A., Violleau, F., Lopez, C., Gaucher-Delmas, M., Madec, M.-  
993 N., Beaucher, E., & Gaucheron, F. (2017). Gradual disaggregation of the casein  
994 micelle improves its emulsifying capacity and decreases the stability of dairy  
995 emulsions. *Food Hydrocolloids*, 63, 189–200.  
996 <https://doi.org/10.1016/j.foodhyd.2016.08.037>
- 997 Liu, S., Huang, S., & Li, L. (2016). Thermoreversible gelation and viscoelasticity of  $\kappa$ -  
998 carrageenan hydrogels. *Journal of Rheology*, 60(2), 203–214.  
999 <https://doi.org/10.1122/1.4938525>
- 1000 Lu, Y., McMahon, D. J., Metzger, L. E., Kommineni, A., & Vollmer, A. H. (2015).  
1001 Solubilization of rehydrated frozen highly concentrated micellar casein for use in  
1002 liquid food applications. *Journal of Dairy Science*, 98(9), 5917–5930.  
1003 <https://doi.org/10.3168/jds.2015-9482>
- 1004 Lu, Y., McMahon, D. J., & Vollmer, A. H. (2016). Investigating cold gelation properties  
1005 of recombined highly concentrated micellar casein concentrate and cream for use  
1006 in cheese making. *Journal of Dairy Science*, 99(7), 5132–5143.  
1007 <https://doi.org/10.3168/jds.2015-10791>
- 1008 Marchin, S., Putaux, J.-L., Pignon, F., & Léonil, J. (2007). Effects of the environmental  
1009 factors on the casein micelle structure studied by cryo transmission electron  
1010 microscopy and small-angle x-ray scattering/ultras-small-angle x-ray scattering.  
1011 *The Journal of Chemical Physics*, 126(4), 045101.  
1012 <https://doi.org/10.1063/1.2409933>



- 1013 McMahon, D. J., & Oommen, B. S. (2008). Supramolecular Structure of the Casein  
 1014 Micelle. *Journal of Dairy Science*, 91(5), 1709–1721.  
 1015 <https://doi.org/10.3168/jds.2007-0819>
- 1016 Nordby, M. H., Kjøniksen, A.-L., Nyström, B., & Roots, J. (2003). Thermoreversible  
 1017 Gelation of Aqueous Mixtures of Pectin and Chitosan. *Rheology*.  
 1018 *Biomacromolecules*, 4(2), 337–343. <https://doi.org/10.1021/bm020107+>
- 1019 O’Connell, J. E., Grinberg, V. Ya., & de Kruif, C. G. (2003). Association behavior of  $\beta$ -  
 1020 casein. *Journal of Colloid and Interface Science*, 258(1), 33–39.  
 1021 [https://doi.org/10.1016/S0021-9797\(02\)00066-8](https://doi.org/10.1016/S0021-9797(02)00066-8)
- 1022 On-Nom, N., Grandison, A. S., & Lewis, M. J. (2010). Measurement of ionic calcium,  
 1023 pH, and soluble divalent cations in milk at high temperature. *Journal of Dairy*  
 1024 *Science*, 93(2), 515–523. <https://doi.org/10.3168/jds.2009-2634>
- 1025 Ozcan-Yilsay, T., Lee, W.-J., Horne, D., & Lucey, J. A. (2007). Effect of Trisodium  
 1026 Citrate on Rheological and Physical Properties and Microstructure of Yogurt.  
 1027 *Journal of Dairy Science*, 90(4), 1644–1652. <https://doi.org/10.3168/jds.2006-538>
- 1028 Saboyainsta, L. V., & Maubois, J.-L. (2000). Current developments of microfiltration  
 1029 technology in the dairy industry. *Le Lait*, 80(6), 541–553.  
 1030 <https://doi.org/10.1051/lait:2000144>
- 1031 Salaün, F., Mietton, B., & Gaucheron, F. (2005). Buffering capacity of dairy products.  
 1032 *International Dairy Journal*, 15(2), 95–109.  
 1033 <https://doi.org/10.1016/j.idairyj.2004.06.007>
- 1034 Sharma, P., Munro, P. A., Dessev, T. T., Wiles, P. G., & Buwalda, R. J. (2016). Effect of  
 1035 shear work input on steady shear rheology and melt functionality of model

- 1036           Mozzarella cheeses. *Food Hydrocolloids*, 54, 266–277.
- 1037           <https://doi.org/10.1016/j.foodhyd.2015.10.009>
- 1038   Sharma, P., Munro, P. A., Dessev, T. T., Wiles, P. G., & Foegeding, E. A. (2018). Strain
- 1039           hardening and anisotropy in tensile fracture properties of sheared model
- 1040           Mozzarella cheeses. *Journal of Dairy Science*, 101(1), 123–134.
- 1041           <https://doi.org/10.3168/jds.2017-13126>
- 1042   Touhami, S., Marciniak, A., Doyen, A., & Brisson, G. (2022). Effect of alkalization
- 1043           and ultra-high-pressure homogenization on casein micelles in raw and pasteurized
- 1044           skim milk. *Journal of Dairy Science*, 105(4), 2815–2827.
- 1045           <https://doi.org/10.3168/jds.2021-20700>
- 1046   Vaia, B., Smiddy, M. A., Kelly, A. L., & Huppertz, T. (2006). Solvent-Mediated
- 1047           Disruption of Bovine Casein Micelles at Alkaline pH. *Journal of Agricultural and*
- 1048           *Food Chemistry*, 54(21), 8288–8293. <https://doi.org/10.1021/jf061417c>
- 1049   Vollmer, A. H., Kieferle, I., Püsl, A., & Kulozik, U. (2021). Effect of pentasodium
- 1050           triphosphate concentration on physicochemical properties, microstructure, and
- 1051           formation of casein fibrils in model processed cheese. *Journal of Dairy Science*,
- 1052           104(11), 11442–11456. <https://doi.org/10.3168/jds.2021-20628>
- 1053   Wang, Q., & Ma, Y. (2020). Effect of temperature and pH on salts equilibria and calcium
- 1054           phosphate in bovine milk. *International Dairy Journal*, 110, 104713.
- 1055           <https://doi.org/10.1016/j.idairyj.2020.104713>
- 1056   Winter, H. H., & Chambon, F. (1986). Analysis of Linear Viscoelasticity of a
- 1057           Crosslinking Polymer at the Gel Point. *Journal of Rheology*, 30(2), 367–382.
- 1058           <https://doi.org/10.1122/1.549853>

- 1059 Younes, E. (2017). Structural Properties of Casein Micelles in Milk, the effect of salt,  
1060 temperature, and pH. *International Journal of Biotechnology and Bioengineering*,  
1061 3(6), 202–215. <https://doi.org/10.25141/2475-3432-2017-6.0202>
- 1062 Zad Bagher Seighalani, F., McMahon, D. J., & Sharma, P. (2021). Determination of  
1063 critical gel-sol transition point of Highly Concentrated Micellar Casein  
1064 Concentrate using multiple waveform rheological technique. *Food Hydrocolloids*,  
1065 120, 106886. <https://doi.org/10.1016/j.foodhyd.2021.106886>
- 1066
- 1067

## CHAPTER 5

## EFFECT OF KAPPA CARRAGEENAN ADDITION ON

## COLD GELLING BEHAVIOR OF MICELLAR CASEIN DISPERSIONS

**ABSTRACT**

This study aims to study the gelation properties of Micellar Casein Concentrate (MCC) in conjunction with the addition of  $\kappa$ -carrageenan and physicochemical modifications in the form of calcium chelation and alkalization via trisodium citrate and sodium hydroxide respectively. Using a 3 stage multi-frequency testing protocol, we observed the rheological properties of modified MCC in response to declining temperature. Ultrastructure analysis via TEM was conducted to observe the effect of  $\kappa$ -carrageenan (KC) inclusion in conjunction with treatments. In addition to these, particle size, zeta potential, and texture profile analysis methods were conducted in order to understand more about the gelling properties of MCC. Alkalization of the sample raised gel strength compared to control samples, although  $\kappa$ -carrageenan inclusion into HC-MCC was the main source of increases in gel strength and gelation temperatures. TEM micrographs depict 2 separate phases within the solution despite high shear homogenization, as well as minimal interaction between these two phases. This study

1090 lays the groundwork for additional work on HC-MCC on understanding cold gel  
1091 formation.

1092

## 1093 **5.1: Introduction**

1094

1095 Modern trends in the food industry have moved towards a clean label approach  
1096 during the formulation of a product. In the dairy industry, many polysaccharide-based  
1097 gums are utilized in various products to improve textural aspects and reduce syneresis  
1098 (Rafiq et al., 2020). While improving these aspects of a food are important, so is taking  
1099 into consideration the concern of consumers. Studies have found that many of these gums  
1100 are perceived negatively by consumers, meaning that reduction in use could lead to better  
1101 product perception (Maruyama et al., 2021). Highly Concentrated-Micellar Casein (HC-  
1102 MCC) is a concentrated form of micellar casein concentrate (MCC), created via the  
1103 microfiltration of milk to concentrate casein within solution. Previous studies have  
1104 observed the formation of a cold gel in HC-MCC or conducted research on its material  
1105 properties (Dunn et al., 2021; Lu et al., 2016; Zad Bagher Seighalani et al., 2021). These  
1106 studies propose that gelation comes from a packing or jamming transition, where an  
1107 increase in entropy within the system combined with steric hinderance between micellar  
1108 structures limit flow and deformation of the sample in cold temperatures. While the exact  
1109 mechanism behind the formation of a cold gel is still not known, there is a potential  
1110 application in the use of HC-MCC as an alternative ingredient in dairy products to  
1111 increase viscosity and stabilize solutions. Due to its composition (17-23% casein in  
1112 solution), it offers a clean label option by utilizing dairy proteins for stabilizing properties

1113 rather than gum-based products currently used. To consider HC-MCC as a potential  
1114 ingredient in the future, a better understanding of its gelation is required to apply it to  
1115 specific foods.

1116       Previous studies have shown that physicochemical modifications such as calcium  
1117 chelation via trisodium citrate (TSC) and alkalization of HC-MCC yield increases in gel  
1118 strength and raise the temperature in which the sample forms a gel (Ozcan-Yilsay et al.,  
1119 2007). The reason behind this change in properties is due to the destabilization of the  
1120 micellar structure in response to the modification applied. While the methods of  
1121 treatment create a different effect on the morphology of casein, both are able to increase  
1122 gel qualities. Calcium chelation removes the structural colloidal calcium phosphate  
1123 (CCP) within the micelle (Udabage et al., 2000). Such a reaction can result in the release  
1124 of free casein fragments into a solution, increasing interactivity between structures. On  
1125 the other hand, alkalization of the sample is thought to increase the negative charges on  
1126 caseins promoting further interaction between protein and water, culminating in the  
1127 dissociation of the micellar structure (Sinaga et al., 2017). Both treatments encourage  
1128 interaction among proteins outside of the micellar structure, which is thought to be the  
1129 reason why gel properties increase compared to unmodified samples. This increased rate  
1130 of interaction, however, is the antithesis of the packing/jamming effect previously  
1131 described, indicating that further research is required to fully understand the mechanisms  
1132 behind gelation.

1133       While polysaccharide-based stabilizers have had declining preference,  $\kappa$ -  
1134 carrageenan (KC) is still a commonly used product within the dairy industry (Campbell  
1135 & Hotchkiss, 2017). KC is well known for its variable conformation in response to

1136 temperature; in temperatures above 50°C, the structure converts from a helix to a coil  
1137 (Bourriot et al., 1999). The helix form of KC assists in the gelation of protein solutions  
1138 by binding to micelles and encouraging interaction with the newly bound polysaccharide  
1139 chains (Drohan et al., 1997; Spagnuolo et al., 2005).

1140         While there have been multiple studies exhibiting the interactions between casein  
1141 and carrageenan mixtures (Bourriot et al., 1999; Spagnuolo et al., 2005; Pang et al.,  
1142 2015), there has been minimal research exhibiting the interaction between KC and casein  
1143 with the addition of calcium chelating salts. This study aims to study the potential  
1144 interactions between KC and modified casein micelles, be it from calcium chelation or  
1145 from pH adjustment. While the addition of KC or a calcium chelating salt to a casein gel  
1146 may not be considered clean label, it will be used to better understand the gelation  
1147 properties of HC-MCC. We also intend to observe how the addition of KC to HC-MCC  
1148 can reduce the minimum amount of protein required to form a gel, and how it may impact  
1149 the other qualities of the gel such as texture and gel strength.

1150

## 1151                                 **5.2: Materials and Methods**

1152

### 1153         **5.2.1: HC-MCC Manufacture and Storage**

1154         HC-MCC used in the study was produced by South Dakota State University in the  
1155 same manner as described in Lu et al., (2015). The MF system was a 4-vessel continuous  
1156 design utilizing polyvinylidene fluoride membranes with a combined surface area of  
1157 57.4m<sup>2</sup>. The subsequent vacuum evaporation of the MCC occurred at 63°C at a pressure  
1158 of -680mbar. The samples will be held in large pails within a -20°C freezer, where they

were taken out and molten to a liquid state via water bath. The liquid HC-MCC is thoroughly mixed and poured into screw cap plastic containers in ~120g quantities. To prevent microbial spoilage, all HC-MCC used had 0.05% wt/wt sodium azide added. Samples not in use returned to the -20°C freezer until ready for use. Sample cups were thawed in a water bath and stored in refrigerators in between tests. All tests were performed in triplicate.

1165

#### 1166 **5.2.1.1: HC-MCC Modifications**

1167 Modifications to the HC-MCC were in 4 categories: dilution, pH adjustment,  
1168 calcium chelating (TSC) salt addition, and KC addition. Adjustment of protein content  
1169 was performed with deionized water. Adjustment of pH was accomplished utilizing  
1170 sodium hydroxide (NaOH) as a base. For pH adjustment, samples were first  
1171 homogeneously mixed using an overhead mixer for 2 minutes, followed by the addition  
1172 of NaOH and were mixed further for 3 minutes. The samples were then held at room  
1173 temperature for 2 hours to allow for the additions to dissolve. The calcium chelating salt  
1174 used in this study was food grade trisodium citrate dihydrate (TSC), sourced from Cargill  
1175 (Eddyville, IA). TSC at a 25mM concentration was added to the samples at 60°C with  
1176 constant stirring using a glass rod immediately prior to loading into the rheometer. For  
1177 some samples, additional heating for 5 seconds in a microwave was required to fully  
1178 incorporate the salt.

1179 Treatment samples from each group were diluted with DI water from 18.5% to  
1180 10% protein and will serve as a baseline for further testing. MCC then had 0.1%, 0.2%,  
1181 or 0.3% wt/wt KC added. The sample was then vortexed within a centrifuge tube at 2800



1182 rpm for 30 seconds and warmed in a water bath to 40°C. Lastly, the sample was  
1183 homogenized using an Omni GLH (Kennesaw, GA) tissue homogenizer to ensure a lack  
1184 of  $\kappa$ -carrageenan aggregation.

1185

### 1186 **5.2.2: SMUF Preparation**

1187 Reagent salts found in Table 3-1 were measured and mixed in proportion to create  
1188 SMUF in 1-liter quantities. The remaining volume is filled with deionized water and  
1189 stirred until the salts are solubilized. The salt solution was filtered using a vacuum flask  
1190 and a Millipore 1.2 $\mu$ m filter (Bedford, MA). To prevent precipitation of phosphates in the  
1191 completed buffer, the SMUF was stored in a refrigerator at 5°C in between uses.

1192

### 1193 **5.2.3: Rheological testing**

1194 Rheological measurements were performed using an Anton Paar MCR 302  
1195 rheometer (Anton Paar GMBH, Graz, Austria) using a concentric cylinder geometry  
1196 setup (model no. CC27). For sample loading, 20ml of sample was heated to 40°C and  
1197 poured into the bottom of the sample cylinder. An oil layer is added on the top via a  
1198 pipette to prevent dehydration during the rheological protocol. Rheological testing was  
1199 conducted in three stages (Figure 3-1). In the first stage a time sweep was conducted by  
1200 holding the sample at 40°C for 5 minutes, recording data every 30 seconds for a total of  
1201 10 data points. The following temperature sweep decreased from 40°C to 5°C and  
1202 recorded data every 41.25 seconds resulting in 51 data points. Lastly, the third stage held  
1203 samples at 5°C for at least 10 hours, making measurements every minute. Rheological

1204 testing was conducted by applying simultaneously multiple angular frequencies (3, 6, 12,  
1205 24, and 48 rad/s), and gelation point was determined by using the criteria described in by  
1206 Zad Bagher Seighalani et al., (2021), where gelation point was defined as the point where  
1207 the loss tangent of the sample is independent of frequencies applied (Winter & Chambon,  
1208 1986). Storage modulus ( $G'$ ) values obtained during the temperature sweep at 20°C, 8°C,  
1209 5°C at the end of the temperature sweep, and holding 5°C for 10 hours during the time  
1210 sweep will be used to compare gel strength between the different treatments.

1211

#### 1212 **5.2.4: Texture Analysis**

1213 Texture analysis of treatments was conducted using a TA-XT Plus texture  
1214 analyzer (Stable Micro System Ltd., Surrey, UK) with a texture profile test using a two-  
1215 bite test with 25% compression. Samples of HC-MCC treatments were poured into 30mm  
1216 diameter cylindrical molds and were allowed to solidify overnight in a 5°C refrigerator  
1217 prior to testing. Fracture properties were tested in compression deformation modes using  
1218 a 1.5cm thick section of sample. Force and compressional data from testing was  
1219 converted into Hencky strain ( $\epsilon$ ) using equation 5 where  $L(t)$  is the height of the  
1220 compressed sample and  $L_0$  is the initial height. A metric to observe the strain hardening  
1221 potential of a sample is the strain hardening ratio (SHR), or the ratio of the slope at the  
1222 beginning of testing compared to the end (Sharma et al., 2018)(Bast et al., 2015). As the  
1223 sample continues to harden in response to strain, the slope will increase, and the ratio can  
1224 describe the level of hardening possible.

1225

### 1226 **5.2.5: Transmission Electron Microscopy**

1227            Ultrastructure analysis of HC-MCC mixtures was performed using the TEM  
1228 method described by (Lu et al., 2015). Samples from each treatment group will undergo  
1229 TEM imaging with 0, 0.1, and 0.3% KC added. Samples underwent rheological testing  
1230 using the sample loading and testing method described above. After testing was  
1231 complete, the CC27 geometry was removed from the rheometer. The bottom of the  
1232 geometry was removed to reveal the sample which were harvested for TEM. Samples  
1233 were fixed using 2% glutaraldehyde and formaldehyde for at least two hours. Samples  
1234 were then rinsed in a sodium cacodylate buffer and postfixed in 2% osmium tetroxide  
1235 solution for 1 hour, followed by rinsing with distilled water in two 10-minute stints. After  
1236 dehydration of the samples via a progressive ethanol series (20 min each in 50%, 70%,  
1237 twice in 95%, and three times in 100% EtOH) samples were transitioned into plastic resin  
1238 and infiltrated with a resin-acetone mix. Infiltration with pure resin followed, and  
1239 polymerization of sample blocks occurred overnight at 65°C. Sections (70-100nm) were  
1240 cut on a Leica EM UC6 ultramicrotome (Leica Microsystems Inc., Buffalo Grove, IL)  
1241 using a diamond knife (Diatome, Hatfield, PA). Sections were double stained for 20  
1242 minutes with saturated aqueous uranyl acetate followed by 10 minutes with Reynold's  
1243 lead citrate. Sections were then analyzed using a transmission electron microscope (TEM,  
1244 JEM 1400 Plus, Jeol USA Inc., Peabody, MA) operated at 120kV, and digital images  
1245 were captured using a Gatan camera (Gatan Inc., Pleasanton, CA).

1246

### 1247 **5.2.6: Particle Size**

1248 Particle size analysis was conducted in using an Anton Paar PSA 1190 micro  
1249 particle size analyzer (Graz, Austria). Sample gels were cured overnight in a refrigerator,  
1250 and mixed with 5°C DI water to ensure the HC-MCC is still in a gelled state before  
1251 loading the sample into the analyzer receptacle. Sample dispersion within the unit was  
1252 accomplished using distilled water with a 5 second debubbling time, and measurements  
1253 occurred over a 30 second period with a pump speed at 120 rpm.

1254

### 1255 **5.2.7: Zeta Potential**

1256 Tests examining casein zeta potential were conducted using an Anton Paar  
1257 Litesizer 500 particle size analyzer (Anton Paar GMBH, Graz, Austria). Testing HC-  
1258 MCC in each treatment and each KC level was conducted using a temperature series  
1259 measurement from 40°C to 5°C, conducting measurements at 40, 30, 20, 10, and 5°C in  
1260 descending order. Samples reached the target temperature for testing and equilibrated for  
1261 10 minutes prior to a measurement to ensure samples are uniformly cooled. The sample  
1262 then sat overnight at 5°C after the temperature sweep and was measured the following  
1263 day to observe any potential difference due to additional holding time at 5°C. HC-MCC  
1264 was diluted in simulated milk ultrafiltrate (SMUF) buffer 1000x and loaded into a model  
1265 no. 225288 zeta potential cuvette (Anton Paar GMBH, Graz, Austria). All measurements  
1266 were conducted using 18V with a maximum of 300 measurements for each reading. Zeta  
1267 potential data was calculated using Smoluchowski approximation which is part of the  
1268 testing software.

1269

### 1270 **5.2.8: Statistical Analysis**

1271 Data points from rheological, particle size, and texture analysis tests were pulled  
1272 from their respective software programs. Statistical significance was measured using a  
1273 GLM model in SAS to compare the effects of modifications. Differences will be  
1274 evaluated using ANOVA and Tukey's HSD adjustment with  $P \leq 0.05$  considered  
1275 statistically significant.

1276

## 1277 **5.3: Results and Discussion**

1278

### 1279 **5.3.1: Particle Size**

1280 With increasing KC content within samples, there was a growing issue during  
1281 initial measurements using an Anton Paar model litesizer 500 nano particle size analyzer  
1282 due to the formation of KC aggregates in micron size, causing issues with data  
1283 interpretation. As KC content increased, the average particle diameter outputs grew  
1284 increasingly erratic. Particle size distribution data showed the conversion from a  
1285 monomodal dispersion in KC free samples to multimodal distributions at erratic sizes  
1286 with 0.3% KC. In addition, the additional peaks observed from KC addition were near the  
1287 limit of detection for the litesizer hardware, rendering the measurements incomplete. To  
1288 correctly capture large particle size species, we conducted particle size analysis on the  
1289 gelled particles using an Anton Paar model PSA 1190 particle size analyzer which was  
1290 better equipped to observe the casein-KC gels on a micro-meter scale rather than on the  
1291 nano-meter scale.

1292           The increase from 0.1% to 0.3% KC within solution resulted in a significant  
1293 decrease in average particle size regardless of treatment group (Table 5-1). Indicating that  
1294 the size of casein within solution decreases as KC content increases. Increased KC  
1295 content results in a multimodal distribution of particles (Figure 5-1), which is confirmed  
1296 by TEM data (Figure 5-5). The effect of pH adjustment and calcium chelation  
1297 significantly increases particle size compared to control groups; other studies have  
1298 described an increase in micelle size in response to alkalization (Y. Liu & Guo, 2008).  
1299 While TEM micrographs depict the disintegration of the micellar structure, alkalization  
1300 could increase the ability of the caseins to hold more moisture. This effect would describe  
1301 the significant increase in particle size at 0.3% KC content compared to control samples.  
1302 In the case of TSC addition, the destabilization of the micelle brought on by calcium  
1303 chelation could also encourage protein-water interactions, as TSC is also known to raise  
1304 the pH of HC-MCC solutions (Chapter 4.3.1).

1305

1306

1307

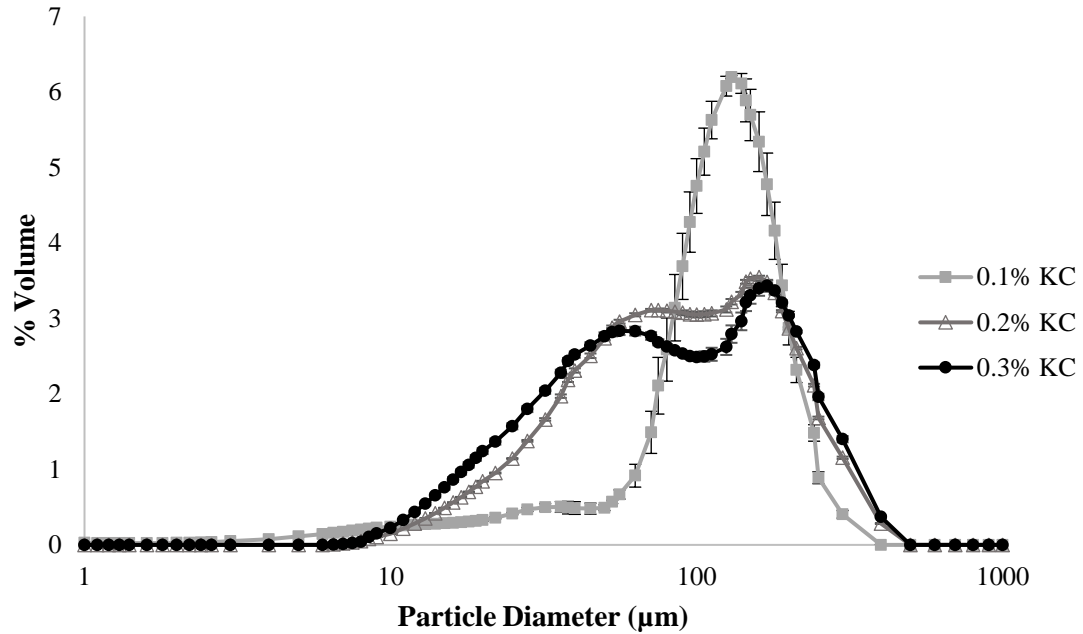


**Figure 5-1:** Comparison of particle size distributions across KC concentrations. All samples included are control samples, bars indicate standard error.

**Table 5-1:** Comparison of Particle Size ( $d_{4,3}$ ) Against KC Content and Treatment.

KC Content (% wt/wt)	Control	25mM TSC	pH 7.0
0.1	$116 \pm 2.99^{Aa}$	$120 \pm 2.22^{Aa}$	$112 \pm 1.08^{Ba}$
0.2	$83.0 \pm 0.464^{Bc}$	$116 \pm 1.64^{ABb}$	$132 \pm 1.27^{Aa}$
0.3	$76.1 \pm 1.87^{Bb}$	$108 \pm 2.59^{Ba}$	$103 \pm 2.35^{Ca}$

Capital letters designate significance across KC content levels, while lower case designates significance across treatment groups. Significance level is  $P < 0.05$

### 1318 **5.3.2: Zeta Potential**

1319           No significant changes in the zeta potential of HC-MCC were observed as a result  
1320 of temperature sweep testing. In addition, no significant differences in values were  
1321 observed after holding the sample overnight at 5°C and resuming testing. It can be  
1322 inferred from this result that the solubility of CCP in response to temperature does not  
1323 have significant effect on the zeta potential of KC-casein mixtures. Increasing  
1324 concentrations of KC within samples also produced an insignificant effect on zeta  
1325 potential. While KC may simply not affect the zeta potential of casein, this finding in  
1326 conjunction with TEM micrographs is further proof that there is minimal interaction  
1327 between KC and casein in our samples. Sun et al., (2016) described a change in zeta  
1328 potential values in response to starches binding to casein, however there was concrete  
1329 evidence in the form of scanning electron microscopy micrographs depicting interaction  
1330 between casein and starch. Treatment effects also produced minimal changes within zeta  
1331 values, although as evidenced within particle size and texture tests, there were minimal  
1332 differences observed as well. In future tests, conducting measurements at different  
1333 concentrations may be recommended to ensure there is adequate sample within the  
1334 SMUF solution.

1335

### 1336 **5.3.3: Texture Analysis**

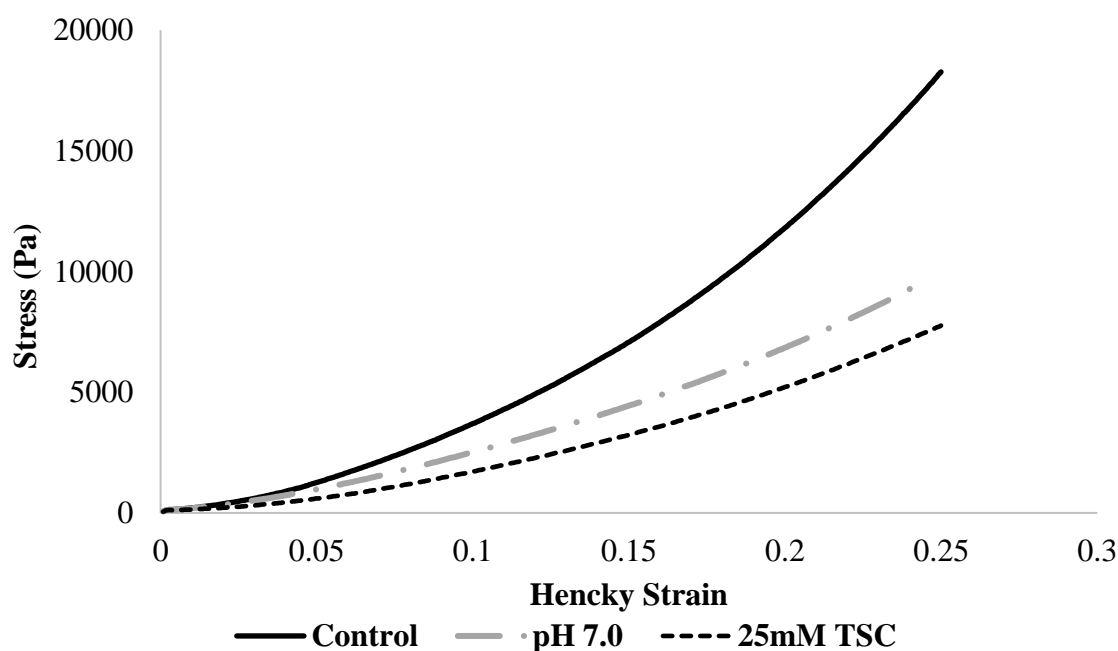
1337           Texture profile analysis was conducted only on the samples added with 0.3% KC,  
1338 because they were able to hold their shape at 25% strain during testing. Maximum stress  
1339 values achieved at 25% strain were higher (23.9 kPa) for control samples than pH (13.5  
1340 kPa) and TSC treated samples (10.1 kPa) (Figure 5-2). A similar pattern was found for



1341 hardness and strain hardening ratio, with control samples being significantly higher than  
1342 either form of treatment (Table 5-2). While comparing these results with small strain  
1343 rheology, it is apparent that large strain rheology exhibits a distinctive behavior, because  
1344 of the way deformation takes in the material.

1345

1346



1347

1348 **Figure 5-2:** Compressional testing of KC-MCC gels. Values are until 25% maximum  
1349 strain.

1350

1351

1352

1353 **Table 5-2:** Texture Analysis Results.

Treatment	Control 0.3% KC	25mM TSC 0.3% KC	pH 7.0 0.3% KC
Maximum Stress (Pa)	23900±1100 <sup>A</sup>	10100±741 <sup>B</sup>	13500±418 <sup>B</sup>
Hardness (g)	291±18.0 <sup>A</sup>	123±8.19 <sup>B</sup>	154±3.25 <sup>B</sup>
Strain Hardening Ratio	3.03±0.289 <sup>A</sup>	1.14±0.0755 <sup>B</sup>	1.30±0.0944 <sup>B</sup>

1354 Capital letters designate significance across treatments at a significance level of  $P < 0.05$ .

1355

1356

1357 **5.3.4: Rheology**1358 **5.3.4.1: Effect of KC addition**

1359 In this study, we diluted 18.5% protein HC-MCC to 10% protein, which did not  
 1360 form cold gels upon cooling to 5°C (Table 5-4). Diluted samples then had KC added in  
 1361 0.1%, 0.2 % and 0.3% quantities. As expected, increases in KC concentration from 0.2%  
 1362 to 0.3% led to a significant increase in gel strength, from 290 Pa to 1300 Pa (Table 5-3).  
 1363 Rheological measurements captured during the temperature sweep exhibited a strong  
 1364 increase in storage modulus values consistently around 27°C (Figure 5-3, Figure 5-6)).  
 1365 This increase was due to KC reaching critical sol-gel temperature within solution (Bui et  
 1366 al., 2019); while the values used in the study are not enough for KC to create a gel alone,  
 1367 they are enough to create a significant increase in dynamic moduli when mixed with HC-  
 1368 MCC. The effect of KC addition to MCC samples was evidenced on the gelling  
 1369 temperature (Table 5-4). Samples with 0.1% KC added did not form a gel during  
 1370 temperature sweep (40°C to 5°C) but formed a gel while holding at 5°C for 10 hrs.

1371 Increasing KC from 0.2% to 0.3% however, increased gelation temperature from 25.3°C  
1372 to 27.8°C (Table 5-4).

1373 **Table 5-3:** Comparison of storage modulus values between treatments and temperatures for kappa carrageenan added MCC samples

Treatment	G' (Pa)			
	20°C	8°C	5°C	5°C + 10hrs
Unmodified 0.1KC	2.23±0.152 <sup>Db</sup>	3.81±0.150 <sup>Eb</sup>	4.56±0.281 <sup>Eab</sup>	7.94±1.50 <sup>Da</sup>
Unmodified 0.2KC	113±20.0 <sup>CDb</sup>	243±41.0 <sup>DCab</sup>	290±48.1 <sup>DEab</sup>	409±71.2 <sup>CDa</sup>
Unmodified 0.3KC	396±31.7 <sup>BCc</sup>	875±72.1 <sup>BCb</sup>	1090±102 <sup>BCab</sup>	1300±33.3 <sup>Ba</sup>
25mM TSC 0KC	0.0640±0.0134 <sup>Db</sup>	1.33±0.377 <sup>Eb</sup>	1.62±0.748 <sup>Eb</sup>	27.1±5.59 <sup>Da</sup>
25mM TSC 0.1KC	17.8±2.51 <sup>Dc</sup>	105±6.13 <sup>Eb</sup>	137±5.86 <sup>Eb</sup>	208±11.6 <sup>CDa</sup>
25mM TSC 0.2KC	292±42.2 <sup>BCDb</sup>	645±80.7 <sup>CDab</sup>	758±90.5 <sup>CDa</sup>	945±116 <sup>BCa</sup>
25mM TSC 0.3KC	580±49.6 <sup>Bc</sup>	1200±94.4 <sup>Bb</sup>	1380±109 <sup>Bab</sup>	1740±141 <sup>Ba</sup>
7.0 0KC	0.00430±0.00252 <sup>Db</sup>	0.00941±0.00528 <sup>Eb</sup>	0.0262±0.00614 <sup>Eb</sup>	3.53±1.08 <sup>Da</sup>
7.0 0.1KC	13.8±3.76 <sup>Db</sup>	106±35.5 <sup>Eb</sup>	141±47.8 <sup>Eb</sup>	414±108 <sup>CDa</sup>
7.0 0.2KC	197±41.8 <sup>CDc</sup>	758±105 <sup>BCb</sup>	931±117 <sup>BCb</sup>	1620±162 <sup>Ba</sup>
7.0 0.3KC	986±197 <sup>Ab</sup>	2070±264 <sup>Aab</sup>	2340±281 <sup>Aab</sup>	3530±523 <sup>Aa</sup>

1374 Capital letters designate significance between the same temperature, lower case designates significance between temperatures.

1375 Significance level P<0.05

**Table 5-4:** Gelation Temperatures of Modified MCC Dispersions

Carrageenan Concentration (wt/wt%)	Treatment		
	Unmodified	25mM TSC	pH 7.0
0	NO GEL	NO GEL*	NO GEL*
0.1	NO GEL*	19.9±0.46 <sup>Ba</sup>	14.6±1.07 <sup>Bb</sup>
0.2	25.3±0.46 <sup>Bb</sup>	29.0±0.24 <sup>Aa</sup>	25.5±0.47 <sup>Ab</sup>
0.3	27.8±0.40 <sup>Ab</sup>	29.5±0.23 <sup>Aa</sup>	27.2±0.41 <sup>Ab</sup>

\* Did not gel during the temperature sweep. Capital letters designate significant

differences between the same treatment, lower case designates significance between KC concentrations. Significance level  $P < 0.05$ .

#### 5.3.4.2: Effect of Calcium Chelation and Alkalization

Physicochemical modifications (TSC and pH) on HC-MCC had less of an effect on the gel strength of samples compared to the effect of KC addition. TSC addition and pH modification resulted in gel formation while holding at 5°C without KC addition. When KC is added to the sample however, the CGT values are similar and appear to be largely dependent on the concentration of KC rather than the additional treatments. While not significant, the increase in KC content from 0.1% to 0.2% in TSC samples raised the storage modulus value of treatments by a factor of 4 and increased further when raised to 0.3% (Table 5-3). KC at all concentrations significantly improved the gel strength of cold gels, exhibiting maximum gel strength for pH 7.0 and 0.3% KC ( $G' = 3500$  Pa). This clearly indicates that combined the impact of pH and KC was the most effective at improving gel strength. The sudden increase in dynamic moduli around 27°C in response

to increasing KC indicates that KC may be forming a gel by itself. The gelling properties of KC are unaffected by pH adjustment from 6.6 to 7.0, or from the use of calcium chelating salts indicating that treatment group modifications only have an effect on the casein within the system.(Ould Eleya & Turgeon, 2000).

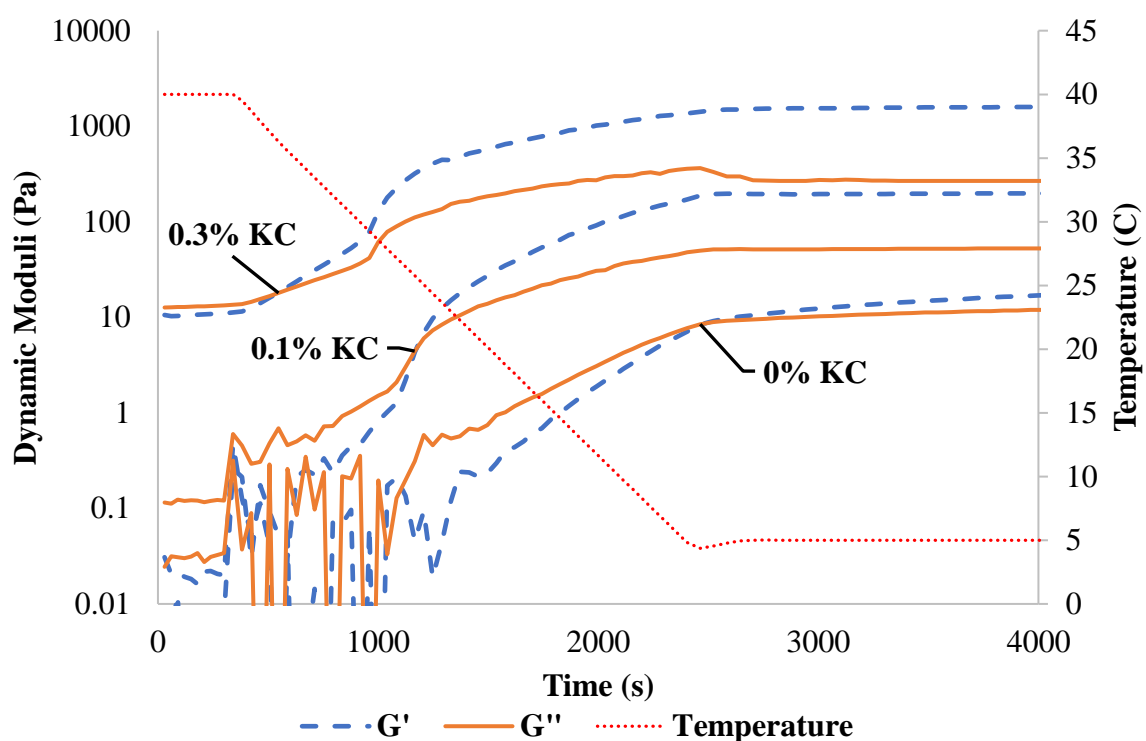


**Figure 5-3:** Temperature sweep data for 25mM TSC treatments. A comparison of dynamic moduli in response to the temperature sweep in the rheological protocol using 3 rad/s frequency.

### 1406 5.3.5: TEM Micrographs

1407 TEM micrographs of MCC samples treated with KC, pH and TSC are presented  
1408 at two magnification levels (2,000x and 20,000x) in Figure 5-4 and 5-5. Without KC  
1409 additions, TSC and pH treated samples had uniform, and monophasic structures. Even  
1410 while utilizing high shear to homogenize the sample, the addition of KC led to the  
1411 creation of a biphasic solution that was made of separate KC and casein phases. Samples  
1412 with at 0.1% and 0.3% added KC exhibited minimal interaction with caseins regardless  
1413 of treatment. In samples 0.3% KC, the casein phase appears to be more compact,  
1414 indicating that KC is absorbing moisture more readily than casein, and compacting the  
1415 casein phase into a denser state. Because of this reduction in moisture, the casein that  
1416 appeared in the micrographs was darker than the other phase potentially due to a lower  
1417 affinity to moisture holding compared to KC. The separate KC phase in the micrographs  
1418 were less dense than casein, and appeared to create mesh like fragments that exhibit  
1419 heavily crosslinking from individual strands. Any potential for interaction (mixing of two  
1420 phases or bond formations) between caseins in any form and KC was observed within the  
1421 border regions of KC and casein areas.

1422

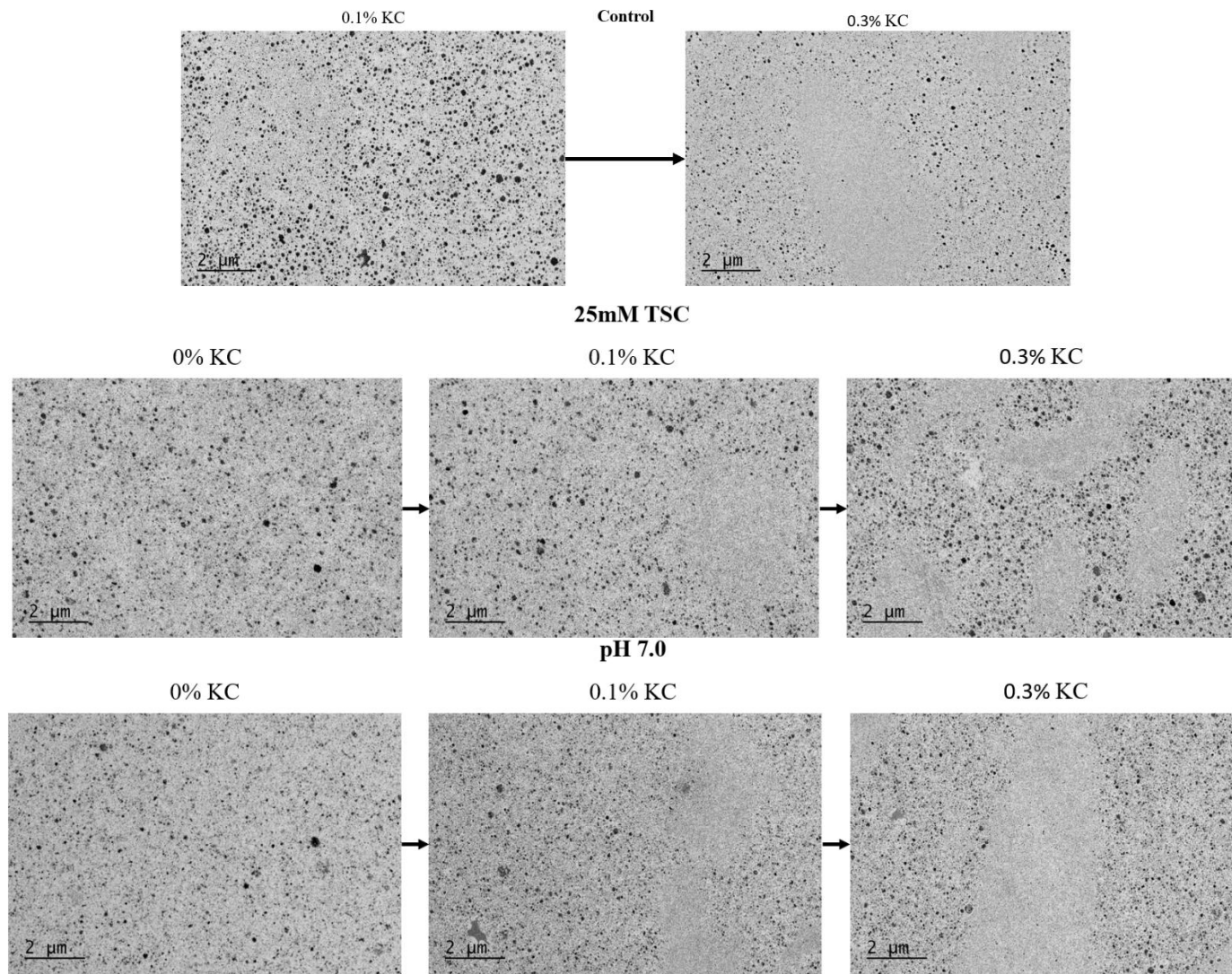


**Figure 5-4:** TEM micrographs of cold gels made from treated MCC samples (10% protein) at 2000x instrumental magnification



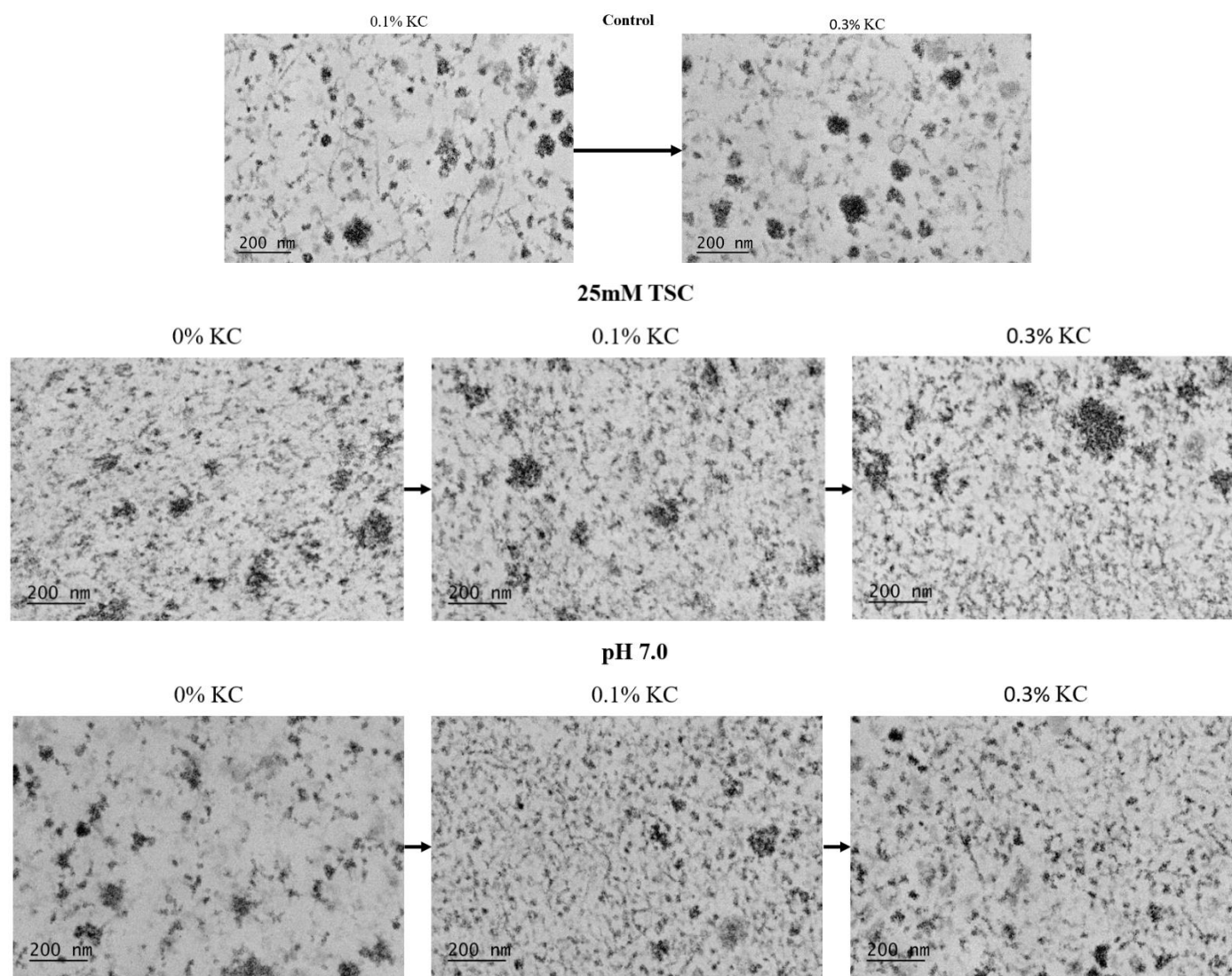


**Figure 5-5:** TEM micrographs of cold gels made from treated MCC samples (10% protein) at 20000x instrumental magnification

There were clear indications of changes in the micellar structures in response to modifications. Samples with 25mM TSC or adjusted to pH 7.0 at 10% protein exhibit similar morphological changes as TEM micrographs conducted on 18.5% protein samples (Figure 4-7). The disintegration of the micellar structure is clearly evident, and there is an abundance of free casein strands within solution compared to control samples. pH 7.0 samples appear to have an increased degree of structural disintegration similar to samples in the previous study (Figure 4-7); this greater fraction of free caseins is likely to interact well with water and the cause for the increase in gel strength over TSC and control samples. The pH at which micellar disintegration is occurring is lower than what was reported by Vaia et al., (2006), but is a similar result compared to the previous chapter (Chapter 4.3.5), which could mean that our MCC sample may have an increased sensitivity to pH adjustment. While still a minimal amount, samples with micellar collapse appear to have a higher degree of interaction between caseins and KC within solution, exhibited in the same border regions as control samples. As the structure of the casein micelle is weakened due to the effect of calcium chelation or alkalization (Touhami et al., 2022), the free caseins will have an increase potential for interaction with the KC phase.

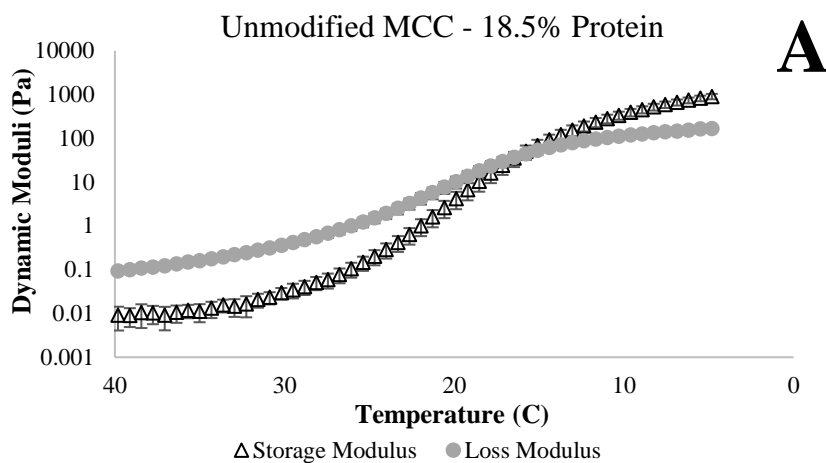
## 5.4: Discussions

The aim of this research was to study the potential of KC to improve the gelling behavior of MCC at a lower protein concentration than previous chapters. When comparing studies on modified HC-MCC (18.5% and 15% protein) from previous

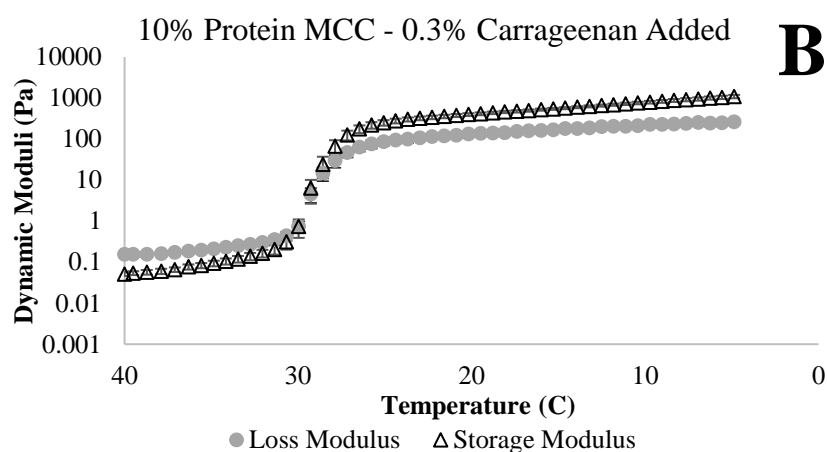
1454 chapters (Chapter 3.3.4, Chapter 4.3.2) and diluted MCC samples (10% protein) from this  
1455 study, the gel strength of samples from previous tests are an order of magnitude higher  
1456 than the samples tested in this study due to differences in protein content. On the other  
1457 hand, the highest CGT in this chapter was 29.5°C (10% protein, 25mM TSC and 0.3%  
1458 KC) which was only 3.5°C lower than highest average CGT (18.5% protein, pH 6.8 with  
1459 10mM TSC) measured in the previous chapters (Table 3-2) While the addition of KC into  
1460 diluted HC-MCC did not increase the gel strength enough to make up for reduced protein  
1461 content, it was able to make a high CGT.

1462         Figure 5-6 compares the temperature sweep and gelation curves of an unmodified  
1463 18.5% protein HC-MCC gel with a diluted, 10% protein gel with 0.3% KC. While the  
1464 storage modulus values at the end of the temperature sweep are similar, the diluted  
1465 sample has a significantly higher CGT. Due to this elevated CGT value, the frequency  
1466 dependence on the sample with added KC did not change significantly from 20°C  
1467 through the end of testing (Figure 5-7). During this period, it maintained a frequency  
1468 dependence ( $n < 0.2$ ) low enough to be considered a strong gel (Faber et al., 2017; Rafe &  
1469 Razavi, 2017). The unmodified samples, however, had a significantly higher frequency  
1470 dependence ( $n \sim 0.7$ ) at 20°C in comparison, but significantly lower value at the end of the  
1471 temperature sweep ( $n = 0.08$ ) and at the end of testing ( $n = 0.05$ ).

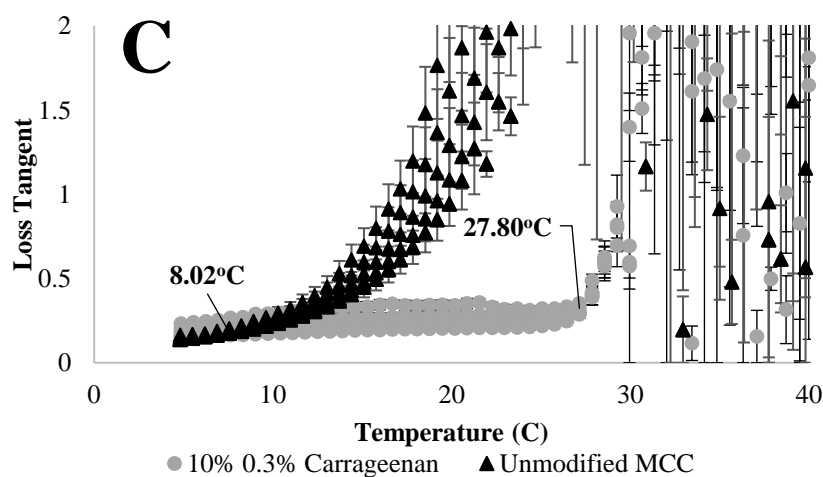
1472



1473



1474



1475

1476 **Figure 5-6:** A and B: Dynamic Moduli of treatments during the temperature sweep. C:

1477 Gelation curves during the temperature sweep with their Respective Gelation Points.

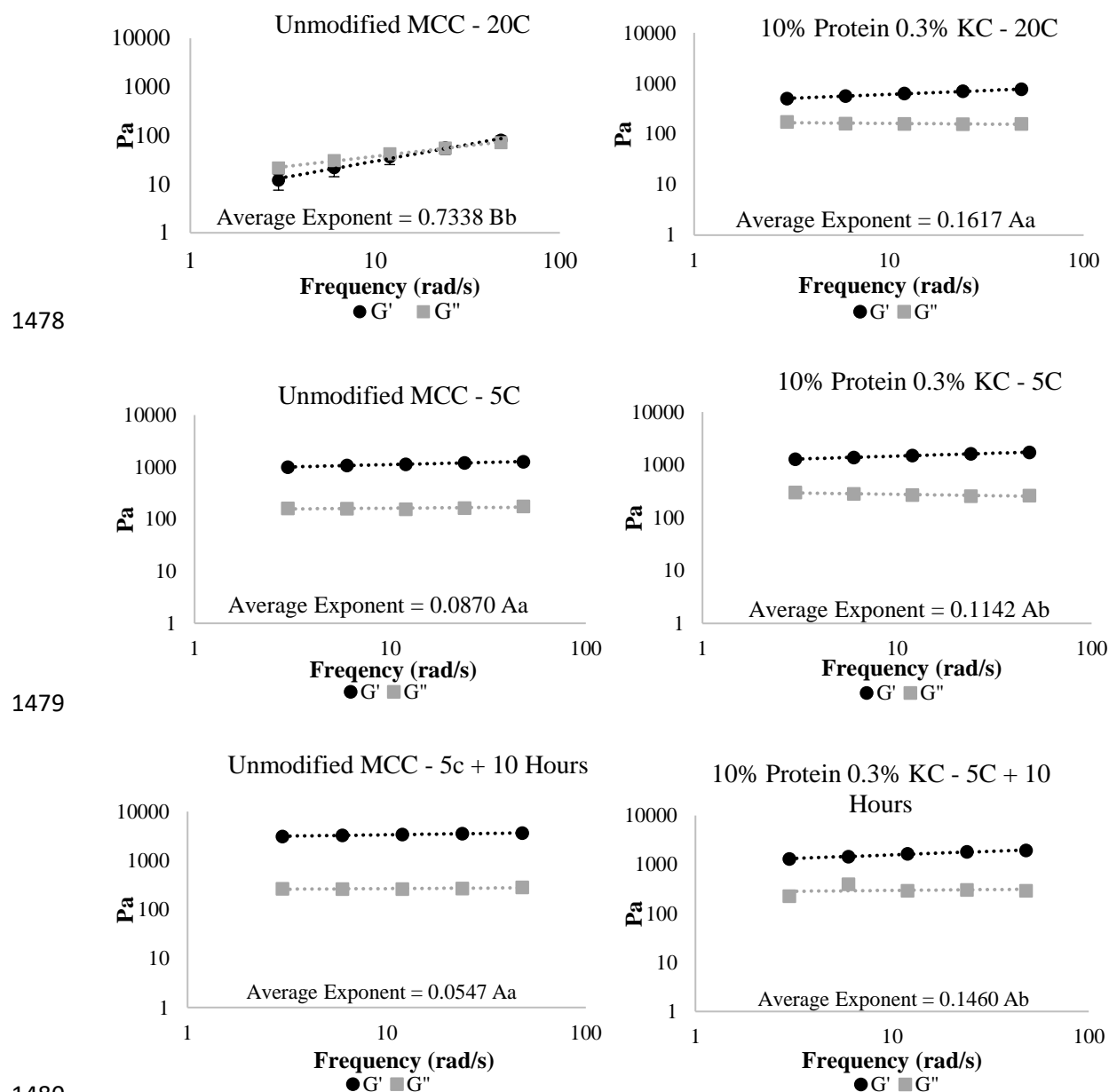


**Figure 5-7:** A comparison of frequency measurements at 20°C, 5°C, and 5°C after 10 hours between unmodified HC-MCC and a diluted sample with 0.3% kappa carrageenan added. The exponent of the slope equation for  $G'$  can be used as a marker for gel strength, with a smaller exponent indicating a stronger gel and less frequency dependence. Capital letters denotes significant difference ( $P < 0.05$ ) between temperatures and lower case denotes significance between treatments.

1487           When comparing texture analysis results from previous chapters, we observed the  
1488   opposite result i.e., pH and TSC modifications reduced the maximum stress, hardness and  
1489   strain hardening ratio over the control. (Chapter 4.3.4). The reduction in protein content  
1490   prohibits dense networks of casein compared to undiluted samples, resulting in less  
1491   resistance to compression forces and a reduction in shear hardening qualities. Control  
1492   samples still maintain a native protein conformation, which could offer more resistance in  
1493   testing typically observed in other dairy samples (Sharma et al., 2018; Zad Bagher  
1494   Seighalani & Joyner, 2019).

1495           When considering the results from TEM micrographs, KC appears to bind  
1496   moisture to a greater extent than casein in any form, reducing the moisture available to  
1497   the casein phase within solution. This offers an explanation as to why a consistent  
1498   increase in  $G'$  was observed in all rheology tests utilizing KC; as there is minimal  
1499   interaction between casein and KC, the concentrated pockets of KC were able to absorb  
1500   available moisture within the system and create a separate KC gel matrix within the MCC  
1501   system. In the formation of this matrix, KC absorbs water from the casein pockets,  
1502   effectively compacts the protein phase closer. The increase in casein density assists in gel  
1503   strength by allowing casein structures to interact as if they were a higher protein  
1504   concentration, therefore increasing potential for casein-casein interactions. In addition,  
1505   TSC and pH modification can lead to conformational changes in casein micelles, which  
1506   can result in increased gel strength (Chapter 3.3.4, Chapter 4.3.2). Furthermore, the  
1507   ability of KC to absorb moisture also offers a potential explanation for particle size data.  
1508   Such competition for moisture results in less hydration of micellar structures and a  
1509   reduction in overall size of casein micelles within control samples.

1510

1511

## 5.5: Conclusions

1512

1513       The addition of KC into diluted MCC dispersions results in significant increases  
1514 in both gel strength and gelation temperature. The use of KC creates separate phases  
1515 within solution that absorb water to a greater extent than casein, resulting in concentrated  
1516 casein pockets within a composite network. Additional physicochemical modifications in  
1517 the form of calcium chelation and alkalization improved gel strength and CGT, at the  
1518 expense of a reduction in textural hardness and strain hardening properties. Interaction  
1519 between KC and HC-MCC was minimal regardless of treatment, indicating that elevated  
1520 gel qualities were due to the water binding effects of KC rather than the formation of a  
1521 KC-casein matrix. In the future, studies with other forms of physicochemical  
1522 modifications could yield additional insights into the cold gelling behavior of MCC  
1523 dispersions.

1524

## References

- 1525
- 1526
- 1527 Bui, V. T. N. T., Nguyen, B. T., Renou, F., & Nicolai, T. (2019). Rheology and  
 1528 microstructure of mixtures of iota and kappa-carrageenan. *Food Hydrocolloids*,  
 1529 89, 180–187. <https://doi.org/10.1016/j.foodhyd.2018.10.034>
- 1530 Campbell, R., & Hotchkiss, S. (2017). Carrageenan Industry Market Overview. In A. Q.  
 1531 Hurtado, A. T. Critchley, & I. C. Neish (Eds.), *Tropical Seaweed Farming*  
 1532 *Trends, Problems and Opportunities: Focus on Kappaphycus and Eucheuma of*  
 1533 *Commerce* (pp. 193–205). Springer International Publishing.  
 1534 [https://doi.org/10.1007/978-3-319-63498-2\\_13](https://doi.org/10.1007/978-3-319-63498-2_13)
- 1535 Dunn, M., Barbano, D. M., & Drake, M. (2021). Viscosity changes and gel formation  
 1536 during storage of liquid micellar casein concentrates. *Journal of Dairy Science*,  
 1537 104(12), 12263–12273. <https://doi.org/10.3168/jds.2021-20658>
- 1538 Faber, T. J., Jaishankar, A., & McKinley, G. H. (2017). Describing the firmness,  
 1539 springiness and rubberiness of food gels using fractional calculus. Part I:  
 1540 Theoretical framework. *Food Hydrocolloids*, 62, 311–324.  
 1541 <https://doi.org/10.1016/j.foodhyd.2016.05.041>
- 1542 Liu, Y., & Guo, R. (2008). PH-dependent structures and properties of casein micelles.  
 1543 *Biophysical Chemistry*, 136(2), 67–73. <https://doi.org/10.1016/j.bpc.2008.03.012>
- 1544 Lu, Y., McMahon, D. J., Metzger, L. E., Kommineni, A., & Vollmer, A. H. (2015).  
 1545 Solubilization of rehydrated frozen highly concentrated micellar casein for use in  
 1546 liquid food applications. *Journal of Dairy Science*, 98(9), 5917–5930.  
 1547 <https://doi.org/10.3168/jds.2015-9482>



- 1548 Lu, Y., McMahon, D. J., & Vollmer, A. H. (2016). Investigating cold gelation properties  
1549 of recombined highly concentrated micellar casein concentrate and cream for use  
1550 in cheese making. *Journal of Dairy Science*, 99(7), 5132–5143.  
1551 <https://doi.org/10.3168/jds.2015-10791>
- 1552 Ould Eleya, M. M., & Turgeon, S. L. (2000). The effects of pH on the rheology of  $\beta$ -  
1553 lactoglobulin/ $\kappa$ -carrageenan mixed gels. *Food Hydrocolloids*, 14(3), 245–251.  
1554 [https://doi.org/10.1016/S0268-005X\(99\)00055-7](https://doi.org/10.1016/S0268-005X(99)00055-7)
- 1555 Ozcan-Yilsay, T., Lee, W.-J., Horne, D., & Lucey, J. A. (2007). Effect of Trisodium  
1556 Citrate on Rheological and Physical Properties and Microstructure of Yogurt.  
1557 *Journal of Dairy Science*, 90(4), 1644–1652. <https://doi.org/10.3168/jds.2006-538>
- 1558 Rafe, A., & Razavi, S. M. A. (2017). Scaling law, fractal analysis and rheological  
1559 characteristics of physical gels cross-linked with sodium trimetaphosphate. *Food*  
1560 *Hydrocolloids*, 62, 58–65. <https://doi.org/10.1016/j.foodhyd.2016.07.021>
- 1561 Rosmaninho, R., Santos, O., Nylander, T., Paulsson, M., Beuf, M., Benezech, T.,  
1562 Yiantsios, S., Andritsos, N., Karabelas, A., Rizzo, G., Müller-Steinhagen, H., &  
1563 Melo, L. F. (2007). Modified stainless steel surfaces targeted to reduce fouling –  
1564 Evaluation of fouling by milk components. *Journal of Food Engineering*, 80(4),  
1565 1176–1187. <https://doi.org/10.1016/j.jfoodeng.2006.09.008>
- 1566 Sharma, P., Munro, P. A., Dessev, T. T., Wiles, P. G., & Foegeding, E. A. (2018). Strain  
1567 hardening and anisotropy in tensile fracture properties of sheared model  
1568 Mozzarella cheeses. *Journal of Dairy Science*, 101(1), 123–134.  
1569 <https://doi.org/10.3168/jds.2017-13126>

- 1570 Sun, N., Liang, Y., Yu, B., Tan, C., & Cui, B. (2016). Interaction of starch and casein.  
 1571 *Food Hydrocolloids*, 60, 572–579. <https://doi.org/10.1016/j.foodhyd.2016.04.029>
- 1572 Touhami, S., Marciniak, A., Doyen, A., & Brisson, G. (2022). Effect of alkalization  
 1573 and ultra-high-pressure homogenization on casein micelles in raw and pasteurized  
 1574 skim milk. *Journal of Dairy Science*, 105(4), 2815–2827.  
 1575 <https://doi.org/10.3168/jds.2021-20700>
- 1576 Udabage, P., McKINNON, I. R., & Augustin, M.-A. (2000). Mineral and casein  
 1577 equilibria in milk: Effects of added salts and calcium-chelating agents. *Journal of*  
 1578 *Dairy Research*, 67(3), 361–370. <https://doi.org/10.1017/S0022029900004271>
- 1579 Vaia, B., Smiddy, M. A., Kelly, A. L., & Huppertz, T. (2006). Solvent-Mediated  
 1580 Disruption of Bovine Casein Micelles at Alkaline pH. *Journal of Agricultural and*  
 1581 *Food Chemistry*, 54(21), 8288–8293. <https://doi.org/10.1021/jf061417c>
- 1582 Winter, H. H., & Chambon, F. (1986). Analysis of Linear Viscoelasticity of a  
 1583 Crosslinking Polymer at the Gel Point. *Journal of Rheology*, 30(2), 367–382.  
 1584 <https://doi.org/10.1122/1.549853>
- 1585 Zad Bagher Seighalani, F., & Joyner, H. (2019). Wear: A new dimension of food  
 1586 rheological behaviors as demonstrated on two cheese types. *Journal of Food*  
 1587 *Engineering*, 263, 337–340. <https://doi.org/10.1016/j.jfoodeng.2019.07.016>
- 1588 Zad Bagher Seighalani, F., McMahon, D. J., & Sharma, P. (2021). Determination of  
 1589 critical gel-sol transition point of Highly Concentrated Micellar Casein  
 1590 Concentrate using multiple waveform rheological technique. *Food Hydrocolloids*,  
 1591 120, 106886. <https://doi.org/10.1016/j.foodhyd.2021.106886>
- 1592
- 1593

## CHAPTER 6

## CONCLUSION

Dispersions of HC-MCC were modified in specific manners (pH modification, TSC and KC addition) that resulted in changes (mostly favorable) in gel strength and the temperature of gelation. In addition to the changes evidenced by rheological testing, ultrastructure analysis confirms that morphological changes were occurring within the micellar structure of casein in response to these treatments. The addition of TSC to HC-MCC, regardless of protein content was found to raise gel strength and gelation temperature when at a native or acidified pH level. Changes in zeta potential and textural properties were also evidenced by calcium chelation, with TSC additions increasing strain hardening qualities, increasing the net negative charge of particles. In high concentrations (50 mM), TSC resulted in reductions in gel strength compared to lower concentrations (25 mM), with TEM micrographs depicting the formation of large casein aggregates. These newly formed structures are likely to be the cause for the reduction in storage modulus ( $G'$ ).

Adjustment of the sample pH also resulted in various structural changes to caseins. It was observed that storage modulus values followed an exponential positive relationship in the pH range of 6.2-6.8, with samples alkalized to 6.8 yielding the strongest gels. As expected, net charge on the casein micelles and particle size increased in response to increasing pH levels. Further alkalization to pH 7.0 continued to increase

1618 gel strength, creating a potential pathway for further testing. TEM conducted on alkalized  
1619 samples shows evidence of micellar disintegration in response to increasing pH levels  
1620 with concurrent gains in gel strength. Potential increases in protein-protein and protein-  
1621 water interactions as a result of micellar collapse is the current hypothesis behind the  
1622 increases in gel qualities.

1623 Tests conducted in chapter 3 led to the conclusion that protein content of the gels  
1624 was the main determinant of gel strength. The addition of KC to diluted gels was found to  
1625 raise the gelation point to a similar temperature level as observed in previous chapters,  
1626 but gel strength and strain hardening qualities were considerably weaker compared to  
1627 samples previously tested. Additional physicochemical modifications to KC added gels  
1628 affected particle size, gel strength, and textural qualities, but KC content was the main  
1629 determinant of gel strength and temperature of gelation. TEM micrographs depicted two  
1630 separate phases within solution; one of casein and one of KC. the water binding capacity  
1631 of the polysaccharide reduces the moisture available to casein, resulting in pockets of  
1632 concentrated protein responsible for encouraging gelation.

1633 Future testing of HC-MCC could explore its potential applications within the food  
1634 industry. The addition of HC-MCC to products such as yogurt to observe its potential  
1635 ability to thicken and prevent syneresis is a potential pathway for a future project. In  
1636 addition, there is still much to learn about the gelation properties of the sample, especially  
1637 when considering the physicochemical modifications applied. Another pathway to  
1638 consider is how different industrial methods of manufacture could affect the gelling  
1639 qualities of the product, and the effect of other milk components (higher mineral content,  
1640 whey protein and lactose fraction, etc.) remaining in solution.

## APPENDIX

**Table A-1:** Confidence Intervals of 18.5% Protein Sample Gelation Temperatures

TSC (mM)	pH			
	6.2	6.4	6.6	6.8
0	8.48 (7.50, 9.45)	10.52 (9.56, 11.48)	10.74 (9.79, 11.71)	30.19 (25.67, 34.72)
10	7.32 (4.74, 9.90)	22.87 (17.94, 27.80)	25.16 (19.66, 30.66)	32.03 (29.09, 36.96)
25	25.84 (20.35, 31.33)	27.22 (22.93, 31.50)	29.05 (25.49, 32.60)	31.33 (30.34, 32.32)
50	21.03 (14.16, 27.90)	25.16 (22.55, 27.76)	24.01 (21.06, 26.95)	26.07 (19.93, 32.22)

**Table A-2:** Confidence Intervals of 15% Protein Sample Gelation Temperatures

TSC (mM)	pH			
	6.2	6.4	6.6	6.8
10	No Gel	No Gel	6.41 (5.43, 7.40)	25.39 (23.67, 27.10)
25	5.06 (4.81, 5.30)	18.06 (12.84, 23.29)	25.15 (19.94, 30.36)	25.62 (22.06, 29.17)
50	14.87 (10.94, 18.80)	24.47 (17.59, 31.35)	16.24 (11.96, 20.51)	26.07 (19.91, 32.23)

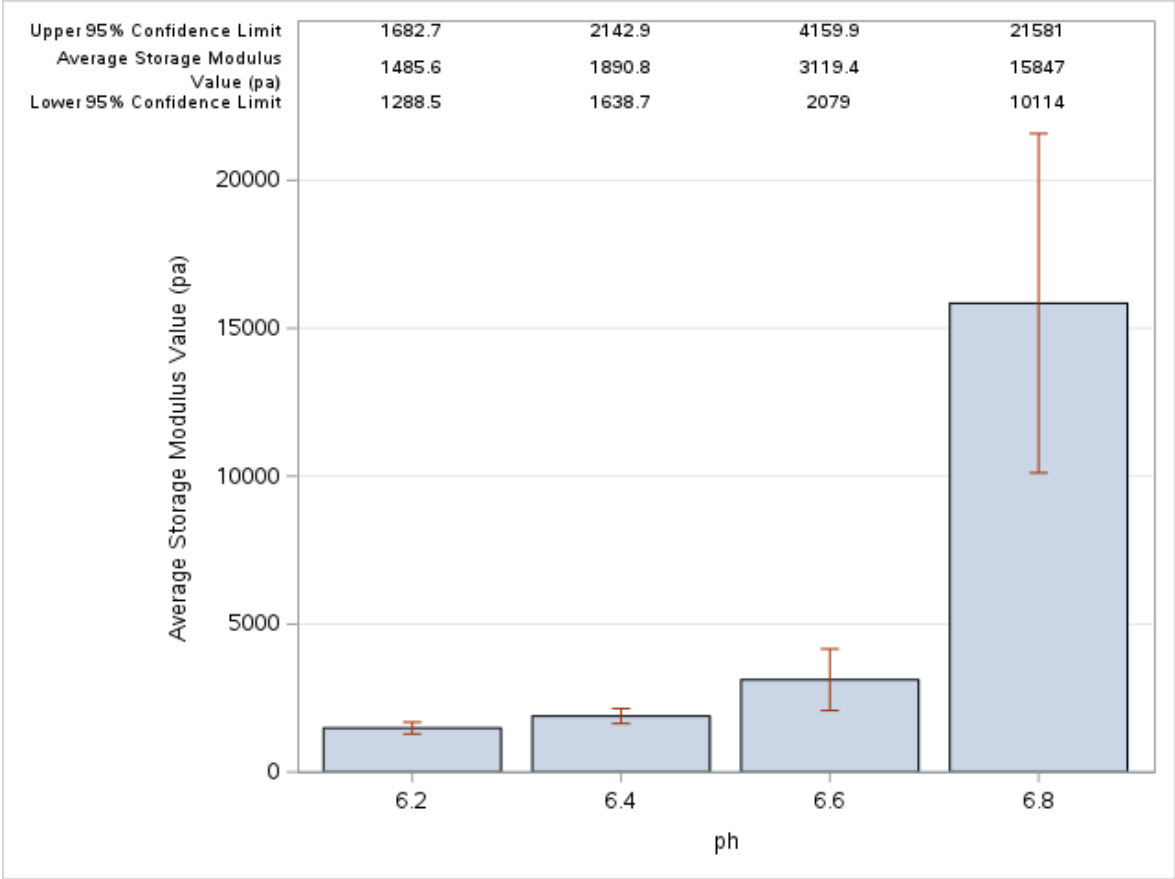
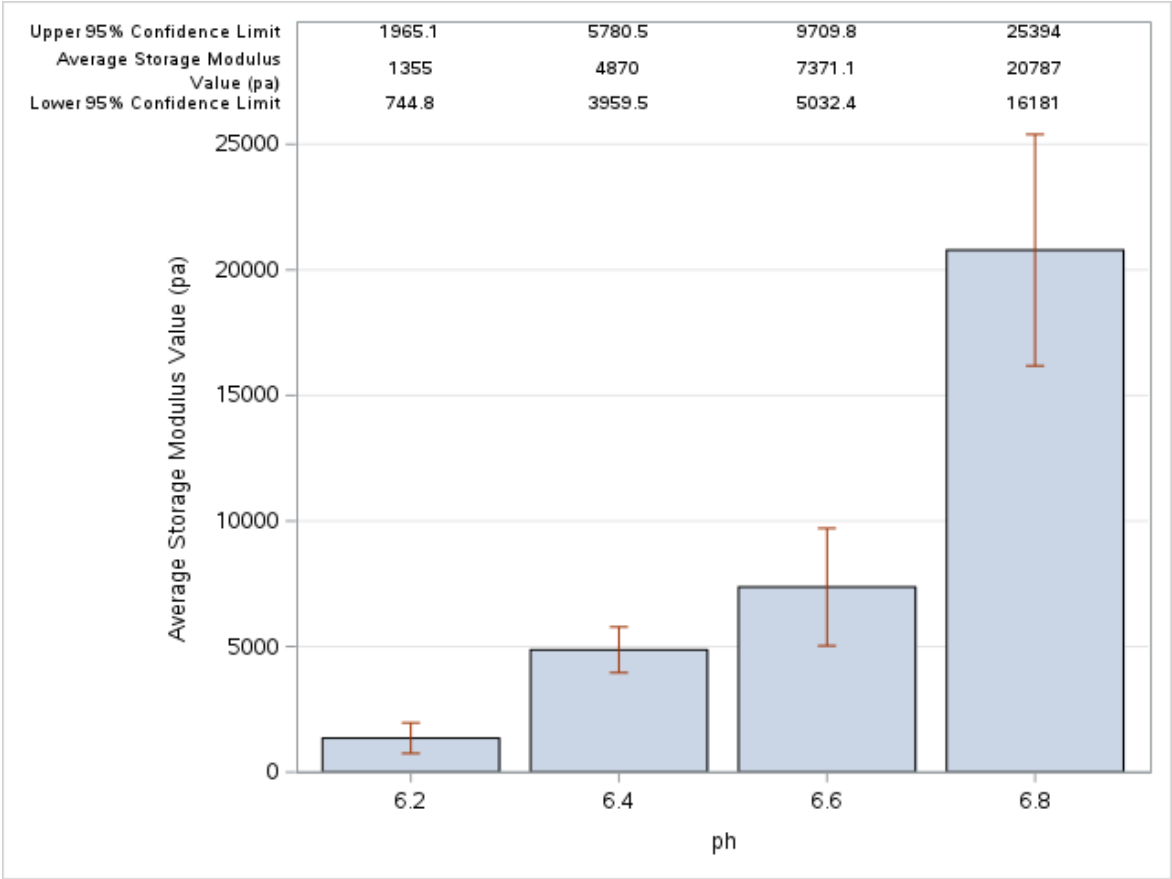
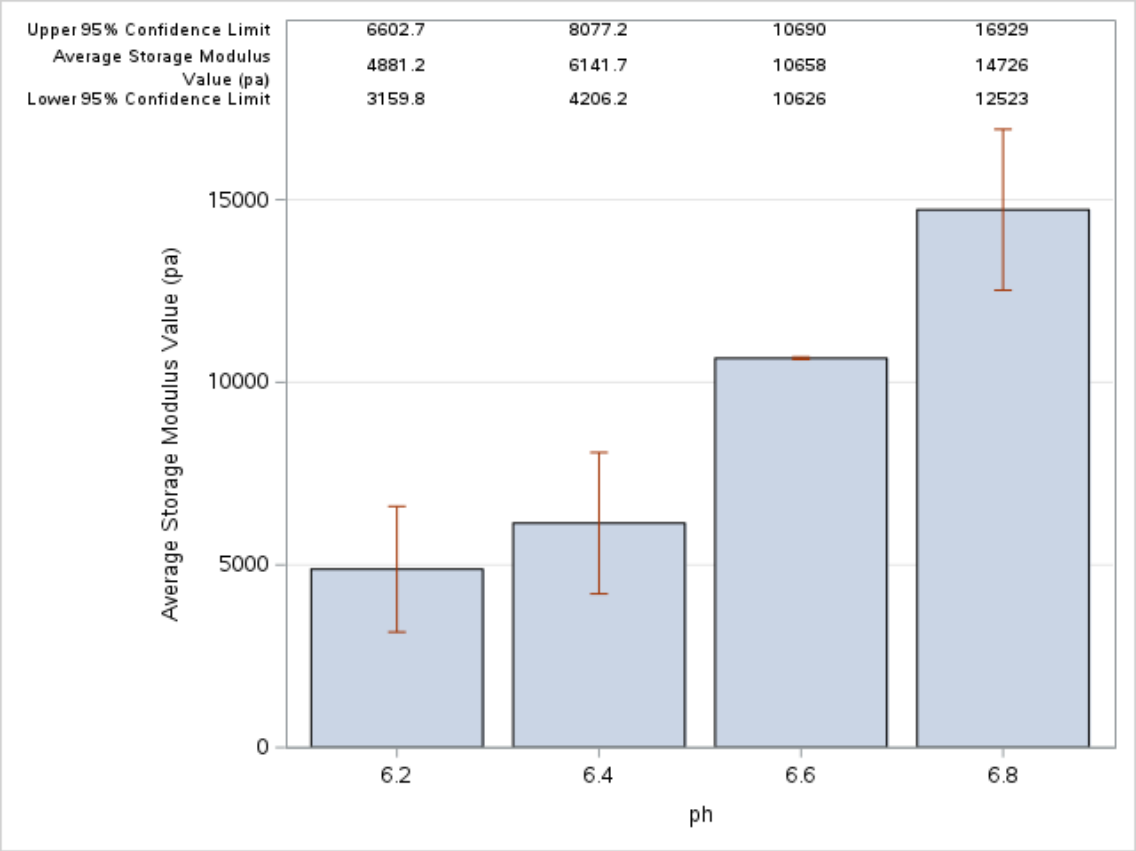


**Figure A-1:** 95% Confidence Intervals of G' Values – 18.5% Protein and 0mM TSC. G' values are recorded after 10 hours of holding at 5°C



1656

1657 **Figure A-2:** 95% Confidence Intercals of G' Values - 18.5% Protein and 10mM TSC. G'  
1658 values are recorded after 10 hours of holding at 5°C



1659

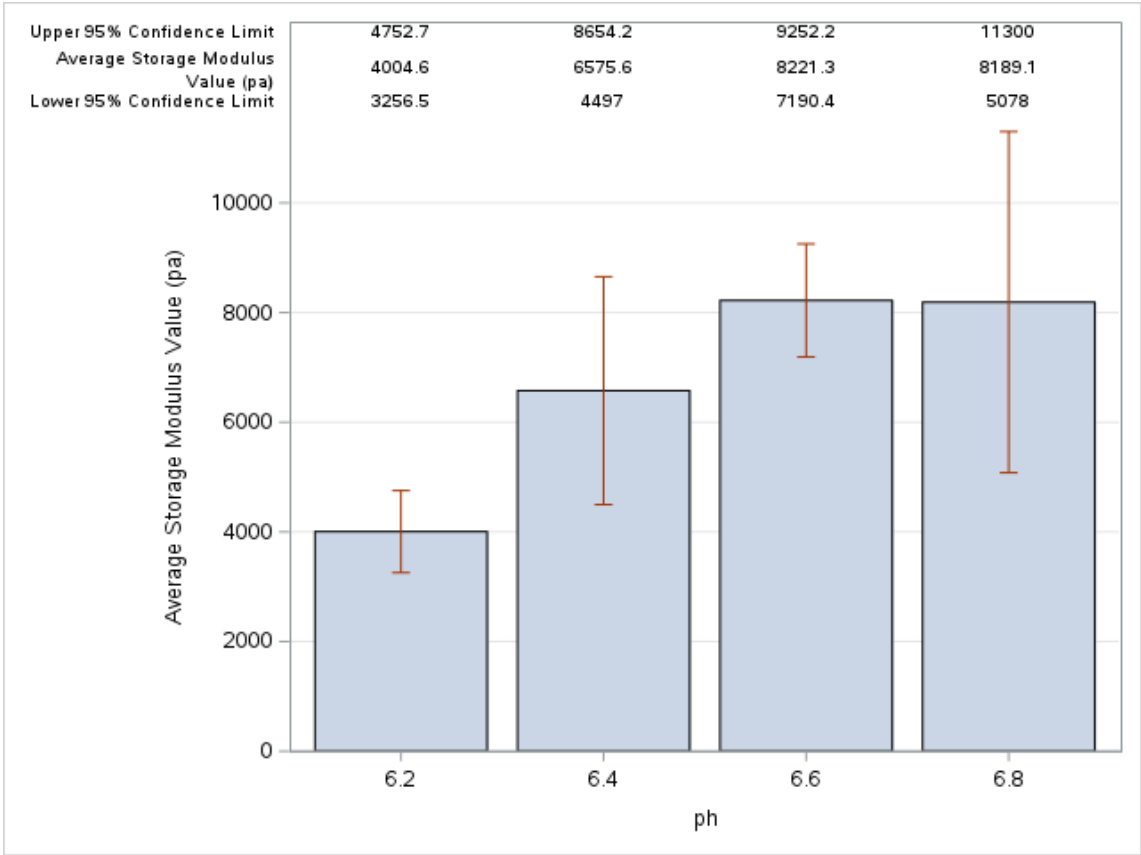
1660 **Figure A-3:** 95% Confidence Intervals of G' Values – 18.5% Protein and 25mM TSC.

1661 G' values are recorded after 10 hours of holding at 5°C

1662

1663





1664

1665 **Figure A-4:** 95% Confidence Intervals of G' Values – 18.5% Protein and 50mM TSC.

1666 G' values are recorded after 10 hours of holding at 5°C